LBL-19545
UC-94c c.2

# Lawrence Berkeley Laboratory
UNIVERSITY OF CALIFORNIA

RECEIVED
LAWRENCE
BERKELEY LABORATORY
JUL 16 1985
LIBRARY AND
DOCUMENTS SECTION

## APPLIED SCIENCE DIVISION

TECHNOLOGY BASE RESEARCH PROJECT FOR
ELECTROCHEMICAL ENERGY STORAGE
Annual Report for 1984

May 1985

TWO-WEEK LOAN COPY
This is a Library Circulating Copy
which may be borrowed for two weeks.

APPLIED SCIENCE
DIVISION

Prepared for the U.S. Department of Energy under Contract DE-AC03-76SF00098

LBL-19545 c.2

## DISCLAIMER

This document was prepared as an account of work sponsored by the United States Government. While this document is believed to contain correct information, neither the United States Government nor any agency thereof, nor the Regents of the University of California, nor any of their employees, makes any warranty, express or implied, or assumes any legal responsibility for the accuracy, completeness, or usefulness of any information, apparatus, product, or process disclosed, or represents that its use would not infringe privately owned rights. Reference herein to any specific commercial product, process, or service by its trade name, trademark, manufacturer, or otherwise, does not necessarily constitute or imply its endorsement, recommendation, or favoring by the United States Government or any agency thereof, or the Regents of the University of California. The views and opinions of authors expressed herein do not necessarily state or reflect those of the United States Government or any agency thereof or the Regents of the University of California.

LBL-19545

# ANNUAL REPORT

# FOR 1984

# TECHNOLOGY BASE RESEARCH PROJECT FOR ELECTROCHEMICAL ENERGY STORAGE

Applied Science Division
Lawrence Berkeley Laboratory
University of California
Berkeley, California 94720

Edited by Kim Kinoshita, Technical Manager

May 23, 1985

This work was supported by the Assistant Secretary for Conservation and Renewable Energy, Office of Energy Systems Research, Energy Storage Division of the U.S. Department of Energy, under Contract No. DE-AC03-76SF00098.

TABLE OF CONTENTS


i. EXECUTIVE SUMMARY v

I. INTRODUCTION 1

II. EXPLORATORY RESEARCH 2

A. Ambient-Temperature Lithium Cells 2

1. All Inorganic Ambient-Temperature Rechargeable Lithium Battery 2

2. Sulfolanes as Electrolytic Solvents for Rechargeable Lithium Batteries 5

B. Sodium/Sulfur Systems 6

1. Study of High Energy Cathodes for Molten-Salt Batteries 6

2. Improved Lifetime of the Hollow-Fiber Sodium/Sulfur Cell 7

C. Thermally-Regenerative System 9

1. Research on Materials Relating to the Sodium Heat Engine 9

III. APPLIED SCIENCE RESEARCH 11

A. Alkaline and Metal/Air Cells 11

1. Battery Electrode Studies 11

2. Reaction Profiles and Electrode Shape Change 14

3. A Semiconductor Approach to the Study of Oxide Films 15

4. Structure of Zincate Ions in Concentrated Aqueous Potassium Hydroxide 17

5. Thermodynamic Framework for Estimating Efficiencies of Alkaline Batteries 19

6. Development of Membranes for the Zinc/Ferricyanide Battery 20

7. Zinc/Nickel Oxide Battery Membrane Separator Studies 22

8. Research on Separators for Alkaline Zinc Batteries 23

9. Supported Liquid-Membrane Battery Separators 24

B. Zinc/Halogen Cells 26

1. Surface Morphology of Metals in Electrodeposition 26
2. Dendritic Zinc Deposition in Flow Batteries 27
3. Zinc Electrode Morphology in Acid Electrolytes 29
4. Transport in Aqueous Battery Systems 31

C. Molten Salt Cells 32

1. Molten-Salt Cell Research 32
2. Investigation of the Mechanism for Capacity Decline of the $FeS_2$ Electrode in Lithium/Iron Disulfide Cells 36
3. New Battery Materials 38

D. Components for Alkali/Sulfur Cells 40

1. Electrochemical Properties of Solid Electrolytes 40
2. Improved β"-Alumina Oxide Electrolytes Through Transformation Toughening 43
3. Principles of Superionic Conduction 44
4. Electrical Conduction and Corrosion Processes in Fast Ion-Conducting Glasses 46
5. Evaluation of New Lithium-Conducting Glasses 48
6. Glass Electrolytes and Advanced Cell Concepts 49
7. Transport Properties of Sodium-Polysulfide Melts 51
8. Mathematical Modeling of the Sulfur Electrode 51

E. Corrosion Processes in High-Temperature, High-Sulfur-Activity Molten Salts 52

1. Behavior of Materials in Sulfur-Polysulfide Melts 52
2. Polysulfide Containment Materials 53
3. Corrosion-Resistant Coatings for High-Temperature High-Sulfur-Activity Applications 58

F. Components for Ambient-Temperature Lithium Cells 59

1. Surface Layers on Battery Materials 59
2. Metal Couples in Non-Aqueous Electrolytes 61
3. Polymeric Electrolytes for Ambient-Temperature Lithium Batteries 62
4. Novel Membranes for Lithium Batteries 64

G . Cross-Cutting Research 66

1. Analysis and Simulation of Electrochemical Systems 66
2. Electrode Kinetics and Electrocatalysis 67
3. Analysis of Ambient-Temperature Sulfur Electrodes 70
4. Engineering Analysis of Electrolytic Gas Evolution 71
5. Bibliography of Convective Transport Correlations 73

IV. AIR SYSTEMS RESEARCH 74

A. Secondary Metal/Air Cells 74

1. Electrocatalysts for Oxygen Electrodes 74
2. Corrosion of Non-Metallic Electrode Materials 76
3. Iron/Air Battery Development 77
4. Research and Development of Bifunctional Oxygen Electrodes 78
5. Electrical and Electrochemical Behavior of Particulate Electrodes 80

B. Aluminum/Air Batteries 82

1. Aluminum/Air Battery Research and Development 82

C. Fuel Cell Research 93

1. Fuel Cells for Vehicles 93
2. Advanced Chemistry and Materials for Fuel Cells 105
3. Alternative Electrolytes for Fuel Cells 108

## EXECUTIVE SUMMARY

The U.S. Department of Energy's Office of Energy Systems Research provides continuing support for an Energy Storage Program, which includes R&D on advanced electrochemical energy storage and conversion systems. A major goal of this program is to develop electrochemical power sources suitable for application in electric vehicles and/or electric load-leveling devices. The program centers on advanced secondary batteries and fuel cells that offer the potential for high performance and low life-cycle costs, both of which are necessary to permit significant penetration into commercial markets.

The DOE Electrochemical Energy Storage Program is divided into two projects: the Exploratory Technology Development and Testing (ETD) Project and the Technology Base Research (TBR) Project. ETD Project management responsibility has been assigned to Sandia National Laboratory (SNL), and the Lawrence Berkeley Laboratory (LBL) is responsible for management of the TBR Project. The ETD and TBR Projects include an integrated matrix of research and development efforts designed to advance progress on several candidate electrochemical systems. The role of the TBR Project is to perform supporting research for the advanced battery systems under development by the ETD Project, and to evaluate new systems with potentially superior performance, durability and/or cost characteristics. The specific goal of the TBR Project is to identify the most promising electrochemical technologies and transfer them to industry and/or the ETD Project for further development and scale-up. This report summarizes the research, financial, and management activities relevant to the TBR Project in CY 1984.

General problem areas addressed by the project include identification of new electrochemical couples for advanced batteries, determination of technical feasibility of the new couples, improvements in battery components and materials, establishment of engineering principles applicable to electrochemical energy storage and conversion, and the assessment of fuel-cell technology for transportation applications. Major emphasis is given to applied research which will lead to superior performance and lower life-cycle costs.

The TBR Project is divided into three major project elements: Exploratory Research, Applied Science Research, and Air Systems Research. Highlights of each project element are summarized according to the appropriate battery system or electrochemical research area.

## Exploratory Research

The objectives of this project element are to identify, evaluate and initiate development of new electrochemical couples with the potential to meet or exceed advanced battery and electrochemical performance goals. Research projects were conducted on ambient-temperature lithium cells, novel Na/S systems, and a thermally-regenerative system.

### Ambient-Temperature Lithium Cells

- Duracell, Inc. has identified the $Li/LiAlCl_4$-$SO_2/C$ system for further development of an all-inorganic ambient-temperature rechargeable lithium battery. Small prototype cells (0.4 Ah, 100 Wh/kg) were fabricated and tested. A cycle life of 60-90 cycles at 100% depth-of-discharge (DOD) has been achieved, and cells on partial discharge (60% DOD) achieved a few hundred cycles.

- EIC has found that the stability of lithium in sulfolane-based electrolytes is good during storage at temperatures up to 70°C. However, lithium electrodes show inadequate cycling efficiencies in these electrolytes due to various factors. Further effort on this project has been discontinued because of the problems encountered with electrolyte purification and poor cycling efficiency of the lithium electrode.

### Sodium/Sulfur Systems

- Experiments at the University of Tennessee on Na/β"-alumina/$SCl_3^+$ in $AlCl_3$-NaCl cells indicate a compromise between high specific energy and long cycle life may be required to achieve a viable battery system. "Sulfur-rich" cells showed high specific energy but the performance degraded with cycling.

- Dow Chemical Company has developed a sensitive technique involving anion chromatography that can detect sulfur corrosion of glass electrolytes of as little as $10^{-6}$ cm of the glass surface. Reaction rates and kinetics of sulfur attack on 16 glasses were determined at 300° and 400°C. The standard Dow D406 glass was found to be the most resistant to attack at 300°C, but it was rapidly attacked at 400°C.

## Thermally-Regenerative System

- Experiments are underway at Ford Motor Company to improve the performance and endurance of electrodes for a thermally-regenerative electrochemical system using sodium (sodium heat engine). Encouraging results were obtained with several cermet electrodes which were produced by sintering of porous β"-alumina layers on commercial β"-alumina tubes, followed by impregnation with molybdenum salt or by flame spraying β"-alumina and metal powder.

# Applied Science Research

The objectives of this project element are to provide and establish scientific and engineering principles applicable to batteries and electrochemical systems; and to identify, characterize and improve materials and components for use in batteries and electrochemical systems. Projects in this element provide research that supports a wide range of battery systems -- alkaline metal/air, flow, solid-electrolyte, molten-salt, and non-aqueous. Other projects are directed at research on improving the understanding of electrochemical engineering principles, corrosion of battery components, surface analysis of electrodes, and electrocatalysis.

## Alkaline Cells

- Experiments at LBL are directed at developing practical means of reducing zinc species solubility in strong alkaline electrolytes. The addition of $Ca(OH)_2$ to the zinc electrodes does not appear to enhance its cycle life.

- Lockheed Missiles and Space Co. has concluded from their studies on porous zinc electrodes in alkaline electrolytes that, to prevent shape change to the zinc electrode during cycling, cell designs should be implemented which maintain uniform lateral current distribution. These modifications could include (i) graded porosity in the separator material, (ii) graded ohmic resistance or porosity of the substrate, and (iii) graded porosity of the counter electrode.

- SRI International has examined the effect of various additives ($Li^+$, $Co^{2+}$, $Fe^{2+}$, $F^-$, ZnO, and PbO) on the charge-discharge behavior of Zn and Ni electrodes in alkaline electrolyte. The addition of $F^-$ ions was found to decrease the $O_2$-evolution overpotential on the Ni electrode and decrease the capacity of the Zn electrode, while the addition of PbO may have some beneficial effect.

- Raman spectroscopy studies of zincate species in KOH at Argonne National Laboratory revealed a spectrum indicative of the presence of $Zn^{2+}$ ions and $[Zn(OH)_4{}^{2-}]_n$ complexes, where $n > 1$.

- Ohio State University has completed measurements on the thermodynamic activity of water in the binary $KOH-H_2O$ system at 25°C.

- Sandia National Laboratory has found that sulfonated polysulfones show encouraging performance as separators for zinc/ferricyanide cells. These separators showed no weight-loss after exposure to alkaline-ferricyanide electrolyte at 50°C for one week, and they exhibited a low resistance (1 - 5 ohm-$cm^2$) and a low rate of ferricyanide permeation ($10^{-5}$ mmol/h/$cm^2$). An average efficiency of 75% was achieved with these separators for over 200 cycles in cell tests.

- A number of membranes (polyvinyl alcohol cross-linked with crown ether) have been fabricated by Brigham Young University. They exhibit conductivities ranging from 0.02 to 0.033 mho/cm; these values are approaching the target of 0.01 mho/cm.

- Hybrid separators developed by Pinnacle Research Institute appear to possess ion selectivity that is comparable to that of ion-exchange membranes.

- The development of supported liquid-membrane separators for Zn/NiOOH cells at Castle Technology Corp. was discontinued due to a change in the priorities for the TBR Project.

## Zinc/Halogen Cells

- The morphology of zinc electrodeposited from 1.0 M $ZnCl_2$ ($0.7 < pH < 4.6$) was investigated at LBL by studying the initial stages of deposition. Kinetic measurements using a potential-step method yielded exchange current densities of ~1 $mA/cm^2$. The density of zinc nodules increased with surface potential at a rate from 200 to 1000 nodules/$mm^2$-mV.

- Illinois Institute of Technology has concluded from their modeling studies that the direct effect of convection on tip growth rate during deposition of zinc nodules is quite small, since tip growth is kinetic rather than mass-transfer controlled. However, the predicted growth rates are smaller that the experimental results by one to two orders of magnitude.

- Brookhaven National Laboratory (BNL) has found that the additions of stoichiometric or excess stoichiometric amounts of $AlCl_3$ to $ZnBr_2$ electrolytes has a favorable effect on the deposition zinc at a zinc electrode. It was observed that the electrode kinetics were slowed, a fine-grain deposit was produced, and dendrite growth was inhibited.

- Lawrence Livermore National Laboratory (LLNL) has completed measurements of the mutual diffusion coefficient (25°C) for the $ZnCl_2$-$H_2O$ system over the concentration range 0.004996-7.2489 mol/kg $H_2O$.

## Molten-Salt Cells

- Argonne National Laboratory has completed development of the electrode performance-evaluation system. Evaluation of negative electrodes of the family $Li_xAl_{1-n}Si_n$ indicate that the composition with $n = 0.5$ has higher specific power that Li-Si electrodes and higher specific energy than Li-Al electrodes. Tests of a dense $FeS_2$ electrode in LiCl-KCl at 410°C indicated a factor of two increase in capacity utilization at high current density (100 $mA/cm^2$) and a cell resistivity that is about 50% lower than that of conventional $FeS_2$ electrodes.

- Thermogravimetric analysis by Gould, Inc. indicates that $FeS_2$ electrodes must be operated at 285°C or lower to avoid sulfur evolution. The loss of sulfur from $FeS_2$ alone is about 70 times greater than that from $FeS_2$ in a eutectic LiCl-KCl electrolyte.

- Stanford University has examined numerous lithium-based systems for negative electrodes; these include Li-Al, Li-Sn, Li-Sb, Li-Bi, Li-Zn, Li-Cd and Li-Pb. It has been found that a number of these binary systems exhibit high chemical diffusion coefficients at near ambient temperatures, so that their electrode reactions should be quite rapid.

Components for Alkali/Sulfur Cells

- Experiments at LBL suggest that the asymmetric polarization observed with sodium electrodes can be minimized or eliminated by the addition of a chemical oxygen scavenger, which reacts with $Na_2O$ at an appreciable rate to yield an insoluble oxide and sodium metal.

- Experimental studies at Rockwell International indicate that $ZrO_2$-toughened β"-alumina should contain between 10-15 vol% $ZrO_2$ to obtain the optimum strength and ionic conductivity.

- A family of glasses with compositions analogous to NASIGLAS has been synthesized by the Massachusetts Institute of Technology. The conductivity at 350°C for several of the sodium-based glasses is as high as $10^{-4}$ $ohm^{-1}cm^{-1}$.

- A novel electrochemical method was developed at the Massachusetts Institute of Technology which is capable of simultaneously determining the electrolytic and chemical stabilities of solid electrolytes. This method indicated that the glass composition $Li_2O$-$B_2O_3$, which contained 2 mol% $Al_2O_3$, behaved as a perfect lithium-ion electrolyte over a wide range of lithium activity (up to 0.08 at 380°C) and temperature (320-400°C).

- LBL has developed a successful procedure for making and blowing lithium-chloroborate glass into thin-walled sealed tubes.

- Argonne National Laboratory has completed evaluation of 24 soda-rich glasses in the soda-alumina-zirconia-silica system for use in Na/S cells. Static corrosion tests in sodium, sulfur, and sodium polysulfide at 400°C for 1000 hr indicated that four of the glasses have relatively little weight-loss (0.8 $mg/cm^2$) in all three environments. Further evaluation of these four materials in Na/S cells is underway.

- LBL is developing mathematical models that are useful for understanding the operation of Na/S cells. The mathematical models provide improved understanding of the operation of the sulfur electrode and the transport processes in sodium-polysulfide melts.

Corrosion Processes in High-Temperature, High-Sulfur Activity Molten Salts

- LBL has employed static corrosion and dynamic polarization tests to characterize the behavior of Mo, Cr and 70% Cr-30% Fe in both sulfur-sodium polysulfide and sulfur-lithium polysulfide melts. The dynamic polarization behavior is found to depend strongly on the identity of the cation in the molten-salt mixture, as well as the metal.

- Argonne National Laboratory has examined the corrosion stability of numerous metals and alloys in sulfur and sodium polysulfide at 350°C. Their results indicate that these materials show vastly different corrosion rates in the two sulfur environments. It appears that materials with corrosion stability (e.g., Al, Ni-Cr-Mo-W and Fe-Cr-Mo alloys) in sulfur may not be as stable in sodium polysulfide and vice-versa.

- Illinois Institute of Technology has deposited a nickel interlayer on low-carbon steel by conventional electroplating and electroless nickel plating. Experiments are underway to coat these samples with molybdenum and to test their stability in a high-sulfur-activity

Components for Ambient-Temperature Lithium Cells

- Surface layers formed on lithium in $LiClO_4$ with < 1 ppm $H_2O$ have been analyzed by LBL. From observations using IR spectroscopy, ESCA analysis, and in-situ X-ray diffraction analysis, it was concluded that $Li_2CO_3$ and a polymeric compound are formed.

- UV-visible spectroscopy experiments of iodine and bromine solutions at LBL have demonstrated that the stable form of the halogen in propylene carbonate is the trihalide.

- The University of Pennsylvania has found that $MgCl_2$ complexes of poly(ethylene oxide) (PEO) exhibit a conductivity at 60°C that is comparable to that of the $LiCF_3SO_3$-PEO complex. These new complexes may be a general group of high-conductivity solid electrolytes for rechargeable lithium batteries.

- Efforts at Case Western Reserve University to develop multi-block copolymers for use as membranes in lithium batteries was discontinued due to difficulties encountered in the synthesis of these materials.

Cross-Cutting Research

- Illinois Institute of Technology has completed a draft "Bibliography of Convective Transport Correlations." Suggestions by reviewers have been incorporated in the draft copy, and the final report will be available in 1985.

- LBL has developed models that are useful in the identification of electrochemical parameters. These models will aid in the design and scale-up of electrochemical systems; they are used to (i) calculate the concentration, potential, and current distribution in thin-gap flow cells, (ii) predict important operating characteristics of $LiAl/FeS_2$ cells, and (iii) predict the effect of redistribution of active material on the cycle life of Zn/NiOOH batteries.

- An electrolyte cell was constructed by LBL which allows observation of coalescence phenomena at gas bubbles generated on microelectrodes. Preliminary results indicate that for bubbles smaller than 1 mm in diameter, the coalescence event is completed within $10^{-5}$ s. Earlier observations by researchers which showed that bubbles could touch without immediate coalescence may have resulted from slight axial misalignment in their electrochemical cells.

- Low-energy electron diffraction (LEED) analysis has been used at LBL to obtain fundamental understanding of the processes occurring at electrode surfaces. The LEED analysis was applied to investigate the anodic reconstruction of metal surfaces and the electrodeposition/dissolution of metals.

- Porous electrodes containing transition-metal sulfides (CuS, $MoS_2$ and CoS), carbon black and PTFE were fabricated at LBL. Experiments are underway to determine the kinetic parameters for the sulfide/polysulfide redox couple.

## Air Systems Research

The objectives of this project element are to identify, characterize and improve materials for air electrodes; and to identify, evaluate, and initiate development of metal/air battery systems and fuel-cell technology for transportation applications.

### Metal/Air Battery Research

- Results obtained by pyrolysis gas chromatography-mass spectroscopy at Case Western Reserve University indicate that heat-treatment to 850°C of metal macrocycles supported on carbon produces volatile fragments that do not contain nitrogen. Data obtained by transmission electron microscopy and Mossbauer spectroscopy suggest that the iron and cobalt tetramethoxyphenyl porphyrins, which are adsorbed on carbon, decompose at 800°C to produce the corresponding oxides. It appears that the supported metal oxides have high catalytic activity for oxygen reduction.

- Experiments at LBL indicate that the catalytic effect of metal oxides on carbon corrosion in alkaline electrolytes does not involve a redox mechanism. Extensive testing of graphitized furnace blacks has identified graphitized Sterling R as the only material with a corrosion rate significantly lower than that of acetylene black.

- Energy Research Corporation has found perovskites of the composition $LaNiO_3$ and $La_{0.5}Sr_{0.5}CoO_3$ show promising performance for bifunctional air electrodes.

- Experimental work on potential transients within fluidized-bed electrodes and moving-bed electrodes has been completed at LBL. This study showed that the phenomenon referred to as "bubbling" (development of regions in the electrode that are almost free of particles) occurs with zinc-coated copper particles, but it does not occur with Sorapec particles.

- Development work on the iron/air battery at Westinghouse Electric Corp. has been discontinued due to the limited life and performance of their bifunctional air electrode containing carbon blacks.

Aluminum/Air Battery R & D

- The major thrusts of the Aluminum/Air battery program were on (i) air cathode development, (ii) hydrargillite crystallization and separation, (iii) integrated experiments involving a coupled cell/crystallizer, (iv) cell design, and (v) development of improved aluminum anodes. Major achievements of the program include:

  - Two experiments were preformed at LLNL in which a single cell was coupled to a crystallizer. Although the experiments lasted only 5 hr (at nominally 120 A), a great deal of important systems-design information was obtained.

  - Experiments at Eltech Systems, Electromedia, and Case Western Reserve University has identified RB (de-ashed) and Norit Ultracarbon, both containing 5-10% CoTMPP, as promising air cathodes.

- Two proprietary aluminum anodes developed by Alcan show promise with an open-circuit corrosion rate of 0.12 $mg/cm^2/min$ and an open-circuit potential of 1.84 V.

- Alcan has obtained some significant results on the agglomeration of hydrargillite. Their measurements indicate that particle agglomeration to >40 μm occurs under "low turbulence" conditions in reasonably short times (2 hr).

Fuel Cell Research

o Los Alamos National Laboratory (LANL) has conducted research in several areas of electrochemistry, theoretical studies, fuel-cell testing, fuel processing, and membrane characterization, as well as managed subcontracts on fuel cell R&D. Major achievements of the fuel-cell program include:

  - Theoretical studies of the PtO and $Pt_2$ molecules were conducted at LANL. These studies indicate that a charge transfer of 0.34 electrons takes place from the Pt atom to the O atom; and the Pt-Pt bond length in $Pt_2$ is 2.33 A, which is less than that for bulk Pt.

  - A six-station, $H_3PO_4$ fuel-cell test stand was completed at LANL to investigate the effects of rapid current pulsing, slow load-current ramping, and temperature cycling on electrode performance.

  - Rutherford back scattering and X-ray photoelectron spectroscopy verified that the activity decay observed with electrodes tested for 2000 hr in the six-station test stand was due to Pt redistribution in the cell. Pt from the cathode appears to migrate and deposit on the anode.

  - LANL investigated the mechanism of methanol steam reforming on active catalysts. The oxygen atom in $CO_2$ is provided by water and not methanol, apparently occurring by rapid oxygen exchange on the catalyst surface.

- A 20-kW fuel-cell system was delivered by Energy Research Corporation, and tests of the system have started at LANL. The original system efficiency of 30% decreased to 26%, but overall the system performed reasonably well.

- United Technologies Corporation has observed that heat-treated macrocyclic (iron tetramethoxyphenylporphyrin) supported on carbon exhibits stable performance in half-cell test in $H_3PO_4$ at 140°C. However, the electrocatalyst decays in performance in full-cell tests; the decay mechanism has not been identified.

- An alternative membrane to Nafion that was tested by the General Electric Company showed encouraging performance. Over 1200 hr of operation were accumulated using this membrane in a cell at 180°F, 30 psig $O_2$ and 30 psig $H_2$.

- The University of Virginia was successful in quenching disorder in a 25 at% Cr-75 at% Pt sample. Previous investigators reported that it was not possible to retain disorder in samples of this composition.

o HREELS (High Resolution Electron Energy Loss Spectroscopy) studies at BNL showed that various adsorbed species involving Pt-O and Pt-C bonds are formed when $H_2O$, $O_2$, CO, and $CH_4$ interact with the (111) face of a Pt single crystal.

o Kinetic studies at LBL using the rotating ring-disk electrode technique indicate that the current for oxygen reduction in dilute $Cs_2CO_3$ is higher than that in KOH at the same concentration. Because $Cs_2CO_3$ solutions are a $CO_2$-rejecting electrolyte, the favorable kinetics for oxygen reduction that was observed is encouraging for the development of alkaline fuel cells using alternatives to alkali-hydroxide electrolytes.

## Planned Activities in 1985

New research projects planned include:

1. An RFP will be issued for research on novel concepts for metal/air batteries.

2. New research projects to address corrosion in electrochemical systems will be considered.

## Management Activities

During 1984, LBL managed 36 subcontracts and conducted a vigorous research program in Electrochemical Energy Storage. LBL staff members attended project review meetings, made site visits to subcontractors, and participated in technical management of various TBR projects. LBL staff members participated in the following reviews, meetings, and workshops:

- EPRI Fuel Cell Workshop, Boston, MA, January 10-11, 1984.
- Energy Storage Program Quarterly Review, Washington, DC, February 8-9, 1984.
- Zinc/Ferricyanide Flow Battery Review Meeting, Palo Alto, CA, February 16, 1984.
- Fuel Cell Review Meeting, LANL, Los Alamos, NM, March 20-21, 1984.
- Sodium-Beta"-Alumina Review Meeting, SNL, Albuquerque, NM, March 29, 1984.
- Second International Meeting on Lithium Batteries, Paris, France, April 25-27, 1984.
- EPRI Zinc/Chloride Battery Review Meeting, Palo Alto, CA, May 2-3, 1984.
- Spring Meeting of the Electrochemical Society, Cincinnati, OH, May 6-11, 1984.
- Aluminum/Air Battery Program Review, Chardon, OH, May 11, 1984.

- Workshop on Conducting Polymers, Rochester, MI, June 4-8, 1984.
- 31st Power Sources Symposium, Cherry Hill, NJ, June 11-14, 1984.
- Sixth DOE Electrochemical Contractor's Review, Washington, DC, June 25-29, 1984.
- 35th Meeting of the International Society of Electrochemistry, Berkeley, CA, August 5-10, 1984.
- 23rd Annual Conference of Metallurgists, Quebec City, Canada, August 19-23, 1984.
- 19th Intersociety Energy Conversion Engineering Conference, San Francisco, CA, August 19-14, 1984.
- Zinc/Ferricyanide Quarterly Review, Palo Alto, CA, August 22, 1984.
- 8th Workshop on Phosphoric Acid Fuel Cell Technology, Long Beach, CA, September 5, 1984.
- Review of the Duracell Program on Inorganic Ambient-Temperature Rechargeable Lithium Battery, Burlington, MA, September 13-14, 1984.
- Fall Meeting of the Electrochemical Society, New Orleans, LA, October 7-12, 1984.
- Lithium-Iron Sulfide Battery Workshop, Palo Alto, CA, October 16, 1984.
- Workshop on Research Needs for Corrosion Prevention and Control in Energy Conservation Systems, Seattle, WA, October 29-November 1, 1984.
- Lead Center Coordination Meeting, LBL, Berkeley, CA, November 7, 1984.
- Aluminum/Air Battery Subcontractors Meeting, LLNL, Livermore, CA, November 8, 1984.
- Fuel Cells for Transportation Advisory Committee Meeting, Albuquerque, NM, November 13-14, 1984.
- Review Meeting on BNL Electrochemistry Program, BNL, Upton, NY, November 19-20, 1984.
- Workshop on Sodium/Sulfur Cells, Albuquerque, NM, November 20, 1984.
- Annual Meeting of the American Institute of Chemical Engineers, San Francisco, CA, November 25-30, 1984.

## Milestones for Technology Base Research Project

Milestones accomplished in Fiscal Year 1984 by the TBR project include:

- A decision was made not to pursue engineering development of the iron/air battery at Westinghouse Electric Corp. due to problems with the present state-of-technology. The corrosion stability of the carbon support that is presently used in their bifunctional air electrode is not adequate to achieve a cycle life of 1000 cycles, and improved electrocatalysts with high activity and stability are not available.

- Development of two computer codes, "SIMPLE" and "M32.bas" by LLNL has been completed. These codes are used to analyze crystallization parameters in the crystallizer of the aluminum/air cell. The computer code has been expanded to take into account the effect of particle size distribution on the crystallizer-cell interaction.

- Fuel-cell endurance tests of macrocyclic electrocatalysts at United Technologies Corporation was recommended based on the promising results obtained in short-term tests. Iron tetramethoxyphenyl porphyrin, which was heat-treated at 850°C, exhibited an intrinsic activity higher than that of Pt on a metal-weight basis to a specific current of 300 mA/mg.

- Rockwell International has found that the addition of tetragonal-$ZrO_2$ (up to 25 vol%) to β"-alumina increased its fracture toughness by up to 66%, and its strength by a factor of two or three. Based on these results and data obtained at LBL on this transformation-toughened β"-alumina, it was recommended that the project at Rockwell International be continued.

- A review of the Duracell, Incorporated program on the development of an all-inorganic rechargeable lithium battery was held to assess their technology. The results of their research are sufficiently encouraging that it was recommended that this battery system continue to receive DOE support.

- Hamilton Standard Electrochemical (formerly a part of the General Electric Company) is investigating proton-exchange membrane/ electrocatalyst assemblies (M&E) with the goal of reducing the cost of the membrane and electrocatalyst, while still maintaining the performance levels presently achieved with Nafion and high loadings of Pt electrocatalyst (4 $mg/cm^2$). The results to date are encouraging, and they indicate that low-cost M&Es are attainable. Based on these developments, it is recommended that the development of low-cost membrane/electrocatalyst assemblies continue.

## Acknowledgement

This work was supported by the Assistant Secretary for Conservation and Renewable Energy, Office of Energy Systems Research, Energy Storage Division of the U.S. Department of Energy under Contract No. DE-AC03-76SF00098. The fuel cell effort at LANL was partially supported by the U.S. Department of Energy, Office of Vehicle and Engine Research and Development. The support from the Department of Energy and the contributions to this project by the participants in the Technology Base Research Project are gratefully acknowledged.

Subcontractor Financial Data - CY 1984

| Subcontractor | Principal Investigator | Project | Contract Value (K$) | Duration (months) | Expiration Date |
|---|---|---|---|---|---|
| EXPLORATORY RESEARCH | | | | | |
| Ambient Temperature Lithium Cells | | | | | |
| Duracell International, Inc. | A. Dey | $Li/SO_2$ | 1500 | 39 | 12-84 |
| EIC Laboratories, Inc. | J. Foos | $Li/Sulfolane/TiS_2$ | 116 | 12 | 4-84 |
| Sodium/Sulfur Cells | | | | | |
| University of Tennessee | G. Mamantov | $Na/SCl_4(NaCl-AlCl_3)$ | 19 | 12 | 3-85 |
| Dow Chemical Company | P. Pierini | Sodium/Sulfur | 290 | 12 | 8-85 |
| Thermally-Regenerative System | | | | | |
| Ford Motor Company | T. K. Hunt | Sodium Heat Engine | 240 | 12 | 2-85 |
| APPLIED SCIENCE RESEARCH | | | | | |
| Lawrence Berkeley Laboratory | E. Cairns, L. DeJonghe, J. Evans, R. Muller, J. Newman, P. Ross, and C. Tobias | Electrochem. Energy Storage | 1500 | 12 | 9-84 |
| Alkaline and Metal/Air Cells | | | | | |
| Lockheed Missiles and Space Co. | T. Katan | Reaction Profiles | 80 | 16 | 12-84 |
| SRI International | M. Madou | Semiconductor Electrode | 84 | 12 | 3-85 |
| Argonne National Laboratory | V. Maroni | Spectroscopic Studies | 25 | 12 | 9-85 |
| Ohio State University | D. Macdonald | Cell Thermodynamics | 57 | 12 | 6-84 |
| Brigham Young Univ. | D. Bennion | Zn/NiOOH Separators | 91 | 12 | 7-84 |
| Pinnacle Research | R. Yeo | Zn/NiOOH Separators | 115 | 12 | 7-84 |
| Castle Technology, Inc. | J. P. Pemsler | Liquid Membranes | 77 | 12 | 4-84 |
| Zinc/Halogen Cells | | | | | |
| Illinois Institute of Technology | J. R. Selman | Zn Deposition | 81 | 12 | 3-85 |
| Brookhaven National Laboratory | J. McBreen | Zn Morphology | 100 | 12 | 9-84 |
| Lawrence Livermore Nat'l Laboratory | D. Miller | Transport Properties | 65 | 12 | 9-84 |
| Molten Salt | | | | | |
| Argonne National Laboratory | J. Battles | Molten Salt Cells | 400 | 12 | 9-84 |
| Gould, Incorporated | H. F. Gibbard | $Li/FeS_2$ | 236 | 16 | 10-85 |
| Stanford University | R. Huggins | New Battery Materials | 395 | 12 | 10-84 |

Subcontractor Financial Data - CY 1984

| Subcontractor | Principal Investigator | Project | Contract Value (K$) | Duration (months) | Expiration Date |
|---|---|---|---|---|---|
| Components for Alkali/Sulfur Cells | | | | | |
| Rockwell International, Inc. | F. Lange | Improved $\beta''Al_2O_3$ | 154 | 12 | 6-84 |
| Massachusetts Institute of Technology | B. Wuensch | Superionic Conductors | 98 | 12 | 5-85 |
| Massachusetts Institute of Technology | H. Tuller | Li Conducting Glasses | 115 | 12 | 3-85 |
| Argonne National Laboratory | M. Roche | Glass Electrolytes | 300 | 12 | 9-84 |
| Corrosion Processes in High-Temperature, High-Sulfur Activity Molten Salt | | | | | |
| Argonne National Laboratory | J. Battles | Polysulfide Containment | 300 | 12 | 9-84 |
| Illinois Institute of Technology | R. Selman | Corrosion Resistant Coatings | 193 | 12 | 8-85 |
| Components for Ambient-Temperature Lithium Cells | | | | | |
| University of Pennsylvania | G. Farrington | Polymeric Electrolytes | 108 | 12 | 2-85 |
| Case Western Reserve University | M. Litt | Novel Membranes | 161 | 17 | 7-84 |
| Cross-Cutting Research | | | | | |
| Illinois Institute of Technology | J. R. Selman | Transport Correlations | 43 | 40 | 6-84 |
| AIR SYSTEMS RESEARCH | | | | | |
| Metal/Air Battery Research | | | | | |
| Case Western Reserve University | E. Yeager | Air Electrodes | 292 | 12 | 2-85 |
| Energy Research Corporation | M. Klein | Bifunctional $O_2$ Electrode | 232 | 12 | 5-85 |
| Westinghouse Corporation | E. Buzzelli | Fe/Air Battery Development | 119 | 7 | 9-84 |
| Aluminum/Air Battery R&D | | | | | |
| Lawrence Livermore Nat'l Laboratory | A. Maimoni | Al/Air Battery R&D | 608 | 12 | 9-84 |
| Eltech Systems Corporation | L. Gestaut | Al/Air Battery | 892 | 24 | 1-86 |
| Fuel Cell R&D | | | | | |
| Los Alamos National Laboratory | J. Huff | Fuel Cell R&D | 1015 | 12 | 9-84 |
| Brookhaven National Laboratory | J. McBreen | Fuel Cell Research | 308 | 12 | 9-84 |
| United Technologies Corporation | J.A. Bett | Alloy Catalysts | 627 | 24 | 4-85 |
| Hamilton Standard (formerly G.E.) | J.F. McElroy | Solid Polymer Electrolyte | 997 | 23 | 12-84 |
| University of Virginia | G. Stoner | Alloy Electrocatalyst | 40 | 15 | 11-84 |

# I. INTRODUCTION

This report summarizes the progress made by the Technology Base Research (TBR) Project for Electrochemical Energy Storage during calendar year 1984. The primary objective of the TBR Project, which is sponsored by the Department of Energy (DOE) and managed by Lawrence Berkeley Laboratory (LBL), is to identify electrochemical technologies that can satisfy stringent performance and economic requirements for electric vehicles and stationary energy storage applications. The ultimate goal is to transfer the most promising electrochemical technologies to the private sector or to another DOE project (e.g., Sandia National Laboratories' Exploratory Technology Development and Testing Project) for further development and scale-up.

Besides LBL, which has overall responsibility for the TBR project, technical management of several projects is shared with Lawrence Livermore National Laboratory (LLNL) and Los Alamos National Laboratory (LANL). Brookhaven National Laboratory (BNL) and Argonne National Laboratory (ANL) participate in the TBR project by providing key research support in several of the project elements.

The TBR project consists of three major project elements:

- Exploratory Research
- Applied Science Research
- Air Systems Research

The objectives and the specific battery and electrochemical systems addressed by each project element are discussed in the following sections, which also include technical summaries that relate to the individual projects. Financial information that relates to the various projects and a description of the management activities for the TBR Project are described in the Executive Summary.

## II. EXPLORATORY RESEARCH

The major thrust of this project element is to evaluate promising electrochemical couples for advanced batteries for electric vehicles. The advanced battery systems that were investigated are ambient-temperature rechargeable lithium cells, new sodium/sulfur battery systems, and a thermally-regenerative electrochemical system using sodium.

### A. AMBIENT-TEMPERATURE LITHIUM CELLS

#### All Inorganic Ambient-Temperature Rechargeable Lithium Battery

(A.N. Dey, Duracell, Inc.)

The objective of this program is to develop an ambient-temperature rechargeable Li battery which can deliver 500-800 cycles at 80% depth of discharge (DOD), with a specific energy of about 150 Wh/kg. The short-term goal is to achieve a cycle life of about 200-300 cycles at 80-100% DOD.

Previous research efforts at Duracell Inc. led to the discovery of several new $SO_2$ electrolytes with inorganic salts such as $LiAlCl_4$ and $LiGaCl_4$ and positive electrode materials including $CuCl_2$ and others. Among the new electrolytes, $LiAlCl_4/SO_2$ demonstrated the best performance with conductivity of about $1 \times 10^{-1}$ $ohm^{-1}cm^{-1}$ at ambient temperature and good cycling efficiency for lithium electrode. Cycling efficiencies of 92-99% have been achieved at current densities of 1-5 $mA/cm^2$.

The $Li/CuCl_2$ system with $LiAlCl_4/SO_2$ electrolyte has an OCV of 3.43 V and a theoretical specific energy of about 1100 Wh/kg. Although experimental prismatic cells have demonstrated 200-300 cycles at 50% DOD, the prototype cells with wound electrode design have shown considerably poorer cycle life. Deep discharge of the $CuCl_2$ electrode to less than 2.6 V causes some irreversible damage and substantially reduces its cycle life. Tests of cells at 55°C also showed significant decrease in cycle life.

Since $CuCl_2$ positive material cannot be discharged to below 2.6 V, and it is more difficult to process for good storage life and reproducible performance, studies in 1984 have been focused on the development of an alternative carbon cathode. Effort was directed at studies of the $Li/LiAlCl_4$-$SO_2/C$ system which has an OCV of 3.29 V and a theoretical specific energy density of about 520 Wh/kg. Previous experimental cells have shown good rate capability and long cycle life on deep discharge. Some cells have demonstrated over 150 cycles at 100% DOD without significant loss of cell capacity.

Small hermetically-sealed Li/C prototype cells with wound electrode design were developed. The cell has an overall dimension of 0.627-inch O.D. and 1.22-inch height. It can deliver about 0.4 Ah at a 50-100 mA rate at 3.0 V. However, the cells showed poorer cycle life compared to the experimental prismatic cells. The prototype cell has specific energy of about 100 Wh/kg; it is believed that the specific energy can be further improved when the system is scaled up to larger sizes.

The structure of the prototype cell was improved to provide a cycle life of about 60-90 cycles at 100% DOD. A gradual loss of capacity of about 1% per cycle was observed for cells on deep discharge. The development of internal shorts after 50-60 cycles on deep discharge is the most common failure mode for these cells. However, cells on partial discharge (60%) can deliver a few hundred cycles. Diagnostic studies of cells that underwent deep discharge showed that the capacity fading of the wound cells is probably caused by poor mechanical structure of the positive electrode and the starvation of the electrolyte on deep discharge.

Studies on cell chemistry of the $Li/LiAlCl_4$-$SO_2/C$ system were carried out. The results indicated that $LiAlCl_4$ and $SO_2$ are involved in the cell reactions to form a complex with the C electrode during discharge and charge. The composition of $LiAlCl_4/SO_2$ electrolyte was optimized to achieve the best low-temperature performance (-20°C), high-temperature (70°C) storage and cycle life of the lithium electrode.

Various separator materials were evaluated to alleviate the problem of internal shorts; polypropylene microporous separator (Celgard) was previously employed in the cells. The separator degraded gradually on cycling, especially with cells under extensive overcharge. High-density polyethylene (HDPE) separator was found to be superior to the polypropylene separator due to its improved chemical stability. Cells made with HDPE separators were less prone to develop internal shorts. However, degradation of the HDPE separators was still observed after numerous cycles or prolonged overcharge.

Capability of sustaining limited overcharge is one of the advantages of the inorganic $Li/LiAlCl_4$-$SO_2/C$ system. Experiments were carried out to investigate the overcharge characteristics and the chemistry of overcharge. The amount of overcharge the cell can sustain depends on the chemical stability and the physical structure of the separator. On overcharge, $Cl_2$ and $AlCl_3$ are generated at the positive electrode and excess lithium is deposited at the negative electrode. Both $Cl_2$ and $AlCl_3$ were found to be highly soluble in the electrolyte. The dissolved $Cl_2$ and $AlCl_3$ diffuse through the separator, and they recombine with the deposited lithium to reform the electrolyte according to the following reactions:

$$1/2Cl_2 + Li \rightarrow LiCl$$

$$LiCl + AlCl_3 \rightarrow LiAlCl_4$$

Cells with separators having better chemical stability and porosity can sustain the significant rates of overcharge necessary to accomplish cell balancing.

Prototype Li/C cells with $LiGaCl_4/SO_2$ electrolyte or mixed electrolytes of $LiGaCl_4/SO_2$ were also studied to investigate the possibility of improving their specific energy. Cells operating with $LiGaCl_4/SO_2$ electrolyte can deliver 50% more capacity (0.6 Ah vs 0.4 Ah) at low rates of discharge than cells with $LiAlCl_4/SO_2$ electrolyte. However, the capacity decreases rapidly with increasing rate of discharge. Cells operating with electrolytes containing $LiGaCl_4$ were also more prone to developing internal shorts. Most cells failed within 20-30 cycles.

It is planned to evaluate new binder materials in an effort to improve the cathode structure so that the capacity fade on cycling can be alleviated. In addition, it is planned to evaluate new separator materials in order to prevent premature cell shorting.

Sulfolanes as Electrolytic Solvents for Rechargeable Lithium Batteries
(J.S. Foos and S.B. Brummer, EIC Laboratories, Inc.)

The purpose of this research was to investigate the use of sulfolane-based electrolytes in secondary lithium batteries. Sulfolane has been shown to give moderately conductive solutions, and to be exceptionally stable to Li. At 70°C, similar cycling efficiencies for lithium electrodes were observed in electrolyte solutions containing a variety of salts, indicating that the stability of Li in sulfolane results primarily from sulfolane-derived films.

Half-cell testing was used throughout most of the investigation. Unfortunately such tests are not expected to be fully predictive of full-cell behavior. Thus, the most promising electrolyte, sulfolane/$LiClO_4$, was evaluated in 0.68 Ah Li/$TiS_2$ cells. Cells of this type had previously been used to evaluate ether-based electrolytes and were modified by using sulfolane-wettable separators. The cells were cycled at 70°C for 15 cycles at 30% depth-of-discharge before polarizing to the voltage limits. This reflects poor cycling behavior for both the Li and $TiS_2$ electrodes. Thus, failure of these cells must be attributed, at least in part, to factors other than poor Li cycling efficiency.

Much of the effort has been concentrated on the purification of sulfolane and its electrolyte solutions in hopes of maximizing the stability of these materials towards Li. An alternative approach is to use additives or reactive co-solvents to form protective films on Li. A co-solvent of particular interest is sulfur dioxide. At low concentrations in sulfolane, sulfur dioxide produces a cathodically-formed protective film on Pt, which can be removed anodically. Concentrated solutions of 5-7 M can be formed in sulfolane at ambient temperature and pressure. These solutions are relatively conductive and show good stability on

storage with Li at 70°C. The conductivity of a LiBr solution is surprisingly high, presumably due to the formation of bromosulfinate anions. Half-cell cycling of Li in sulfur dioxide-sulfolane electrolytes were generally unsuccessful, possibly due in part to problems with the separator. In a flooded half cell, a Li cycling efficiency of ~70% was observed over 17 cycles.

Further effort on this project has been discontinued because of the problems encountered with electrolyte purification and poor cycling efficiency of the lithium electrode.

Publications


1. J. S. Foos and L. M. Rembetsy, "Lithium Cycling in Sulfolane-Based Electrolytes", in Proceedings of the Symposium on Lithium Batteries, Edited by A. N. Dey, Volume 84-1, The Electrochemical Society, Inc., Pennington, NJ (1984).

2. J.S. Foos, L.M. Rembetsy and S.B. Brummer, "Research To Explore The Feasibility of Sulfolanes As Electrolytic Solvents for Rechargeable Lithium Batteries," LBL-18414, September 1984.


## B. SODIUM/SULFUR SYSTEMS

### Study of High Energy Cathodes for Molten-Salt Batteries

(G. Mamantov, University of Tennessee)

The objective of this program was to investigate the electrochemical and chemical processes taking place in the Na/β"-alumina/$SCl_3^+$ in $AlCl_3$-NaCl cell, which operates at 180-250°C. This cell exhibits two major discharge steps corresponding to the following reactions:

$$SCl_3AlCl_4 + 3\ AlCl_3 + 4\ Na \rightarrow S + 4\ NaAlCl_4$$

Open-circuit voltage = 4.35V

Theoretical specific energy = 552 Wh/kg

and

$$S + NaAlCl_4 + 2\ Na \rightarrow NaAlSCl_2 + 2\ NaCl$$

Open circuit voltage = 2.75 V

Theoretical specific energy = 174 Wh/kg

The theoretical specific energy for the overall reaction is 726 Wh/kg, which is based on the mass of the reactants for the overall reaction (0.8455 kg), but excludes the weight of $\beta''$-$Al_2O_3$.

Since 1978 more than 45 laboratory cells have been investigated. For four of the eleven cells studied in the latter part of 1983 and 1984, more than 150 deep charge-discharge cycles were achieved. Both reticulated-vitreous-carbon and tungsten cathode current collectors were used in these cells. Although a high specific energy has been achieved with some of the "sulfur-rich" cells, the performance of such cells decreases with the number of cycles indicating that a compromise between high specific energy and long cycle life will probably have to be reached. Electrochemical studies of sulfur in the room-temperature melt aluminum chloride-N-(n-butyl) pyridinium chloride indicate the lack of stability of S(IV) in this melt.

Publications


1. E. J. Cairns, G. Mamantov, R. P. Tischer, and D. R. Vissers, "The Chemistry and Status of Rechargeable Molten Salt Batteries," in Proceedings of the Fourth International Symposium on Molten Salts, The Electrochemical Society, Inc., Pennington, NJ (1984) p. 284.

2. G. Mamantov and J. Hvistendahl, "Rechargeable High Voltage Low Temperature Molten Salt Cell Na/$\beta''$-Alumina/$SCl_3^+$ in $AlCl_3$-NaCl," J. Electroanal. Chem. 168, 451 (1984).


## Improved Lifetime of the Hollow-Fiber Sodium/Sulfur Cell

(P.E. Pierini, Dow Chemical Company)

The objective of this project is to improve the lifetime and reliability of hollow-fiber electrolytes for Na/S cells. The project consists of two parts. In the first part, the thermodynamic stability of the glass electrolytes to sulfur disproportionation reactions was calculated, assuming the following reactions.

$$Na_2O \text{ (in glass)} + S \rightarrow Na_2SO_4 + Na_2S_x$$

$$Na_2O \text{ (in glass)} + S \rightarrow Na_2SO_3 + Na_2S_x$$

In the second part, the corrosion rates of the glass electrolytes were determined and the results compared with the calculated stabilities.

Thermodynamic Stability: Calculations were first made for the free energy of reactions of sulfur with $Na_2O$ to yield sodium polysulfide and sodium sulfate. These values were compared to literature values. Attempts were then made to calculate the activities of $Na_2O$ in the various glasses. Literature data from high-temperature melts of some sodium borates and sodium silicates were used. They were corrected for temperature and composition changes to make them applicable to the glasses at 300°C.

The variation in the literature data, as well as the variability introduced by estimations of glass/crystal transitions and borate/silicate mixing, made the limits of error in the final calculations of glass stability too wide for useful application.

Experimental Corrosion Rates: By use of a very sensitive technique involving anion chromatography, a method was developed that can determine attack by sulfur on the glass which results in corrosion of as little as 100 Å of the glass surface. Reaction rates and kinetics of sulfur attack on 16 different glasses were determined at 300°C and 400°C. At the 300°C operating temperature of the Dow Na/S cell, the standard Dow D406 glass in the LBO series is the most resistant to attack by sulfur. At 400°C, it is attacked more rapidly.

The glass corrosion rate is observed to increase with increasing soda content for most of the glasses. An interesting point observation is the apparent arrest of glass corrosion for the LBA series of glasses at 300°C for time periods up to 65 days. This contrasts to continued corrosion detected on LBA glasses at 400°C.

For a fixed surface area of glass, corrosion rates at 400°C tend to increase as the mass of sulfur is decreased. Thus, larger reactivities are observed at greater ratios of glass surface area/volume of sulfur (S/V). This type of behavior is common in corrosion tests where the products of corrosion influence the corrosion rate. However, at 300°C, corrosion rates appear to be essentially independent of S/V ratios within experimental error.

## C. THERMALLY-REGENERATIVE SYSTEM

### Research on Materials Relating to the Sodium Heat Engine

(T.K. Hunt, Ford Motor Company)

The Sodium Heat Engine (SHE) is a new type of energy conversion device capable of the direct conversion of heat into electrical energy using a thermal source delivering heat at 700-1000°C. The objective of this research is to investigate the stability of SHE electrodes and the mechanism by which they can operate at extremely low interfacial polarizations. In addition, research is directed at improving the high-performance endurance of SHE electrode systems.

Sputtered-molybdenum SHE electrodes exhibit ideal initial performance, which is observed to degrade by a factor of 2 or 3 in a few hundred hours at operating temperatures in the range above 800°C. To tie the degradation phenomenon to changes in the electrode, liquid electrodes (expected to have unchanged morphology) were investigated. Pure Sn and Sn-Zr alloy electrodes exhibit no change in output for periods up to 400 hours at 800°C, well beyond the endurance shown by refractory metal alloys.

Experiments on the sodium-molybdenum-oxygen system and x-ray measurements of the species present at the electrode-electrolyte interface have led to the conclusion that the near ideal performance of molybdenum electrodes is obtained because molten sodium/molybdenum compounds at the interfaces and within the electrode provide a means for rapid ion transport. Investigation of SHE electrodes using current-interrupt methods shows a loss of neutral sodium permeability with time. This loss appears to be responsible for the increase in concentration polarization leading to degradation. Studies of the molybdenum-sodium-oxygen-beta"-alumina system have given the conditions for formation of various sodium/molybdenum compounds, a number of which are expected to be molten at normal SHE operating temperatures. Loss of electrode performance can occur when these compounds are lost to the electrode-electrolyte system via decomposition or evaporation. This scenario is also consistent with

observations of electrode rejuvenation upon exposure to oxygen and with the short-term increase in the output of current-loaded electrodes. In the latter case, it is probable that the sodium content (charge carrier density) of the mixed conductor material increases in response to the higher sodium activity at the electrode-electrolyte interface under current loading.

Sputtered TiN electrodes, providing a strictly solid-solid interface, have been tested and have delivered performance approaching 1/2 the ideal value. These electrodes also suffer performance degradation at high temperatures which may be associated with changes in the electrode film morphology, as observed by SEM.

Several cermet electrode systems were investigated with emphasis on use of beta"-alumina/metal composites. These cermets were produced by sintering of porous beta"-alumina layers on commercial beta"-alumina tubes, followed by impregnation with molybdenum from solution or by codeposition of beta"-alumina and metal powders using a 'flame-spray' technique. The latter approach has produced mixed conducting layers which retain the beta"-alumina structure and adhere well to the beta"-alumina tubes. Peak power outputs above 0.5 $W/cm^2$ have been observed in each of these systems, and some tests have shown excellent endurance at power levels as high as 0.55 $W/cm^2$.

Presentations

1. T.K. Hunt and N. Weber, "Sodium Heat Engine Performance," 35th Meeting of the International Society of Electrochemistry, Berkeley, CA, August 5-10, 1984.

2 N. Weber and T.K. Hunt, "High Temperature Stability of Beta"-Alumina," 35th Meeting of the International Society of Electrochemistry, Berkeley, CA, August 5-10, 1984.

## III. APPLIED SCIENCE RESEARCH

The objectives of this project element are to provide and establish scientific and engineering principles applicable to batteries and electrochemical systems; and to identify, characterize and improve materials and components for use in batteries and electrochemical systems. Projects in this element provide research that supports a wide range of battery systems -- alkaline, flow, molten salt, non-aqueous, and solid-electrolyte. Other projects are directed at research on improving the understanding of electrochemical engineering principles, corrosion of battery components, surface analysis of electrodes, and electrocatalysis.

### A. ALKALINE AND METAL/AIR CELLS

#### Battery Electrode Studies

(E.J. Cairns and F.R. McLarnon, Lawrence Berkeley Laboratory)

The purpose of this research is to study the behavior of electrodes used in secondary batteries and to investigate practical means for improving their performance and lifetime. The approach used in this investigation is to study life-and performance-limiting phenomena of the rechargeable-alkaline zinc electrode under realistic cell operating conditions. Rechargeable batteries of current interest that use zinc electrodes include Zn/air, Zn/NiOOH, Zn/AgO, $Zn/Cl_2$, $Zn/Br_2$, and $Zn/Fe(CN)_6^{-3}$.

Knowledge of the concentrations and concentration gradients inside a cycling zinc electrode would help evaluate proposed theories of zinc active material redistribution and identify means by which the rate of capacity loss can be reduced. In order to provide continuous, in-situ measurements of electrolyte species concentrations, a system of "micro-reference electrodes" is being developed for use in model Zn/NiOOH cells. A special cell for measuring the rest potentials of zinc and cadmium "micro-reference electrodes" was built, and equations were developed to calculate KOH and $K_2Zn(OH)_4$ activity coefficients from the rest potentials. Computer programs were then developed for fitting

single and binary electrolyte data with Pitzer's equations (1,2). Pitzer's equations were then used to correlate KOH activity coefficients up to 15 molal. Experimental data were not available for $KOH-K_2Zn(OH)_4$ electrolytes. An algorithm for calculating concentrations inside a cycling porous zinc electrode from the micro-electrode potentials, using an activity-coefficient correlation and a model for the liquid-junction potential, was developed.

The addition of calcium hydroxide to the zinc electrode was investigated as a practical means of reducing zinc species solubility in strong alkaline electrolytes. The reduced zinc solubility is expected to slow the rate of active material redistribution in the zinc electrode, thereby increasing its cycle life. Identical pairs of electrodes, containing 0%, 40%, 25%, and 10% $Ca(OH)_2$ by weight, were fabricated and cycled. The Zn electrode containing no $Ca(OH)_2$ was cycled to 100% depth-of-discharge 150 times, and the cell retained over 90% of its original capacity. An X-ray of the electrode showed significant movement of Zn away from the center of the electrode toward the tab side. The 40%-$Ca(OH)_2$ cells shorted within the first few cycles. Analysis indicated that these cells shorted because they could not accept the same charge current density as the $Ca(OH)_2$-free cell. The charge current density for the 25%-$Ca(OH)_2$ cells was adjusted to a value 25% lower than that typically used for $Ca(OH)_2$-free cells, and after 100 cycles these cells showed some Zn migration to the edges of the electrode, but their capacity remained at 100% of the original value. The 10%-$Ca(OH)_2$ cells were operated for 70 cycles at which point the cells exhibited 60% of their design capacity. Problems with the nickel-oxide electrodes limited the cell capacity to less than 85% of the design value throughout its life. The 25%-$Ca(OH)_2$ cells also showed problems, albeit to a lesser extent, traced to the NiOOH electrodes. The 10%-$Ca(OH)_2$ cells were able to accept the same charge current density as the $Ca(OH)_2$-free cells, but X-ray analysis of the Zn electrodes after 70 cycles indicated significant Zn redistribution.

The current collector of the zinc electrode in a Zn/NiOOH cell was modeled as a network of resistors, and the potential and current associated with each node was obtained using a Kirchhoff's Current Law analysis. The current flowing across the electrolyte was plotted as a function of position on the current collector. Future experimental work is planned to correlate the calculated current distribution with experimental results to determine the effect of current distribution on cycle life and zinc deposit quality. Design considerations included: placement of tabs, conductivity of the collector as a function of changes in mesh dimensions, and the possibility of enhanced collector function by addition of dispersed conductive material to give a larger area for collection of current.

Factors limiting the cycle life of the zinc electrode are redistribution of active material over the face of the electrode (3,4) and passivation (5) (formation of oxide layers over the surface of the electrode). A one-dimensional, time-dependent model is being developed to predict the cause and extent of Zn redistribution and passivation as the electrode is cycled. This model will take into account changes in current density, overpotential and species concentration. The equations for the model are being derived, and are nearly complete. An exhaustive literature search is being carried out to identify the parameters that must be measured experimentally. Experiments are being set up to measure the electronic conductivity of the zinc electrode at various states of charge, and to determine if the electrolyte becomes supersaturated with zinc species during discharge. Both of these are important in determining the type of model used. Also, the properties of the separator must be measured. These, plus completion of the model are the immediate goals.

References

1. K.S. Pitzer and G. Moyorga, J. Phys. Chem. 77, 2300 (1973).

2. K.S. Pitzer and J.J. Kim, J. Amer. Chem. Soc. 96, 5701 (1974).

3. J. McBreen, "Zinc Electrode Shape Change in Secondary Cells," J. Electrochem. Soc. 119, 1620 (1972).

4. K.W. Choi, D.N. Bennion and J. Newman, J. Electrochem. Soc. 123, 1616 (1976); ibid., 123, 1628 (1976).

5. W.C. Sunu, and D.N. Bennion, J. Electrochem. Soc. 127, 2007 (1980); ibid. 127, 2017 (1980).

Publications

1. J.T. Nichols, F.R. McLarnon and E.J. Cairns, "Zinc Electrode Cycle-Life Performance in Alkaline Electrolytes Having Reduced Zinc Species Solubility", accepted for publication in Chem. Eng. Comm. (1985). LBL-18793.

2. T.C. Adler, F.R. McLarnon and E.J. Cairns, "Studies of the Zinc Electrode: Effects of Charging Regime and Electrolyte Composition", 35th Meeting of the International Society of Electrochemistry, Berkeley, CA (1984), Paper No. A6-4.

3. R.I. Goldberg, F.R. McLarnon and E.J. Cairns, "Novel Current Collectors for the Zinc Electrode in Zn/NiOOH Cells - Interim Report", LBID-984 (1984).

## Reaction Profiles and Electrode Shape Change

(T. Katan, Lockheed Missiles and Space Company, Inc.)

An experimental program was conducted to determine the concentration profiles that are developed during cycling of porous alkaline zinc electrodes and the effect of pore size on these profiles. Shape changes that occur in model pore electrodes were investigated. Various analog electrochemical cells were operated to isolate and evaluate the individual processes that cause zinc migration during cycling.

Experimental evidence indicates that both edge effects and osmosis are responsible for shape change. Edge effects can penetrate up to 1.5 mm into the electrode at a frontal current density of 200 $mA/cm^2$, with the edge of the electrode being 20 mV more negative during discharge, and generating a corrosion current of about 0.4 $mA/cm^2$. Also during discharge, the increase in zincate-ion concentration at the zinc electrode can cause osmotic flow through a cellophane separator towards the zinc at rates higher than $1.5 \times 10^{-4}$ $cm^3/cm^2$-s. Both of these processes are sufficient in themselves to cause shape change during cycling at moderate current densities, 20 to 100 $mA/cm^2$. Electroosmosis was found to be at least one order of magnitude less than osmosis, and it is considered negligible.

In general, to prevent shape change it is recommended that cell designs be implemented that maintain uniform lateral current distribution, e.g., by using (a) graded porosity in separator material, (b) graded ohmic resistance or porosity of substrate, and (c) graded porosity of counter electrode, such that less current is drawn from the edges. Additionally, semi-permeable membranes that generate osmotic flow should be avoided.

The shape-change phenomenon was essentially stopped with planar electrodes by roughening the edges of the zinc electrode substrate to decrease the local current density at the edges. Also effective was the use of a counter electrode which was a few millimeters smaller than the zinc negative. In tests of over 1000 cycles, only a polypropylene screen separator was used with a silver-oxide counter electrode.

Penetration depths of the reaction profile were found to be essentially constant, indicating that a typical zinc electrode should be no more than 0.02-cm thick. The reaction profiles at various current densities showed very little polarization, less than 60 mV, until current densities in excess of 500 $mA/cm^2$ were applied and the IR drop within the electrode became comparable to the overall polarization. Penetration depths at the edges, measured laterally to the overall current, became greater with increasing current density once a critical current density was exceeded.

## A Semiconductor Approach to the Study of Oxide Films

(M.J. Madou, SRI International)

Impedance measurements and photoeffect studies on nickel and zinc electrodes were performed in alkaline media to study the properties of semiconductive oxide films on these electrodes. In addition, the effect of additives on these electrodes in alkaline electrolyte was investigated.

The Mott-Schottky plot for a Ni electrode in an alkaline electrolyte with a Li additive was obtained from the impedance studies. It was found that the slope of the Mott-Schottky plot (which is inversely proportional to the acceptor concentration in the oxide) was not influenced

by the presence of Li. This indicates that Li, in this case, does not act as an acceptor. Based on some theories, Li increases the p-type conductivity of NiO and improves its electrode performance. We found the influence of Li on the Ni electrode to be different, and its effect is discussed below.

An anodic photoeffect (onset at wavelengths corresponding to 3 eV) was found on a Zn electrode in an alkaline medium which indicates the n-type character of the oxide on this electrode in the passive region. In a photocurrent-time plot, obtained while chopping the light irradiating the electrode, one can clearly distinguish two separate features in the light-on cycle, most likely indicating two modifications of zinc oxide.

Impedance measurements on Zn in alkaline media with and without fluoride ions revealed two well-resolved semicircles in a typical Nyquist plot. The high-frequency one represents an ideal RC-parallel equivalent circuit, and the second one indicates a diffusional process. The impedance of the electrode in $F^-$-containing solution is higher, indicating the presence of a more-insulating film.

Some of the relevant findings on the effects of different additives on Ni and Zn electrodes are summarized below. The majority of these results were obtained by cyclic voltammetry.

<u>Ni Electrode</u>: Without $Li^+$ present, the oxygen evolution rate on Ni at a fixed potential increases as a function of time due to a type of aging effect of the NiO. This phenomenon is delayed in the presence of $Li^+$. In the potential range where evolution occurs, the discharged electrode behaves as an n-type electrode, and the $Li^+$ is not effective as an acceptor. Also, the effect is present for NiO films of different thickness, except for the very thinnest (a monolayer on a single crystal). In all cases, the presence of $Li^+$ causes the charge and discharge peaks to shift towards more cathodic potentials in the cyclic voltammogram. The presence of $Co^{++}$ ions in the electrolyte leads to an increase in charge capacity, especially in the region before the onset of oxygen evolution. Also, the rate of oxygen evolution seems to be suppressed. Adding $Co^{++}$ to the electrolyte, rather than incorporating

it in the positive plate, might thus be a way to improve Ni-electrode performance. Addition of $Zn^{++}$ ions to the electrolyte leads to a decrease in oxygen overpotential and a shift in the charge and discharge peaks towards more positive potentials. A slight increase in electrode capacity is also noticed. Addition of $F^-$ ions to the electrolyte has a drastic affect on oxygen evolution on NiO electrodes. It results in a decrease in the oxygen overpotential. Addition of PbO results in an increase in capacitance of the Ni electrode, and charge and discharge peaks shift to more anodic potentials. Addition of PbO seems to lead to similar results as those obtained with the addition of $Co^{++}$ ions.

Zn Electrode: The addition of $F^-$ ions to the alkaline electrolyte results in a substantial decrease in currents (charge and discharge) of Zn electrodes. Addition of PbO has a beneficial effect on the capacity of Zn electrodes. It also depassivates, to some extent, the Zn electrode at very positive potentials (passive region). When low concentrations of ZnO are added to the alkaline electrolyte, the hydrogen overpotential on Zn is somewhat suppressed. At higher concentrations, the electrode exhibits much higher passive currents. Addition of iron to the electrolyte has a negative effect on the electrode performance because its presence reduces the hydrogen evolution overpotential.

## Structure of Zincate Ions in Concentrated Aqueous Potassium Hydroxide

(V.A. Maroni, Argonne National Laboratory)

The objective of this task is to elucidate the coordination chemistry of $Zn^{2+}$ ions in concentrated aqueous potassium hydroxide under conditions that emulate those in alkaline batteries with zinc electrodes. A combination of Raman spectroscopy and $^{67}Zn$ NMR spectroscopy is being used to probe the structure of the zincate species present in solution as a function of $Zn^{2+}$ concentration, pH, and $Zn^{2+}/OH^-$ ratio. There have been prior Raman and $^1H$ NMR studies of the aqueous zinc-hydroxyl system (1-3); however, the conclusions of these investigations have shown some disagreement, and several characteristics of the data are not yet fully understood.

For the Raman studies, two series of solutions each consisting of four samples with $Zn^{2+}$ concentrations, [Zn], in the range from 0.3 to 3.0M were prepared. In one series, appropriately measured quantities of ZnO were added to a saturated solution of KOH in $H_2O$ (~18M KOH); in the second series, varying quantities of ZnO were placed in a fixed quantity of water and just enough KOH was added to each sample to bring all the ZnO into solution. In this way, solutions of varying [Zn] with an excess of KOH were obtained in the first case, and solutions with just enough KOH to hold the $Zn^{2+}$ present in solution were obtained in the second case. Raman spectra of ~18M KOH and 5M KOH were also taken to provide a specific elucidation of the spectral features that arise due to the presence of $Zn^{2+}$. The Raman spectra obtained in this study show only two features that are clearly associated with the presence of $Zn^{2+}$ - a polarized band at 464 ± 1 $cm^{-1}$ and a depolarized band at 415 ± 1 $cm^{-1}$. These results confirm the findings of Sharma (1) that a shoulder on the exciting line at ~260 $cm^{-1}$ is not associated with any zinc species because (i) it appears in the spectrum of aqueous (zinc-free) KOH and (ii) its intensity is much more sensitive to KOH concentration than to [Zn] even where zinc is present in solution. Furthermore, it is found (for the first time) that this band is polarized and therefore corresponds to a totally symmetric vibration; hence, it cannot be assigned to the bending mode(s) of $Zn(OH)_4^{2-}$, as postulated by Fordyce and Baum (2) and Jackovitz and Langer (3).

There is another interesting feature in the Raman spectra of the KOH and ZnO-KOH solutions that had not been explored by previous investigators. A significant change is observed in the shape of the spectral features in the 2800 to 3800 $cm^{-1}$ region, i.e., the region of the $O\text{-}H^-$ and H-O-H stretching frequencies. A sharp, polarized peak at 3600 $cm^{-1}$ is clearly associated with the $O\text{-}H^-$ stretch. The rather small value of the depolarization ratio for this band shows that the hydroxyl ions are complexed in a nearly centrosymmetric environment, e.g., in $[Zn(OH)_4^{2-}]_n$, where the value of n could be anywhere from 1 to a considerably larger value indicative of a highly associated, symmetrical-solution structure. A much broader Raman scattering between 2800 and 3800 $cm^{-1}$ underlies the $OH^-$ peak at ~3600 $cm^{-1}$. The band shape and polarization characteristics of this broad feature are sensitive to both pH and the presence of zinc.

The changes in this spectral region are being investigated to determine how the structure of the aqueous KOH medium is affected by addition of ZnO. The effects on solution structure when zinc is added in a form other than ZnO, e.g., as $Zn(ClO_4)_2$, or $ZnI_2$, are also being examined.

An attempt has been made to record infrared (IR) spectra of KOH and ZnO-KOH solutions in the 200-800 $cm^{-1}$ region using a variable path-length cell with polyethylene windows. The results of this effort indicate that there is little chance of making definitive IR measurements of zinc-containing species below 800 $cm^{-1}$. The previously published infrared results for this system (2) were not reproduced, and there appears to be little validity to the conclusions drawn from this prior work.

In future work on this project, the analysis of the Raman data will be completed and a $^{67}Zn$ NMR study will be undertaken to further probe the structure and dynamics of the chemical environment surrounding $Zn^{2+}$ cations in alkaline aqueous media.

References

1. S.K. Sharma, J. Chem. Phys. 58, 1626 (1973).

2. J.S. Fordyce and R.L. Baum, J. Chem. Phys. 43, 843 (1965).

3. J.F. Jackovitz and A. Langer, "A Spectroscopic Investigation of the Zinc-Hydroxy System," in Zinc-Silver Oxide Batteries, A. Fleischer and J.J. Lander, Eds., John Wiley & Sons, Inc., New York, NY (1971) p. 29.

## Thermodynamic Framework for Estimating Efficiencies of Alkaline Batteries

(D.D. Macdonald, Ohio State University)

The thermodynamic activity of water in a binary KOH-$H_2O$ system has been measured using an electrochemical cell, $H_2$(Pt) / KOH in $H_2O$ / Hg, HgO(Pt), in the concentration range between 1 and 8 molal and the temperature range of 0-80°C. From the equilibrium voltage, the activity of water can be directly calculated without making assumptions about the degree of dissociation of the solute or any other solution parameters. The measured values of activity are greater than those found in previous

vapor-pressure studies, but are consistent with previous EMF measurements of KOH concentration cells at 25°C. These values are invariant with temperature for concentrations up to 4.0 molal, but between 6.0 and 8.0 molal the $H_2O$ activity first decreases by ~10% and then increases by ~15% as the temperature is increased. The general activity trend is consistent with, though smaller than, the results in the higher concentration ranges of the previous vapor-pressure studies. The activity of water reported here can be used to refine previous calculations on the theoretical efficiencies of alkaline battery systems.

## Development of Membranes for the Zinc/Ferricyanide Battery

(C. Arnold and R.A. Assink, Sandia National Laboratory)

The objective of this project is to develop an inexpensive, chemically-stable membrane for the zinc/ferricyanide battery. The approaches taken are 1) to evaluate custom-made fluorocarbon-based grafted membranes, and 2) to synthesize and evaluate sulfonated polysulfones.

It was observed that grafted membranes which utilized a fluorocarbon support exhibited high stability in alkaline-ferricyanide. In an effort to optimize conductivity and selectivity, Sandia National Laboratory requested that RAI Research Corp. prepare a series of membranes in which the type of fluorocarbon substrate, degree of crosslinking and film thickness were varied systematically. Styrene and divinyl benzene monomers were radiatively grafted into poly(tetrafluoroethylene) (PTFE) and poly(tetrafluoroethylene-co-hexafluoropropylene) (FEP) and subsequently sulfonated. The best balance of conductivity, selectivity and stability was achieved with 0.0127-cm thick PTFE which was lightly crosslinked (membrane IB). In cycling tests with this membrane, in which a complexing agent was added to the electrolyte to facilitate zinc deposition, average cell efficiencies of 80% over 700 cycles were realized.

In another cycling test, membrane IB was removed after 67 cycles to determine if there was any change in properties as a result of cycling. It was found that the ion-exchange capacity decreased by 75 ± 9%. A hydrogen loss of 64 ± 9%, determined by nuclear-magnetic-resonance

measurements, agreed well with the loss of ion-exchange capacity. This result indicates that the loss of ion-exchange capacity is due to loss of the graft itself, and not a fouling phenomenon. In spite of the graft loss, the conductivity of the membrane increased, and the membrane retained its mechanical strength. An accelerated-aging study has been initiated to determine if the graft loss is limited to a fraction of the total graft, as suggested by the membrane's long life in the cycling cell, or if graft loss continues until the membrane becomes totally inactive.

It has been reported that alkyl groups adjacent to an aromatic ring undergo oxidation in the presence of alkaline-ferricyanide, but that the aromatic ring itself is not attacked (1). This suggests that membranes derived from sulfonated aromatic polymers such as sulfonated polysulfones should have adequate stability in alkaline-ferricyanide electrolytes. Sulfonated polysulfones are readily prepared via sulfonation of relatively inexpensive ($3.80/lb) aromatic polysulfones using an $SO_3$-complex of triethylphosphate. With this sulfonating agent, chain cleavage is reported to be minimal (2). Sulfonated polysulfones were isolated as white powders which were readily soluble in dimethylformamide (DMF), and they could be cast into films. The films were found to be mechanically strong and impervious to attack by ferricyanide. No weight loss was observed after exposure to alkaline-ferricyanide for one week at 50°C. Furthermore, these membranes exhibited low resistances (1-5 ohm-$cm^2$) and a low rate of ferricyanide permeation ($10^{-5}$ mmoles/h/$cm^2$). In cycling tests carried out at Lockheed Missile and Space Co., average efficiencies of 75% over greater than 200 cycles were realized. The following approaches are now being taken to further improve the performance of sulfonated polysulfones: 1) increase voltaic efficiency by increasing the degree of sulfonation and/or porosity; 2) prepare composite membranes by impregnating the sulfonated polysulfone into inert microporous supports. The latter approach would allow membranes to be manufactured by simply drawing the porous substrate through a solution of the polyelectrolyte and drying.

References

1. R. Weissgerber and O. Kruber, Ber. 52, 352 (1919).

2. A. Noshay and L.M. Robeson, J. Appl. Polym. Sci. 20, 1885 (1976).

## Zinc/Nickel Oxide Battery Membrane Separator Studies

(D.N. Bennion and J.S. Bradshaw, Brigham Young University)

The purpose of this research is to develop anion-exchange membranes suitable for application in secondary alkaline batteries. It is hypothesized that anion-exchange membranes will decrease zinc-electrode shape change and dendrite formation, as well as reduce voltage losses in alkaline batteries. Such membranes can be fabricated by incorporating macrocyclic compounds such as crown ethers into a polymer material. By locating a cation, such as a potassium ion, in the interior of the macrocyclic molecule, fixed cationic sites can be created in the membrane. Theoretically, this would reduce the flow of cations and enhance the transport of anions through the membrane, as well as change the direction of water flow in the cell during cycling.

During this year, polypropylene membranes were tested extensively. These membranes were fabricated using two different methods. The first method involved mixing polypropylene together with the KOH salt of the macrocyclic compound, and then pressing the mixture in a mold using a heated press. An alternative method for making membranes was developed which involved dissolving the polypropylene and KOH/macrocycle complex together in boiling 1,1,2,2-tetrachloroethane followed by evaporating the solvent. Several of these membranes were tested for ionic conductivity in a 4M KOH/water solution at room temperature. Conductivities ranged from $10^{-7}$ - $5 \times 10^{-4}$ mho/cm, which are below the target goal of 0.01 mho/cm. It is thought that the low conductivities are due to uneven distribution of the macrocyclic compounds and low water content in the membrane. Comparison to other results from our laboratory on Nafion membranes indicates that the target conductivity should be realized if fixed charge sites are properly dispersed and water content is increased by about 50%. Work is proceeding to create polypropylene membranes with a more even distribution of crown ethers and higher water

content.

Two additional polymers were tested as membrane materials, vinylidine chloride-vinyl chloride copolymer and polyvinyl alcohol. Stability tests of the vinylidine chloride-vinyl chloride showed that it suffered attack by KOH/water solution, so it is unsuitable for the present application.

Sheibley and coworkers (1,2) have found that polyvinyl alcohol, normally unstable in aqueous solutions, can be stabilized by crosslinking polyvinyl alcohol using dialdehyde compounds. Using an adaptation of their methods, it was found that certain crown ethers can be used in place of dialdehydes as a crosslinking agent. Membranes with improved stability in aqueous solutions and with macrocyclic structures chemically bonded to the polymer can be created. A number of these membranes were fabricated and tested for their ionic conductivity in 4M KOH/water solution at room temperature. Measured values ranged from 0.02-0.033 mho/cm, within the target range. It is intended to further refine these polyvinyl alcohol membranes to verify their potential as battery membrane separators.

References

1. D.W. Sheibley, M.A. Manzo, O.D. Gonzalez-Sanabria, "Cross-Linked Polyvinyl Alcohol Films as Alkaline Battery Separators," J. Electrochemical Soc. 130, 2255 (1983).

2. L.C. Hsu, D.W. Sheibley, "Inexpensive Cross-Linked Polymeric Separators Made from Water-Soluble Polymers," J. Electrochemical Soc. 129, 2251 (1982).

## Research on Separators for Alkaline Zinc Batteries

(R.S. Yeo, Pinnacle Research Institute)

The objective of this project is to develop hybrid separators to improve the cycle life of alkaline zinc batteries. These hybrid separators were synthesized and fabricated by Dr. J. Lee (RAI Research Corporation). These new separators exhibit the favorable properties of both ion-exchange membranes and microporous separators. The hybrid separator should be highly specific for fast transport of electrolyte while inhibiting zincate ion diffusion.

The separators are being prepared by radiation-grafting of a monomer, such as acrylic acid, onto a microporous film. The ion-exchange capacity was directly proportional to the extent of grafting; the ion-exchange capacity of a sample with 36% graft is 2.1 meq/g. The fixed-ion concentration is as high as 8 mole/l, while the zincate ion concentration in the hybrid separators is less than 0.1 mole/l. This implies that the ion selectivity of the hybrid separators is as effective as that of ion-exchange membranes.

The transport numbers were measured for a series of hybrid separators. The cation transport number decreases as the concentration of electrolyte increases. The cation transport number increases with increasing percent graft, up to ca. 8%, then gradually decreases. The water transport number shows a rather similar pattern.

Preliminary results for zinc/nickel oxide cells containing hybrid separators (designated 229-4C) in 35% KOH electrolyte showed a low cell polarization. No evidence of dendrite shorting was found in any of the cells containing a one-layer hybrid separator.

Publications

1. R.S. Yeo and J. Lee, "Novel Hybrid Separators for Alkaline Zinc Batteries", in Advances in Battery Materials and Processes., Ed. by J. McBreen, R.S. Yeo, D-T. Chin and A.C.C. Tseung, The Electrochemical Society, Inc., Pennington, NJ (1984) p. 206.

2. R.S. Yeo, "Structural and Transport Properties of Hybrid Battery Separators", Extended Abstract #657, Electrochemical Society Meeting, New Orleans, LA, Oct. 7-12, 1984.

Supported Liquid-Membrane Battery Separators

(J.P. Pemsler, Castle Technology Corporation)

The objective of this project was to develop supported liquid-membrane (SLM) separators to improve the cycle life of zinc/nickel oxide batteries. In particular, a separator that prevents zinc dendrite growth from shorting the cell and reduces capacity loss due to zinc-electrode shape change is being sought. A number of ion-exchange/solvent-modifier systems for incorporation into SLMs were developed. SLMs prepared with these reagents exhibited resistances in

the range of 0.4-10 ohm-$cm^2$, selectively transported hydroxyl ions over zincate ions by a factor of $10^6$-$10^7$, and possessed electrochemical and chemical stability in alkaline electrolytes.

In order to evaluate these SLM separators under conditions closely resembling those in a commercial Zn/NiOOH cell, an accelerated cycle-life test was devised using commercial electrodes. Previous experimental studies indicated that a new design for the cell hardware was required to accommodate the SLM separator. The new cell design was tailored to allow for the total thickness of the electrodes, wicks and SLM without placing excess mechanical pressure on the electrode package, which could cause excess electrode gassing, localized heating, or electrolyte-wick dryout.

The cycle life of cells containing the two SLM separators that performed best in 5M KOH electrolyte consistently exceeded the cycle life of control cells containing one, two or three layers of Celgard 3501 separators. No evidence of dendrite "hot shorting" was found in any of the cells containing SLMs. Improved cycle life with the new cell design was also obtained in 7M KOH electrolyte; the cycle life of cells containing a single-layer SLM exceeded those of single and double layers of Celgard 3501. However, one control cell containing three layers of Celgard 3501 achieved 375 cycles, surpassing the cycle life of cells containing SLMs.

Analysis of failed SLM cells indicated that capacity loss was due to a combination of effects including zinc wick dryout, edge effects, soft shorts, and macro-and micro-shape changes. However, visual observations indicated the shape changes were less pronounced on cells with SLM separators than that with control cells.

At this time no further development of SLM separators for Zn/NiOOH cells is planned due to a shift in the emphasis of the TBR Project. However, evaluation of SLM separators for zinc/ferricyanide batteries is underway at Sandia National Laboratory.

## B. ZINC/HALOGEN CELLS

### Surface Morphology of Metals in Electrodeposition

(C.W. Tobias, Lawrence Berkeley Laboratory)

The objective of this project is to develop a pragmatic understanding of the detail processes and their interactions in the macrocrystallization of metals, which is necessary for the design and optimization of rechargeable galvanic cells. Particularly neglected is the area of macrocrystallization involving substantial thicknesses of metal deposits. Hydrodynamic flow not only affects the limiting rate of deposition, it also produces an imprint on the developing deposit. The genesis of these phenomena must be understood before rational control of such effects may be achieved.

The development of morphology of electrodeposited zinc was investigated by studying the initial stages of deposition. Zinc was deposited galvanostatically from 1.0 M $ZnCl_2$ electrolyte ($0.7 < pH < 4.6$) on rotating-disk electrodes at current densities from 5 to 130 $mA/cm^2$. Glassy carbon (Pine), pyrolytic graphite (Union Carbide), pyrolytic graphite (Gould), graphite-loaded polymer (Exxon), and platinum substrates were used. The number densities of nodules (diameter greater than 1 μm), which are typically encountered during incipient morphological development, were measured using scanning electron microscopy and image analysis. Nodule densities up to $7 \times 10^4$ nodules/$mm^2$ were measured. Results may be summarized as follows:

1) Nucleation processes were discernible through cyclic voltammetry.

2) Potential-step kinetic measurements yielded exchange current densities on the order of 1 $mA/cm^2$.

3) The nodule density increased with surface overpotential at a rate from 200 to 1000 nodules/$mm^2$-mV.

4) The potential between the working and reference electrodes exhibited a transient-potential peak during the first few seconds of deposition. The relative magnitude of the peak potential is inversely related to the number of available nucleation sites.

5) A parallel exists between the magnitude of this peak and the number density of nodules on a given substrate. Substrates rank in order of decreasing activity towards zinc nucleation:

- HOPG pyrolytic graphite (Union Carbide)
- platinum
- pyrolytic graphite (Gould),
- graphite-loaded polymer (Exxon)
- glassy carbon (Pine)

Publication

1. R.C. Anderson (M.S. Thesis) with C.W. Tobias, "Studies on Zinc Electrodes Electrodeposited from Acid Electrolytes", LBL-18646 (1984).

## Dendritic Zinc Deposition in Flow Batteries

(J.R. Selman, Illinois Institute of Technology)

The objectives of this project are to investigate the formation and growth rates of dendritic or nodular deposits at zinc electrodes in flowing acidic halide solutions by experimental and analytical methods. Of particular interest are the effect of convection on the growth rate and the influence of solution chemistry (speciation) on the kinetics and mass-transfer characteristics of the deposition process.

During 1984, a rotating-concentric-cylindrical electrode (RCCE) cell with a small (0.65 cm) electrode gap was designed and constructed. This cell accommodates a rotating inner electrode of the same diameter (0.65 cm) as the previous cell. This cell should allow closer in-situ observation and growth-rate measurement in the early stages of nodular growth.

The mass-transfer characteristics at low rotation rates were determined by the limiting-current method using a nickel electrode and potassium ferri/ferrocyanide in NaOH. Very good agreement was obtained with literature data for mass transfer at the inner electrode (at larger gap width and higher Re number). The correlation of Eisenberg et al (1) is followed down to $Re_d = 950$, while the Schmidt number Sc tends to a value of $1.1 \times 10^{-4}$ at the lowest rotation rates ($Re_d = 350$). The results for mass-transfer at the outer electrode are correlated by

$$k/v = 0.0605\ Re_d^{-0.49} Sc^{-0.644}$$

over the range $650 < Re_d < 5150$. This correlation appears to be more reliable than those in the literature (2).

A systematic analysis was undertaken of the effect of kinetic parameters on the growth rate in the specific flow geometry of the RCCE cell, using an improved model which includes convection. This modeling study has led to the following conclusions. The direct effect of convection on tip growth rate is quite small, since tip growth is kinetically rather than mass-transfer controlled even when $i_o$ is large (e.g., 10-20 $mA/cm^2$). Convection also indirectly increases tip growth rate by decreasing the thickness of the diffusion layer and increasing the concentration level near the electrode. This indirect convection effect causes a much larger increase in growth rate and also lengthens the apparent induction time. However, the predicted growth rates are smaller than the experimental results observed by one or two orders of magnitude. It was concluded, therefore, that ohmic resistance plays an important role in nodular growth when the electrode gap is small, as it is here, as well as in typical battery applications. Furthermore, the presence of surrounding dendrite precursors or nodules, i.e., substrate roughness, effectively increases the growth rate of the tips and shortens the induction time compared to isolated dendrites on smooth substrates.

Studies of anodic zinc dissolution at a corroding electrode in flowing solution have been undertaken. The objective is to determine the dissolution kinetics of zinc in a solution containing both acid and dissolved halogen. Initial experimental results indicate large exchange current densities (up to 60 $mA/cm^2$). However, complications are caused by the complexation of the corrodant ($Br_2$ as $Br_3^-$ ion), as well as nonuniform corrosion-rate distribution on the test electrode (rotating hemispherical electrode). The relative nonuniformity has been computed, following well-established procedures (3), and appears to be approximately 40% for an exchange current density of 7 $mA/cm^2$. The implications of a multistep reaction mechanism for the corrosion-potential measurement are now being studied.

References

1. M. Eisenberg, C. W. Tobias and C. R. Wilke, J. Electrochem. Soc. 101 , 306 (1954).

2. A. J. Arvia and J. S. W. Carrozza, Electrochim. Acta 7, 65 (1962).

3. K. Nisancogliu and J. Newman, J. Electrochem. Soc. 119, 69 (1972).

## Zinc Electrode Morphology in Acid Electrolytes

(J. McBreen, Brookhaven National Laboratory)

The objective of this research is to elucidate the factors affecting the kinetics and morphology of zinc deposition in $ZnCl_2$ and $ZnBr_2$ electrolytes. A further objective is to devise methods to slow the kinetics in $ZnBr_2$ electrolytes, and thereby inhibit dendritic growth and achieve higher electrode capacity in $Zn/Br_2$ batteries. In 1984, work focused on the effect of zinc crystal orientation on the deposition kinetics and morphology and the effect of electrolyte composition on the kinetics in $ZnBr_2$ electrolytes.

The investigation of the effect of crystal orientation on zinc deposition was carried out in 3M $ZnCl_2$ (pH = 0.5). The techniques used were the potential-step method and scanning electron microscopy. The two crystal orientations investigated were the basal plane (1000) and a plane perpendicular to the basal plane (close to (1120)).

The crystal orientation was found to have a large effect on the kinetics and morphology of zinc deposition. On the plane perpendicular to the basal plane, the current transients obtained by the potential-step method indicate a classic layer-type growth where there is no increase in the surface area of the deposit with time, as confirmed by both electrochemical measurements and electron microscopy. It was possible to carry out zinc deposition between 10 mV (~2 $mA/cm^2$) and 60 mV (~5 $mA/cm^2$) in 10 mV intervals over a period of several minutes. On switching the potential up or down between any of these values, the same current was obtained, thus indicating a stable deposit of constant area. Scanning electron microscopy confirmed a layer-type deposit consisting of overlapping layers bounded on one side by the basal plane and on the other by one of the prismatic planes. Thus, the plane edges were

orthogonal to one another.

On the basal plane of zinc single crystals, the kinetics and morphology were completely different. At potentials below 20 mV, the current transients were flat, corresponding to a layer growth mechanism, and above 20 mV, the transients displayed a stepwise rise in the current followed by a steady rise to a steady-state current plateau. This behavior indicates a simultaneous layer growth mechanism with nucleation and growth of three-dimensional centers. Electron microscopy confirmed that a layer-type deposit bounded by either the primary or secondary prismatic planes was produced at low overpotentials (<20 mV). At higher potentials, the nucleation of three-dimensional protrusions were observed; these may be the precursors of dendrites.

Previous work has shown that the addition of heavy metal ions (e.g., $Pb^{++}$, $Bi^{+++}$) in fluorinated surfactants slowed down the kinetics of zinc deposition in both $ZnCl_2$ and $ZnBr_2$ electrolytes. However, neither of these approaches are completely satisfactory since the metal ions can be displaced from the electrolyte by zinc, and the surfactants can be oxidized at the positive electrode. Previous work has also shown that the kinetics were dependent on the anion (i.e., kinetics are slower in $ZnCl_2$ than in $ZnBr_2$ and additions of KCl slow the kinetics in $ZnBr_2$). Accordingly, the approach taken in this study is to add other anions to the electrolyte. Additions of $AlCl_3$ increased the solubility with a concomitant decrease in zinc deposition kinetics. Since it was found that $AlCl_3$ alone would decrease the kinetics, an extensive study was made on the effect of $AlCl_3$ additions on the kinetics of zinc deposition in $ZnBr_2$ electrolytes. It was found that additions of stoichiometric or excess stoichiometric amounts of $AlCl_3$ decreased the kinetics, produced a fine-grained deposit, and inhibited dendrite growth. Compounds such as $ZnAlCl_5$ and $ZnAl_2Br_8$ are reported in the literature, so the effects may be due to complex or compound formation. This looks like a promising approach since these additives are not affected by displacement by zinc or oxidation at the positive electrode.

Publications

1. J. McBreen, "Rechargeable Zinc Batteries", presented at the Sixth Australian Electrochemical Conference, Deakin University, Geelong, Australia; J. Electroanal. Chem. 168, 415 (1984).

2. J. McBreen, "Effect of Charging Methods on Battery Electrodes", Proceedings of the Symposium on Battery Materials and Processes, Edited by J. McBreen, R.S. Yeo, D-T. Chin and A.C.C. Tseung, The Electrochemical Society, Inc., Pennington, NJ (1984), p. 292.

3. J. McBreen, "Nickel/Zinc Batteries", Power Sources for Electric Vehicles, Edited by B.D. McNicol and D.A.J. Rand, Elsevier Press, Amsterdam (1984) p. 541.

Transport in Aqueous Battery Systems

(D.G. Miller and J.A. Rard, Lawrence Livermore National Laboratory)

The purpose of this research is to obtain experimental data on mutual diffusion coefficients, which are required to model battery systems of interest to DOE. Mutual diffusion coefficients are being measured for aqueous $ZnCl_2$ and $ZnCl_2$-KCl mixtures at 25.00 ± 0.005°C by using Rayleigh interferometry.

Eleven composition of high-purity $ZnCl_2$ were studied during this period, and this completes the measurements for this binary system. These measurements cover the concentration range 0.004981 to 5.6517 mol/dm$^3$ (0.004996 to 7.2489 mol/kg $H_2O$).

Diffusion measurements were made for a 1.5016 mol/dm$^3$ $ZnCl_2$-4.0044 mol/dm$^3$ KCl electrolyte. The resulting diffusion coefficients are $10^5D_{11}$ = 0.9829 ± 0.0679, $10^5D_{12}$ = 0.0636 ± 0.0019, $10^5D_{21}$ = -0.1741 ± 0.0160, and $10^5D_{22}$ = 1.4052 ± 0.0917 cm$^2$/s. Here 1 denotes $ZnCl_2$ and 2 denotes KCl. The moderately large negative crossterm coefficient is due to complex formation.

Diffusion measurements were also made for 1.5000 mol/dm$^3$ $ZnCl_2$ - 1.2500 mol/dm$^3$ KCl. In this case, the diffusion coefficients could not be extracted since our non-linear least-squares computer programs did not converge. This results when the two main-term coefficients are close in value, and the two cross-term coefficients are small. When this occurs, the system behaves almost like a pseudo-binary system (which is described by a single diffusion coefficient). Consequently, an attempt

to extract all four numerical coefficients has severe numerical problems. This situation corresponds closely to a ternary system whose diffusion matrix has two equal eigenvalues. The general solution of the diffusion equation for this case, and the relations between the $D_{ij}$ and convenient least-square variables have been obtained. Programming these results remains to be done.

Publication

1. J.A. Rard and D.G. Miller, "Densities and Apparent Molal Volumes of Aqueous Manganese, Cadmium, and Zinc Chlorides at 25°C", J. Chem. Eng. Data 29, 151 (1984).

## C. MOLTEN SALT CELLS

### Molten-Salt Cell Research

(J.E. Battles, Argonne National Laboratory)

The objectives of this program are to generate the scientific and technical base of information from which major improvements in the performance of molten-electrolyte cells can be derived. These efforts are directed toward the development of a cell that will deliver a specific energy of 200 Wh/kg at the 4-h rate and a specific power of 200 W/kg at 50% depth-of-discharge. The cells have lithium-alloy negative electrodes and metal-disulfide positive electrodes.

The research during the past year was directed at efforts in three related areas: (1) development of an electrode performance-evaluation system, (2) electrochemical characterization of candidate positive- and negative-electrode materials adequate to meet the cell performance goals, and (3) studies of cell designs to meet those goals.

A system for measuring and analyzing the properties of porous, reactive electrode beds has been developed, which incorporates techniques and test-cell designs that were perfected in this research program. The test cell, which features a one-dimensional current distribution, has a reference electrode and voltage taps for direct measurement of electrode potential and voltage drop across the electrode bed. In addition, it is equipped with thickness-variation and mechanical stress sensors. The

system is being used to study the performance of advanced electrode materials as influenced by experimental conditions such as electrolyte and electrode composition, loading density, temperature, and applied pressure. Data under both constant-current and pulse-current cycling are acquired by the system and stored in a computer. The data are processed to produce tables and diagrams that summarize the electrode performance in engineering terms such as area-specific resistance (ohm-$cm^2$), capacity (Ah), specific energy (Wh/kg), and specific power (W/kg). The electrochemical characteristics of Li-Al-Si negative electrodes and iron- or nickel-disulfide positive electrodes in LiCl-KCl and LiF-LiCl-LiBr electrolytes were investigated in this reporting period.

The compositions of the negative electrodes are expressed by the formula $Li_x(Al_{1-n}Si_n)$. The compositions tested were n = 0, 0.12, 0.5, and 1.0. The Li-Al-Si negative electrodes possessed higher specific power than Li-Si electrodes, and higher specific energy than Li-Al electrodes. Tests of other ternary compositions will be needed to complete this study. However, an improved electrode material, $Li_x(Al_{0.5}Si_{0.5})$, has been found as a result of the studies conducted to date. This electrode may be cycled between the nominal compositions of LiAlSi and $Li_4AlSi$ and has high specific capacity (1.3 Ah/g) and a low area-specific resistance (less than 0.5 ohm-$cm^2$).

The area-specific resistance of $NiS_x$ and $FeS_x$ electrodes is considerably lower when they are operated in a $Li_2S$-saturated LiF-LiCl-LiBr electrolyte instead of LiCl-KCl eutectic electrolyte. For instance, $NiS_x$ electrodes (for $0 < x < 1$) had an area-specific resistance of about 0.25 ohm-$cm^2$ in the former electrolyte and about 0.65 ohm-$cm^2$ in the latter. With the former electrolyte, however, the formation of soluble polysulfides at states of charge corresponding to $x > 1.6$ in the positive electrode and their subsequent reaction with the negative electrode lowered the coulombic efficiency to an unacceptable valve. Consequently, use of the LiF-LiCl-LiBr electrolyte does not appear to be advisable for cells that employ disulfide electrodes. Alternatives that maintain the excellent power characteristics of the LiF-LiCl-LiBr electrolyte without the loss in coulombic efficiency are being sought.

The specific energy of a given cell design normally increases by only 20% on substituting $FeS_2$ for FeS because the net effect of the substitution is a slight increase in cell voltage with little or no increase in cell capacity. However, a 50% increase in specific energy appears to be possible by cycling exclusively on the high-voltage plateau of the $FeS_2$ electrode, even though in this mode of operation the coulombic capacity is only half that for utilization of both plateaus. This is because the discharge product, $Li_2FeS_2$, is very dense (2.8 $g/cm^3$) compared to $Li_2S$ (1.66 $g/cm^3$), which permits a 50% increase in the initial loading density.

Preliminary tests of a dense, upper-plateau $FeS_2$ electrode in LiCl-KCl electrolyte at 410°C indicated a factor of two increase in capacity utilization at high current density (100 $mA/cm^2$) and a cell resistivity that is about 50% lower than that of conventional $FeS_2$ electrodes. These improvements for the $FeS_2$ electrode give promise of increasing cell cycle life through reduction of the cell operating temperature. Tests of the upper-plateau $FeS_2$ electrode in a LiCl-LiBr-KCl-KBr electrolyte with a 310°C melting-point are underway to assess the improvements in performance at an even lower operating temperature. Also, efforts are proceeding with the design of a full-size, multi-electrode test cell for investigating this new electrode in an actual cell environment.

Publications and Presentations


1. M. Hiroi and H. Shimotake, "Effective Conductivities of an FeS Positive in LiCl-KCl Eutectic Electrolyte at Different States of Charge," J. Appl. Electrochem. 14, 341 (1984).

2. R.K. Steunenberg, "Lithium/Metal Sulfide Molten Salt Batteries: Present Status and Future Potential," in Progress in Batteries and Solar Cells, Vol. 5, JEC Press, Inc., Cleveland, OH (1984) p. 320.

3. H. Shimotake and L.G. Bartholme, "Positive-Electrode Current Collector for Liquid-Metal Cells," U. S. Patent No. 4,440,837 (April 3, 1984).

4. E.J. Cairns, G. Mamantov, R.P. Tischer and D.R. Vissers, "The Chemistry and Status of Rechargeable Molten-Salt Batteries," Proceeding of the Fourth International Symposium on Molten Salts, Edited by M. Blander et al., Vol. 84-2, The Electrochemical Society, Inc., Pennington, NJ (1984) p. 284.

5. M. Hiroi and H. Shimotake, "Effective Conductivities of FeS Positives in LiCl-LiBr-LiF Electrolyte at Different States of Charge," Presented at the 25th Battery Symposium in Japan, Electrochemical Society of Japan, Nagoya, Japan, November 13-14, 1984.

6. T.D. Kaun and M.E. Anderson, "A LiAl/FeS Cell Design for Improved Specific Power and Energy," Extended Abstracts, Vol. 84-2, Fall Meeting of the Electrochemical Society, New Orleans, LA, October 7-12, 1984.

7. L. Redey, "Characterization of Voltage Losses During High-Intensity Current Pulses in Reactive, Porous Electrodes of Molten-Salt Cells", Presented at the 35th Meeting of the International Society of Electrochemistry, Berkeley, CA, August 5-10, 1984.

8. L. Redey and D.R. Vissers, "Electrochemical Characteristics of High-Temperature Li-Al-Si Electrodes", Extended Abstracts, Vol. 84-2, Fall Meeting of the Electrochemical Society, New Orleans, LA, October 7-12, 1984.

9. L. Redey and D.R. Vissers, "Electrochemical Performance of Porous Nickel Sulfide Electrodes", Presented at the 35th Meeting of the International Society of Electrochemistry, Berkeley, CA, August 5-10, 1984.

10. L. Redey and D.R. Vissers, "Electrode Characterization of Li-Al/FeS Cells by Voltage-Loss Investigations", Proceedings of the Symposium on Porous Electrodes: Theory and Practice", Edited by H.C. Maru et al., Vol. 84-8, The Electrochemical Society, Inc., Pennington, NJ (1984) p. 322.

11. L. Redey and D.R. Vissers, "Resistance Characterization of Nickel Sulfide Electrodes in LiCl Containing Molten Salt Electrolytes", Proceedings of the Symposium on Advances in Battery Materials and Processes, J. McBreen, ed., Vol. 84-4, The Electrochemical Society, Inc., Pennington, NJ (1984) p. 53.

12. H. Shimotake, A.A. Chilenskas, R. Malecha and N.P. Yao, "Thermal Management of a Lithium/Iron Sulfide Battery", Proceedings of the 19th Intersociety Energy Conversion Conference, San Francisco, CA, August 19-24, 1984, Vol. 2, (1984) p. 793.

13. Z. Tomczuk, J. James and D.R. Vissers, "Electrochemical Investigation of Li-Si Electrodes", Extended Abstracts Vol. 84-2, Fall Meeting of the Electrochemical Society, New Orleans, LA, October 7-12, 1984.

14. Z. Tomczuk and D.R. Vissers, "EMF Measurements on Li-Al/$FeS_2$ Cells", Presented at the IUPAC Conference on Chemical Thermodynamics, Hamilton, Canada, August 13-17, 1984.

15. Z. Tomczuk, D.R. Vissers and M.L. Saboungi, "Solubility of $Li_2S$ in LiF-LiCl-LiBr Electrolyte: Measurements and Calculations", Proceedings of the Fourth International Syposium on Molten Salts, Edited by M. Blander et al., Vol. 84-2, The Electrochemical Society, Inc., Pennington, NJ (1984) p. 352.

## Investigation of the Mechanism for Capacity Decline of the $FeS_2$ Electrode in Lithium/Iron Disulfide Cells

(H.F. Gibbard, Gould, Inc.)

The object of this project is to determine the cause of capacity decline in lithium-alloy/$FeS_2$ high-temperature, molten-salt cells; currently the major impediment to the development of this high specific-energy couple. By post-test examinations of cells, the capacity decline has been shown to be caused by the evolution of a sulfur species from the disulfide positive active material and subsequent transport through the electrolyte to non-active areas of the cell where it is found as $Li_2S$. It is our hypothesis that the thermal instability of $FeS_2$, together with the small but finite solubility of sulfur in the electrolyte, accounts for the sulfur loss and resulting capacity decline. The goals of this work then are (1) to determine a stable operating temperature for an $FeS_2$ electrode using thermogravimetric analysis, (2) to investigate the effects of electrolytes and Li-Fe-S phases on sulfur evolution, and (3) to demonstrate stable operation of an $FeS_2$ cell.

Thermogravimetric analysis has shown that the $FeS_2$ material must be operated at 285°C or below to avoid sulfur evolution. Operation at higher temperatures leads to increasing rates of sulfur loss as shown in Figure 1. With pure $FeS_2$ material, temperatures as high as 305°C can be held for at least 12 hours without sulfur evolution because of the difficulty of nucleating $Fe_{(1-x)}S$. Once nucleation takes place, however, sulfur evolves at a slow but measurable rate.

Work on investigating the effect of electrolytes and ternary phases has recently begun. The results indicate that sulfur evolution from $FeS_2$ alone is 70 times greater than the sulfur evolution from $FeS_2$ in an eutectic LiCl-KCl electrolyte within the same temperature range. This could indicate that the rate-limiting step for sulfur loss is transport

through the electrolyte. Thus, an appropriate electrolyte might be found that could inhibit sulfur loss either by a low solubility for sulfur or a slow diffusion rate of sulfur in the electrolyte. This might enable the use of an $FeS_2$ cell at a higher operating temperature than 285°C while still controlling sulfur loss, thus increasing the number of candidate electrolytes.

Future research plans include expansion of the studies on the effect of electrolytes on sulfur evolution from $FeS_2$. Sulfur evolution from some of the Li-Fe-S ternary phases, both pure and with electrolyte, will also be examined. After the thermogravimetric studies are completed, the results will be applied in electrolyte selection and operating temperature to guide in the building and operating of an $FeS_2$ cell that will demonstrate stable operation.

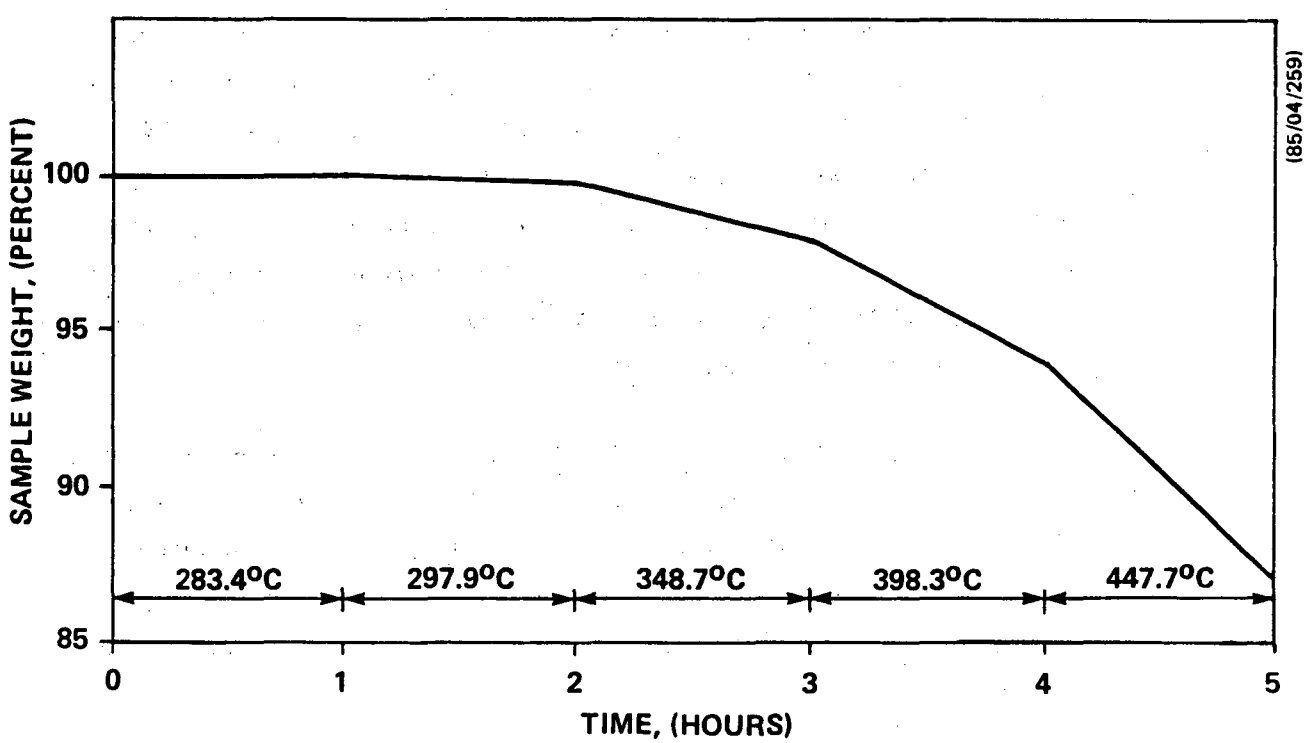


Figure 1. Weight loss in $FeS_2$ due to sulfur evolution.

New Battery Materials

(R.A. Huggins, Stanford University)

The objective of this program is to develop materials for electrolyte or electrode components for high-performance lithium-based secondary batteries. In addition, some effort has been expended to develop experimental and theoretical methods which can be employed to evaluate new materials and relevant phenomena.

Negative Electrode Materials: Work on negative electrodes for use in lithium-based systems is aimed at the investigation of lithium alloys that undergo displacement reactions. This approach avoids the formation of filamentary growth and the related problems of shape change, capacity loss and cell shorting, which are characteristically found when cycling pure lithium electrodes.

Experimental work has involved determination of the fundamental thermodynamic and transport parameters that control the potential, capacity, and kinetic behavior of such materials. Earlier work on this program, which established the important principles, involved the use of molten-salt cells to investigate a number of binary alloy systems at temperatures near 400°C. More recent work has extended these studies to ambient temperatures. In addition, some work has been done to explore potentially-interesting ternary alloys.

A significant amount of information is now in hand concerning potentials and capacities of all the constant-voltage plateaus in the Li-Al, Li-Sn, Li-Sb, Li-Bi, Li-Zn, Li-Cd and Li-Pb systems. It has been found that a number of these binary phases have high chemical diffusion coefficient at ambient temperatures, so that their electrode reactions should be quite fast.

Positive Electrode Materials: The possibility of synthesizing and stabilizing crystal structures with desirable kinetic properties by the introduction of a second alkali metal ion was demonstrated previously. Recent work has extended these concepts and applied them to several additional transition metal-oxide phases, as well as ternary and quaternary structures in the vanadium-bronze family. The latter undergo

insertion reactions with lithium, and they have been shown to have quite attractive thermodynamic and kinetic properties. The cycling properties of these electrode materials were also examined. Cyclability of the layered vanadium oxide was found to be particularly satisfactory.

Solid Electrolytes: Work was recently started to investigate the properties of a family of inorganic polymeric materials that can be prepared in either crystalline or glassy form. The central members of this family are $SiS_2$ and $SiSe_2$, which have crystal structures consisting of parallel chains of distorted edge-sharing $SiS_4$ or $SiSe_4$ tetrahedra. Experiments have shown that they can exist over an appreciable range of stoichiometry; in the case of $SiS_x$, the value of x can vary from 1.85 to 2.4.

The layered alkali zirconium phosphates, $M_2Zr(PO_4)_2$, were prepared by ion-exchange techniques. It was found that a high-temperature modification of the lithium member of this family shows high ionic conductivity. The thermodynamic stability and minority-carrier conduction in several families of lithium solid electrolytes has been addressed by thermodynamic calculations and experimental measurements.

Intermediate Temperature Molten Salts: Work on intermediate-temperature molten salts has two objectives: to find useful lithium-conducting salts with liquidus temperatures below 200°C, and to investigate their stability ranges and compatibility with both high-lithium-activity negative electrodes and useful positive electrodes. Interesting salts have now been found with melting points as low as 100°C that form solid-electrolyte protective layers, and which demonstrate good reversibility with pure lithium electrodes. Others have been found whose thermodynamic properties allow their use with reversible aluminum negative electrodes and lithium-reacting positive electrodes.

Publications

1. N.A. Godshall, I.D. Raistrick and R.A. Huggins "Relationships Among Electrochemical, Thermodynamic, and Oxygen Potential Quantities in Lithium-Transition Metal-Oxygen Molten Salt Cells" J. Electrochem. Soc. 131, 543 (1984)

2. Robert A. Huggins and Bernard A. Boukamp, "All-Solid Electrodes with Mixed Conductor Matrix", U.S. Patent 4,436,796 (March 13, 1984).

3. I.D. Raistrick and R.A. Huggins, "Lithium Ion-Conducting Solid Electrolytes", in Lithium Battery Technology, Edited by H.V. Venkatasetty, John Wiley and Sons, Inc., New York, NY (1984) p. 205.

4. G.J. Reynolds and R.A. Huggins, "Phase Equilibria in the Li-Mn-O Ternary System", in Proceedings of the Symposium on Advances in Battery Materials and Processes, Edited by J. McBreen, D-T. Chin, R.S. Yeo and A.C.C. Tseung, The Electrochemical Society, Inc., Pennington, NJ (1984) p. 1.

5. Jiqiang Wang and R,A. Huggins, "A New Low-Melting-Point Electrolyte $LiNO_3$-$KNO_3$-$CsNO_3$ for Use in Intermediate Temperature Lithium Cells", in Proceedings of the Symposium on Advances in Battery Materials and Processes, Edited by J. McBreen, D-T. Chin, R.S. Yeo and A.C.C. Tseung, The Electrochemical Society, Inc., Pennington, NJ (1984) p. 64.

6. G.J.Reynolds, M.C.Y. Lee and R.A. Huggins, "Measurements of the Partial Electronic Conductivity in Lithium Chloride-Potassium Chloride Molten Salts", in Proceedings of the 4th International Symposium on Molten Salts, Edited by M. Blander, D.S. Newman, G. Mamantov, M.L. Saboungi and K. Johnson, The Electrochemical Society, Inc., Pennington, NJ (1984) p. 519.

7. J. Poris, I.D. Raistrick and R.A. Huggins, "Nitrite Molten Salt for Use in Intermediate Temperature Lithium Cells", in Proceedings of the 4th International Symposium on Molten Salts, Edited by M. Blander, D.S. Newman, G. Mamantov, M.L. Saboungi and K. Johnson, The Electrochemical Soc., Inc., Pennington, NJ (1984) p. 313.

8. I.D. Raistrick and R.A. Huggins, "Use of Lithium Aluminum Chloride Molten Salt as an Electrolyte in Lithium Cells", in Proceedings of the 4th International Symposium on Molten Salts, Edited by M. Blander, D.S. Newman, G. Mamantov, M.L. Saboungi and K. Johnson, The Electrochemical Society, Inc., Pennington, NJ (1984) p. 82.

## D. COMPONENTS FOR ALKALI/SULFUR CELLS

### Electrochemical Properties of Solid Electrolytes

(L.C. De Jonghe, Lawrence Berkeley Laboratory)

The purpose of this research is to characterize the electrochemical behavior of sodium beta"-alumina in the Na/S battery, and explore the possibilities of new low-temperature cathode materials.

A study of the critical current density for onset of Mode I electrolyte degradation was performed for both fracture-toughened beta"-alumina with dispersed zirconia and single-phase electrolyte. Theory developed in this program and elsewhere predicts that the critical current density for crack propagation is proportional to the fracture toughness raised to the fourth power. Therefore, the fracture toughness has an important effect on Mode I failure. One would expect to observe higher current densities for onset of Mode I degradation in beta"-alumina toughened by zirconia dispersion than for single-phase electrolyte. So far, the toughened ceramics showed comparable resistance to crack propagation under current load. This observation is understood when the surfaces of the ceramics in question are examined by optical and scanning electron microscopy. The single-phase electrolyte was fine grained and reasonably free of processing surface flaws, whereas the surface of the toughened ceramics were badly pitted, exhibiting high porosity due to agglomeration of the zirconia. Since propagation of Mode I cracks depends also on the distribution of surface flaws and the microstructure of the material around the flaws, it is not surprising that the poorly-processed toughened electrolytes did not show the expected increased resistance to Mode I failure. Noteworthy was that polishing of the untoughtened ceramics prior to use in the cell reduced their performance in testing, probably due to increased surface flaws; however, polishing the toughened ceramics <u>improved</u> their performance, implying that polishing put the surface under compression through transformation toughening. If the quality of the toughened electrolytes can be improved to an acceptable level, a more meaningful comparison and correlation with theory can be made.

In order to establish the cause of asymmetric polarization reported by various groups for the Na/Na cell with sodium beta"-alumina electrolyte, current-potential curves and current and potential-pulse measurements were done on this cell over the temperature range of 160 to 350°C. A three-electrode configuration was employed in order to separate the inner-sodium working electrode/electrolyte interface from the outer-sodium counter electrode/electrolyte interface. The inner-sodium working electrode (WE) was varied in sodium-oxide content from electrolytically-pure sodium to oxide-saturated sodium. Vanadium foil

was added to the sodium WE for some experiments in order to chemically reduce the $Na_2O$ and set the soluble oxide concentration to a very low value. The experimental observations clearly showed that the presence of oxides modifies the electrochemistry of the sodium beta"-alumina interface. At 300°C, the highest resistance polarization was observed for the oxide-saturated sodium. At this temperature, the addition of vanadium foil to the working electrode reduced the observed resistance polarization and removed any asymmetry previously exhibited. The polarization observed in the experiments always manifested itself as a larger resistance for discharging sodium out of the tube than for charging sodium into the tube. The asymmetric polarization was much more pronounced at 160°C, being largest for oxide-saturated sodium. The electrochemical studies suggested that the additional voltage drop at the working electrode was due to the resistance of a film or adsorption layer to the transfer of sodium ions; the most likely source being an oxide film, possibly $Na_2O$. At the operating temperature of the sodium/sulfur battery, this asymmetric polarization can be minimized or eliminated by the addition of a chemical oxygen scavenger, which reacts with $Na_2O$ at an appreciable rate to yield an insoluble oxide and sodium metal. Possible choices for oxide gettering are vanadium, titanium, and zirconium, or their alloys.

In an effort to assess the corrosive nature of the sodium polysulfide electrode towards beta"-alumina, discs of the ceramic electrolyte were sealed into pyrex ampoules with various $Na_2S_x$ compositions ranging from pure sulfur to $Na_2S_2$, and heated to 450°C for a period of one to fifty days. Optical microscopy, scanning electron microscopy, and weight-loss determinations indicated that the electrolyte is in fact stable towards the positive electrode material under static conditions. Therefore, the observed sulfur-side attack of the electrolyte is most likely due to processes occurring during current flow. Electrochemical experiments on Na/S cells are underway to examine the nature of dynamic sulfur-side attack of the beta"-alumina electrolyte.

Publications

1. D.C. Hitchcock and L.C. De Jonghe, "Solid Electrolyte Degradation with Applied Stress", LBL-18218 (July, 1984).

2. C. Mailhe, "Electrochemical Processes at the Sodium/Sodium Beta"-Alumina Interface", LBL-17687, MS Thesis (May, 1984).

Improved β"-Alumina Oxide Electrolytes Through Transformation Toughening

(F.F. Lange, Rockwell International Science Center)

The use of tetragonal $ZrO_2$ to toughen ceramics (transformation toughening) is now well established both experimentally and theoretically, and reviews have been published. This approach has been applied to several ceramic systems, including recently Na β"-$Al_2O_3$. This material, along with Na β-$Al_2O_3$, are conductors of sodium ions and as such, are being used as a solid electrolyte in high-specific-energy batteries, e.g., the sodium/sulfur battery. The technical feasibility of this battery has been demonstrated, but its lifetime is often limited by degradation of the β"- or β-$Al_2O_3$ electrolyte. Two failure modes have been identified, and analysis of one of these modes indicates that the critical current density for initiation of failure depends on the fracture toughness of the β"-$Al_2O_3$. It is feasible, therefore, that improvements in the mechanical properties of the electrolyte have the potential to improve the reliability of the Na/S battery.

The objectives of this project are to fabricate β"-$Al_2O_3$/$ZrO_2$ composites by an alternative procedure to the dry-pressing route and to determine the amount of $ZrO_2$ that can be used to maximize the strength/ionic resistivity ratio. The fabrication technique chosen was that of slip casting, as this approach should allow the $ZrO_2$ phase to be well dispersed without the detrimental presence of agglomerates, which can act as failure origins in ceramics.

During this year, effort was concentrated on improving the dispersion and mixing of the β"-$Al_2O_3$ and $ZrO_2$ powders, determining the effect of the $ZrO_2$ phase on $Na^+$ conductivity, and determining the role of $ZrO_2$(t) on strengthening. It was shown that $ZrO_2$(t) additions not only increase fracture toughness, but also limit the size of the β"-$Al_2O_3$ grains. The strengthening produced by $ZrO_2$(t) was thus due to two

concurrent phenomena, viz., an increased $K_c$ and a limitation on the large, abnormal $\beta''$-$Al_2O_3$ grains which are the major flaw population in the single-phase material. This was shown by incorporating cubic $ZrO_2$, which did not significantly increase $K_c$ but did result in some strengthening due to its effect of limiting abnormal grain growth. Failure occurred from other processing flaws, viz., two-phase agglomerates and $ZrO_2$ hard agglomerates, indicating that further processing improvements will further increase strength.

Conductivity measurements at 300°C as a function of $ZrO_2$ content showed that the $ZrO_2$ reduced conductivity more than that expected from percolation theory; resistivity increased from 5.5 ohm-cm for single-phase $\beta''$-$Al_2O_3$ to ~7.5 ohm-cm for the composite containing 15 v/o $ZrO_2$ (tetragonal or cubic). Experiments, where the grain size of $\beta''$-$Al_2O_3$ was varied at constant $ZrO_2$ content, indicated that the conductivity was controlled by both the inert $ZrO_2$ phase and its effect of limiting grain growth to produce a smaller-grained material. These results suggest that the composite which is optimized for both strength and conductivity would contain between 10 to 15 v/o $ZrO_2$(t).

## Principles of Superionic Conduction

(B.J. Wuensch, Massachusetts Institute of Technology)

The objective of this program is to provide insight into the factors which control fast alkali ion conduction in materials of potential relevance to battery systems. Exploratory syntheses and electrical conductivity measurements are performed on promising new structure-types, or on new compositions of known conductors which have been modified by crystal-chemical substitution. In systems in which transport is found to be especially sensitive to composition or temperature, the conduction mechanism is examined through neutron scattering analysis of the changes in the structural framework which accompany chemical substitution, and also the distribution and thermal-vibration amplitudes of mobile alkali ions.

Under investigation as potential new fast-ion conducting materials is a family of alkali silicates, $A^{+}_{2+x}M^{3+}_{x}M^{4+}_{1-x}Si_6O_{15}$. The structures of type compounds $K_2TiSi_6O_{15}$ and $K_3NdSi_6O_{15}$ were recently established by Russian workers, but their electrical properties have not been previously examined. The structures consist of $MO_6$ octahedra and $SiO_4$ tetrahedra, which form a system of connected channels. The alkali ions occupy interstices and display the unusually large thermal vibration amplitudes which are the hallmark of a shallow potential well and a characteristic of fast-ion conduction. Moreover, the possibility of substituting octahedral cations of different radius and charge provides a means for varying vacancy/charge-carrier concentration and framework geometry with a degree of flexibility analogous to that available in the NASICON system. The high silica content of these phases resulted in glass formation when synthesis was attempted by solid-state reactions. Hydrothermal synthesis was therefore employed. Synthesis of the prototype K-Ti and K-Nd phases has been successfully achieved by this method. A series of glass solid solutions have been prepared in six different systems as starting charges for further hydrothermal reactions with $A^{+}$ = Na, K; $M^{4+}$ = Ti, Zr; $M^{3+}$ = Y, Nd, La and x = 0, 0.5 and 1.0. As these glasses have compositions somewhat analogous to the highly-conducting "NASIGLAS", $Na_{1+x}Zr_{2-x/3}Si_3P_{3-x}O_{12-2x/3}$ studied at Argonne National Laboratory, it was felt that these materials might have useful conductivities in glassy form. Moreover, a comparison of the transport properties of a given composition when in amorphous and, eventually, in crystalline form would be of interest in understanding the transport properties of the system.

Accordingly, prior to performing the hydrothermal syntheses, complex impedance analyses of the glass specimens have been performed as a function of temperature, 350 to 660°C, and frequency, 50 Hz to 100 kHz, for glasses in the following systems:

| | |
|---|---|
| $K_2TiSi_6O_{15}$ - $K_3YSi_6O_{15}$ | $Na_2TiSi_6O_{15}$ - $Na_3YSi_6O_{15}$ |
| $K_2TiSi_6O_{15}$ - $K_3NdSi_6O_{15}$ | $Na_2TiSi_6O_{15}$ - $Na_3NdSi_6O_{15}$ |
| $K_2TiSi_6O_{15}$ - $K_3LaSi_6O_{15}$ | $Na_2ZrSi_6O_{15}$ - $Na_3YSi_6O_{15}$ |

Activation energies were found to range from 16.6 to 18.9 kcal/mole and 20 to 23 kcal/mole for the Na and K glasses, respectively. A comparison of the properties of the glasses is interesting in that the number of octahedral and tetrahedral ions in the framework remains fixed in all compositions, unlike previous studies of the transport properties of soda-silica or soda-lime-silica glasses in which a change in charge carrier concentration was invariably coupled with a change in network structure. The pre-exponential term, $\sigma_0 T$, in the present work was found to increase in proportion to alkali content, indicating that a constant fraction (or all) of the alkali ions are mobile. Activation energy decreased with increasing alkali content (as has been found for other alkali-silicate glasses), but a striking linear correlation of activation energy with ionic radius of the octahedral cation was found, independent of the alkali concentration. The influence of framework composition on activation energy for transport thus seems primarily a change in mobility effected by an opening of the glass structure. The conductivity at 350°C for several Na glasses is quite respectable, being as large as $10^{-4}$ $ohm^{-1}$ $cm^{-1}$ for the Na-Y glass. Addition of the high-valence network cation does not decrease the ionic conductivity as had been found in some previous studies. Several Na compositions have $\sigma_{350}$ equal to that of a pure alkali-silicate glass of comparable Na content. The relatively high conductivities found for glasses in these systems and the significant effect of chemical substitutions on transport properties strongly suggest that interesting results will be obtained for the crystalline forms of these phases.

## Electrical Conduction and Corrosion Processes in Fast Ion-Conducting Glasses

(H.L. Tuller, Massachusetts Institute of Technology)

A major objective of this research program has been to develop glasses that exhibit fast ion conduction (FIC) in the temperature regime of interest (<350°C) for Li/S batteries, and that also possess the physical attributes which eliminate the shortcomings of ceramic components, such as current-blocking grain boundaries, anisotropic ion transport (e.g., in β"-alumina), high-temperature fabrication and relatively large wall thickness. In particular, attention was focused on the transport,

electrochemical, and corrosion-resistant properties of alkali ion-conducting glasses.

A major accomplishment in 1984 was the development of a novel electrochemical method that is capable of simultaneously determining the electrolytic and chemical stabilities of solid electrolytes, and thereby identifying glasses with the requisite chemical stability. Using this method, data are generated continuously and in-situ, rendering this technique very powerful for rapidly screening potential solid electrolytes. Specifically, electrochemical cells of the type LiAl/glass/LiSn/glass/LiAl, which include a working and reference cell, were used to vary and monitor the activity of lithium $a_{Li}$ from extremely low values in the Sn (initially-pure) inner electrode to values approaching unity by controlled titration from one of the LiAl reference electrodes. When the activity at which the electrolyte reacts with the titrated species is exceeded, an arrest in the emf-versus-time plot is detected. Further, by monitoring the time delay for which particular activities of lithium are achieved in the LiSn alloy electrode, the kinetics of Li penetration into the glass and the resulting growth of reaction layers on specific glass electrolytes are deduced.

This method was applied to investigate FIC Li-borate glasses, and the following features were established:

- The glass composition $Li_2O.B_2O_3$, which contained 2 mol% $Al_2O_3$ to suppress crystallization in the melt, behaved as a perfect Li-ion electrolyte over a wide range of Li activity (up to 0.08 at 380°C) and temperature (320-400°C). This type of glass was successfully used both to titrate Li in an electrochemical cell and to monitor activities of Li in open-circuit cells.

- The aforementioned glass was found to serve as an ideal electrolyte. This feature was used to determine the solubility and thermodynamic properties of Li in molten Sn, the working electrode in the electrochemical cell.

- The chlorine-containing glass composition, $Li_2O.B_2O_3.LiCl$, was found to react with Li at very low activities ($\simeq 10^{-9}$), and it formed a crystalline reaction layer of composition $3Li_2O.B_2O_3$. The growth of the layer was found to be diffusion controlled. The reaction layer was predominantly ionic in nature and did not interfere with the passage of current across the cell. When the reaction layer grows too thick, however, the volume mismatch between it and the glass substrate can cause cracking.

- The chemical diffusion coefficient in the reaction layer was measured using the above approach. It was about 1 x $10^{-9}$ $cm^2/s$ at 380°C, and the activation energy for diffusion was ~0.7eV. Diffusion of electrons across the reaction layer was found to be rate limiting.

- The effect of the electric field on the reaction kinetics was not large, but given sufficient time its effect could be detected by the induced asymmetry in the reaction layers.

AC impedance measurements were begun on a series of glasses based on lithium diborate, to which CaO was added in the range of 1-10% $(CaCO_3)_2/Li_2O_3$. These glasses showed an unexpected increase in conductivity with respect to the CaO-free glass, peaking at about 2%. Work is continuing to confirm these results, as well as extending these measurements to other glasses containing lithium and borates.

Publications and Presentations

1. H.L. Tuller, M.W. Barsoum, "Glass Solid Electrolytes: Past, Present and Near Future--the Year 2004," Symposium on Glass Science and Technology, Vienna, July 1984.

2. H.L. Tuller, "Fast-Ion Conducting Glasses: Theory and Applications," Metallurgy, Materials Science Colloquium, Columbia University, N.Y., October 1984.

3. M.W. Barsoum and H.L. Tuller, "Novel Electrochem. Methods for the Determination of Solid Electrolyte Stability Domains", Presented at the Fall Meeting of the Electrochemical Society, New Orleans, LA, Oct. 1984.

4. M.W. Barsoum and H.L. Tuller, "The Reaction Kinetics and Electrochemical Stability Domains of Amorphous Li-Borate Based Solid Electrolytes," Presented at the Fall Meeting of the Electrochemical Society, New Orleans, LA, October 1984.

Evaluation of New Lithium-Conducting Glasses

(E.J. Cairns and F.R. McLarnon, Lawrence Berkeley Laboratory)

Several borate glasses have been developed that, upon addition of $Li_2O$ and LiCl, show lithium-ion conductivities as high as 2 x $10^{-2}$ $ohm^{-1}$ $cm^{-1}$ at 300°C. It has also been observed that the structure of the glasses is maintained in the presence of molten lithium. The aim of this investigation is to construct and operate a Li/S or Li alloy/S cell that employs a borate fast-ion-conducting glass as the electrolyte.

A succcessful procedure for making and blowing lithium--chloroborate glass into thin-walled sealed tubes has been developed. These tubes have been tested statically for stability in molten sulfur/polysulfides at 380°C. A thin white film was observed to form on the glass in the polysulfide melts. The composition of this film and its effect on conductivity are not yet known.

Several electrochemical cells have been constructed using the thin-walled tubes, but each has experienced mechanical failure within a few hours at 380°C. Current work is directed at eliminating the mechanical problems of cell assembly which appear to be causing the failures.

Glass Electrolytes and Advanced Cell Concepts

(M. Roche, Argonne National Laboratory)

The objective of this research project is to develop a glass electrode that has high ionic conductivity ($10^{-2}$ohm$^{-1}$cm$^{-1}$ at 300°C), is stable in the sodium/sulfur cell environment, and can be fabricated at reasonable cost. Earlier experiments, thermodynamic calculations, and a review of the literature led to the selection of soda-rich glasses in the soda-alumina-zirconia-silica system.

During the past year, 24 glass compositions in the above system were prepared and characterized. Resistivity, activation energy for conduction, and glass transition temperature were determined as a function of composition. These data have been analyzed by multiple linear regression to permit prediction of the properties of all glasses of interest in the quaternary system. The soda-rich quaternary glasses (38 to 42 mol% soda) had conductivities of 2 to 8 x $10^{-3}$ ohm$^{-1}$cm$^{-1}$, activation energies for conduction of about 0.5 eV, and glass transition temperatures of 500 to 700°C.

The glasses were subjected to static corrosion tests in high-purity sodium, sulfur, and sodium tetrasulfide at 400°C for 1000 h; Ceramatec beta"-alumina and Dow borate glass were included in these corrosion tests for comparison of their properties with those of the quaternary silicate glasses. For purposes of identification of the most promising glass compositions, the corrosion tests were carried out at a

temperature higher than the normal operating temperature (about 330°C) of the sodium/sulfur cell.

Four of the soda-rich quaternary glasses, the beta"-alumina ceramic, and the Dow borate glass survived the corrosion tests with relatively low weight changes (less than 0.8 $mg/cm^2$) in all three environments. Detailed examinations of these samples using scanning electron microscopy, optical microscopy, and Auger electron spectroscopy are in progress. However, a few preliminary observations are worthy of note. The beta"-alumina was blackened by exposure to sodium; the Dow glass was not; however, the Dow glass exhibited some yellowing and internal cracking in the $Na_2S_4$ test. The surfaces of some of the soda-rich quaternary glass samples were blackened in the sodium test, but experimental evidence indicates that this blackening was due to reduction of impurities such as iron. The soda-rich quaternary silicate glasses, which are made with high-purity quartz instead of 99.9% pure silica, are transparent after the sodium-exposure test and show only a minor surface discoloration. In general, the glass and ceramic samples survived the sulfur corrosion test with only minor (or no) surface damage. However, at very high soda concentrations (about 46 mol%), sodium sulfate was detected on the glass surfaces. Sodium sulfate is the expected product of the sulfur-soda reaction.

In-cell verification tests in single-tube cells have been initiated using electrolyte tubes fabricated (drawn from the melt at 950°C) from one of the quaternary glasses that survived the corrosion test, i.e., P-glass (41.4 mol% $Na_2O$, 8.2 mol% $Al_2O_3$, 5.8 mol% $ZrO_2$, balance $SiO_2$). A Na/P-glass/S cell, with the sulfur electrode inside the tube, was operated for 100 h (eight cycles) before sulfur evaporation from the open-ended tube forced termination of the test. A method for sealing the glass tube is now being developed.

Future efforts in this program will focus on studying glass corrosion resistance and structure/property relationships. Also, in-cell verification tests will be continued to determine the cycle life of electrolyte tubes.

Publication

1. G. H. Kucera and M. F. Roche, "Investigation of Sodium-Ion Conducting Glasses in the $Na_2O$-$ZrO_2$-$Al_2O_3$-$SiO_2$ System," Extended Abstracts Vol. 84-2, Fall Meeting of the Electrochemical Society, New Orleans, LA, October 7-12, 1984.

## Transport Properties of Sodium-Polysulfide Melts

(J.S. Newman, Lawrence Berkeley Laboratory)

Sodium/sulfur cells are attractive for both vehicle propulsion and utility load-leveling applications. Because the rate-limiting process at the sulfur cathode is the diffusion of charged species within the melt, optimal design of sulfur electrodes will depend upon the availability and accuracy of diffusion-coefficient data for polysulfide melts. An experimental apparatus has been designed to measure the diffusion coefficient of sodium ions in melts of sodium polysulfides.

The method of restricted diffusion is being used to determine differential diffusion coefficients in sodium-polysulfide melts. The experimental apparatus to perform the measurements has been modified and tested. A model of the transport processes in the sodium-sulfur melts has been developed, and fundamental system parameters have been determined.

Diffusion-coefficient data in sodium-sulfur melts will be measured as a function of melt composition and temperature. Fundamental interaction parameters defined in the recently developed model of transport processes in sodium-sulfur melts will be determined and compared to the previous results.

## Mathematical Modeling of Sulfur Electrode

(E.J. Cairns and F.R. McLarnon, Lawrence Berkeley Laboratory)

Mathematical models of the sodium/sulfur cell have been developed, usually to provide improved understanding of the operation of the sulfur electrode. These are one-dimensional models and therefore have limited capability to account for phenomena such as convection, which require a two- or three-dimensional framework. Examination of the physical

properties of sulfur and sodium polysulfides leads to the conclusion that variations in density, viscosity, and wetting cannot be ignored. Work is underway to develop a two-dimensional model of a tubular sodium/sulfur cell, which accounts for the actual behavior of an operating cell. In addition to computer modeling, electronic and ionic potential profiles will be measured throughout the cathode via the use of small reference electrodes.

## E. CORROSION PROCESSES IN HIGH-TEMPERATURE, HIGH-SULFUR-ACTIVITY MOLTEN SALTS

### Behavior of Materials in Sulfur-Polysulfide Melts

(E.J. Cairns and F.R. McLarnon, Lawrence Berkeley Laboratory)

In order to better understand the behavior of various metals for use as current-collector and cell-container materials in sodium/sulfur and lithium/sulfur cells, two types of studies were performed: 1) cyclic voltammetry in $Na_2S_4$ and $Li_2S_{3.8}$ (both of which are representative of single-phase polysulfide melt compositions) molten-salt electrolytes at chromium and molybdenum electrodes, and 2) static corrosion tests of molybdenum, chromium and a 70% Cr-30% Fe alloy in both lithium and sodium polysulfides and molten sulfur. The sodium-polysulfide voltammetry was conducted at 300 and 350°C, and lithium-polysulfide voltammetry was performed at 400°C. The voltammetry experiments employed sweep rates ranging from 5 to 500 mV/sec, and the electrode potentials covered the full range expected in the respective cell systems. The static corrosion tests were performed at 350°C in $Na_2S_3$, 400°C in $Li_2S_{3.8}$, and at both temperatures in molten sulfur. Samples were prepared in the form of flat disks to minimize geometry effects, and the samples corroded at 400°C were analyzed (after cutting, mounting and polishing) by SEM, EDAX and X-ray diffraction techniques. The samples corroded at 350°C were analyzed by SEM and EDAX methods only.

The design of the cell used in the voltammetry experiments has been described elsewhere (Publication 1). Data from these experiments were compared with sodium-polysulfide voltammetry data reported in the literature, which had been gathered using carbon, aluminum and platinum

electrodes. A model was developed to help understand the results of cathodic sweeps in both systems, and the different results for the various metal/melt combinations are explained using thermodynamic and electrochemical arguments.

The data from the static-corrosion studies were compared with reported corrosion mechanisms of the same metals and alloys in sulfur vapor, and the possible influence of solubility of the scale in the melts was measured, as well as rate data for the corrosion of the three materials in sulfur and $Li_2S_{3.8}$.

Publications


1. J.C. Dobson, F.R. McLarnon and E.J. Cairns, "Corrosion of Metals by Sulfur/Polysulfide Melts", 166th Meeting of the Electrochemical Society, New Orleans, LA (1984), p. 163, Paper No. 110.

2. E.J. Cairns, G. Mamantov, R.P. Tischer, and D.R. Vissers, "The Chemistry and Status of Rechargeable Molten-Salt Batteries", in Proceedings of the Fourth International Symposium on Molten Salts, 84-2, Edited by M. Blander, D.S. Newman, G. Mamantov, M-L. Saboungi, and K. Johnson, The Electrochemical Society, Inc., Pennington, NJ (1984) p. 312; LBL-18103.

3. E.J. Cairns, "High Temperature Batteries and Battery Materials", 166th Meeting of The Electrochemical Society, New Orleans, LA (1984), p. 150, Paper No. 101; LBL-17762.


Polysulfide Containment Materials

(J.E. Battles, Argonne National Laboratory)

The objective of this task is to develop new alloys for positive-side current collection and containment in Na/S and $Li/FeS_2$ cells, or other cells with high sulfur activity and high electrical potential at the positive electrode. During the past year, static corrosion testing was continued in sulfur and sodium polysulfides at 350°C for various metals and several commercial, high-chromium alloys. Extensive metallographic, X-ray diffraction, and SEM-EDS analyses are used for characterization of the corrosion products, microstructure, and composition.

A comparison was made of the data for all of the metal and alloy systems that have been corrosion tested so far (listed in Fig. 1). The corrosion behavior was found to change significantly on going from sulfur to sodium polysulfide ($Na_2S_3$) because of a change in the scale composition and morphology. For materials tested in sulfur, the corrosion scale is generally multi-layered and composed of simple metal sulfides, and the corrosion rate appears to be controlled by ionic diffusion through the scale. This produces parabolic kinetics when a dense scale is formed and logarithmic kinetics when a porous inner scale is formed. The results for materials tested in $Na_2S_3$ are summarized in Table 1. With $Na_2S_3$, the corrosion scales are more complex and are generally composed of ternary sodium-metal sulfides, most of which are at least partially soluble in the polysulfide. This creates considerable variation in the corrosion kinetics, as shown by the data in Fig. 1.

Based on a comparison of results obtained for chromium and other metals and alloys, chromium demonstrates relatively unique corrosion behavior in that the corrosion rate is lower in $Na_2S_3$ than it is in sulfur, whereas the opposite is true for other materials. The corrosion reactions for chromium in $Na_2S_3$ and sulfur (to 2500 h) obeyed logarithmic and parabolic rate laws, respectively. In both media, the corrosion scale was bilayer, with the inner layer being $Cr_3S_4$. The outer layer was $Cr_2S_3$ for corrosion in sulfur and $NaCrS_2$ for corrosion in $Na_2S_3$.

Commercial high-chromium alloys have also been corrosion tested, in addition to the E-Brite-26-1 and Nichrome alloys reported previously. The nominal compositions of these alloys are given in Table 2. In sulfur, the corrosion rates of these new alloys were lower than those for chromium alone. Further, the corrosion rate decreased as the chromium content of the alloy decreased, as shown in Fig. 2. The reverse effect was found for the corrosion of these alloys in $Na_2S_3$, i.e., the corrosion rate increased as the amount of chromium in the alloy was decreased, and the corrosion rates of the alloys were higher than those for chromium alone. For the alloys with molybdenum and tungsten additions tested in $Na_2S_3$, the scale showed little tendency toward spalling; this effect did not occur with the E-Brite-26-1 alloy, where extensive

spalling occurred. In all cases, the scale was a single layer of primarily $NaCrS_2$, with the formation of crystals of either $Na_3FeS_3$ or $NiS_2$ in the melt. A series of modified E-Brite alloys has now been prepared to test the effect of additional alloying elements, i.e., Al, Ti, Y, and Zr.

The corrosion rate of aluminum in sulfur was very low. However, this was not the case for aluminum in $Na_2S_3$, where the corrosion rate was about two orders of magnitude higher. The reaction kinetics followed a parabolic rate law, at least up to 1000 h, and the rate constant was about thirty times larger than that for chromium in sulfur (see curves 5 and 10 in Fig. 1). The scale formed on the aluminum tested in the $Na_2S_3$ appeared as a layer of crystallites, and some of the crystals had diffused into the melt. The composition of the crystals has not been fully determined, although they are probably a sodium-aluminum-sulfide with an $Na_2S:Al_2S_3$ ratio higher than in $NaAlS_2$.

An aluminum-9.6 wt % magnesium alloy was also corrosion tested. In $Na_2S_3$, the corrosion reaction for this alloy was effectively eliminated by the formation of a passivating layer of MgS on the metal surface, as suggested by curve 7 in Fig. 1. The corrosion testing of additional alloys of aluminum-magnesium is planned.

Publications

1. A.P. Brown and J.E. Battles, "The Direct Synthesis of Sodium Polysulfides from Sodium and Sulfur", Synth. Reac. Inorg. Met. Org. Chem. 14, 945 (1984).

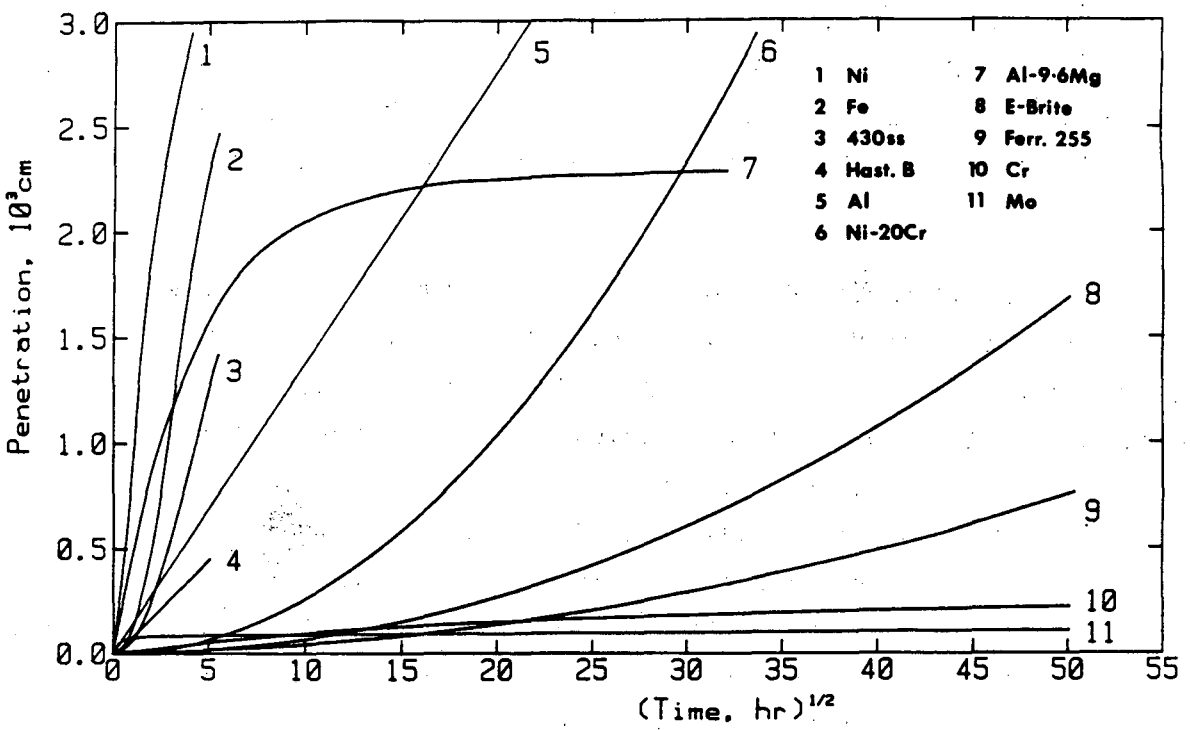


Figure 1. Corrosion Behavior of Various Metals and Alloys in $Na_2S_3$ at 350°C.

Table 1. Rate Laws and Probable Contributing Mechanisms for the Corrosion of Various Metals and Alloys in $Na_2S_3$ at 350°C.*

| Selected Materials | Rate Law | Mechanism |
|---|---|---|
| Molybdenum, aluminum-9.6 magnesium | 'Zero' order | Film Formation |
| Chromium, nickel | Logarithmic | Porous inner scale |
| | | Pore blocking |
| Aluminum, Hastelloy B | Parabolic | Ionic diffusion |
| Low Carbon Steel, Type 430 SS | Parabolic/ linear | Dissolution |
| High-chromium alloys | Mixed Linear/ Parabolic | Interfacial/Ionic Diffusion |

* In sulfur, these materials showed either logarithmic or parabolic corrosion kinetics.

Table 2. Nominal Composition of Commercial High-Chromium Alloys That Were Corrosion Tested

| Alloy | Nominal Composition |
|---|---|
| E-Brite-26-1 | Fe-26Cr-1Mo |
| Nichrome | Ni-20Cr |
| Cabot Alloy 230 | Ni-22Cr-14W-2Mo |
| Ferralium 255 | Fe-26Cr-3.3Mo-7Ni |
| Hastelloy C-22 | Ni-22Cr-13Mo-3Fe-3W |
| Hastelloy G-30 | Ni-29Cr-20Fe-5.5 Mo |

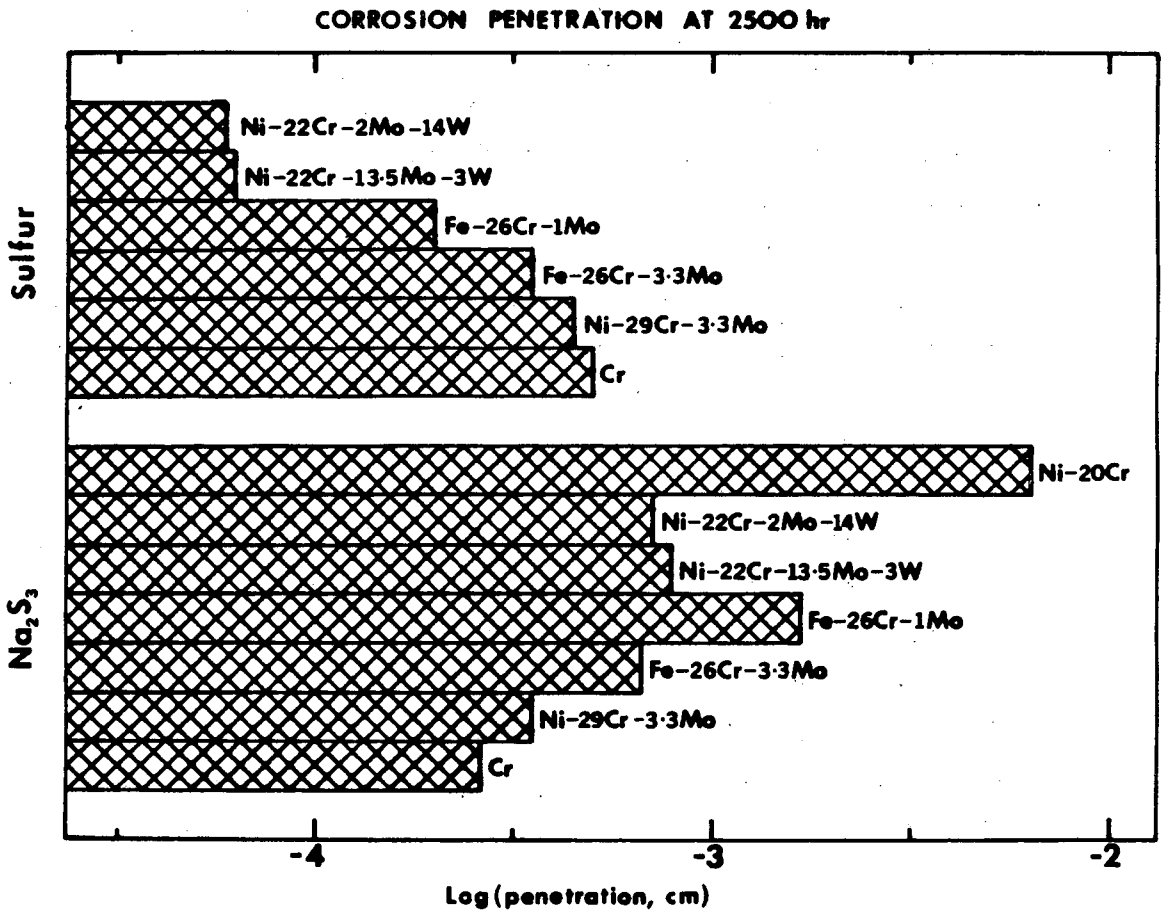


Figure 2. Corrosion Penetration of Various High-Chromium Alloys after 2500 h of Corrosion in Sulfur or $Na_2S_3$ at 350°C.

## Corrosion-Resistant Coatings for High-Temperature High-Sulfur-Activity Applications

(J.R. Selman, Illinois Institute of Technology)

The objective of this project is to explore molten-salt deposition and chemical vapor-deposition (CVD) as methods for preparing corrosion-resistant coatings of molybdenum, molybdenum carbide, or titanium nitride on low-carbon steel. The application of these coatings is in high-temperature sulfur-rich environments such as positive-electrode current collectors for Na/S and Li-alloy/$FeS_2$ batteries.

One of the keys to producing a strongly adherent, defect-free deposit of molybdenum on low-carbon steel is by the use of a nickel interlayer. The first stage of this program involved the evaluation of several commercially-feasible techniques for producing a uniform nickel deposit on 1018 steel. Several electroplating and electroless plating techniques were evaluated. Electroplating is capable of producing a strong defect-free deposit of pure nickel, while the advantage of electroless plating is that it can produce a uniform layer of nickel on all faces of an object at the same time. The disadvantage of electroless nickel plating is that the nickel deposit is not pure but contains as much as 1% phosphorous. It is not known at the present time if the presence of these impurities will interfere with the CVD process. Therefore, samples of 1018 steel were cut and coated by both techniques using a commercial electroplating-bath formulation that produced a very pure nickel deposit and a basic electroless plating bath that exhibited excellent long-term stability. Both sets of samples are being coated with molybdenum via CVD, and the adherence and uniformity of the Mo layer will be evaluated by scratch testing and by microscopic examination. Final selection of the optimum method for depositing the nickel interlayer will be made, and corrosion tests in molten-salt baths will then be initiated.

## F. COMPONENTS FOR AMBIENT-TEMPERATURE LITHIUM CELLS

### Surface Layers on Battery Materials

(R.H. Muller, Lawrence Berkeley Laboratory)

The purpose of this work is to advance the understanding of the properties of surface layers on battery electrode materials that are important for the functioning of rechargeable galvanic cells with high energy and power capabilities, high energy efficiency, acceptable charge retention and long cycle life. Means are sought to achieve superior, predictable properties of surface layers and to form them consistently in order to provide enhanced battery operation. Present studies concern surface layers on lithium in representative nonaqueous battery electrolytes and oxide formation on metals in aqueous media.

Surface layers formed on Li in $LiClO_4$/propylene carbonate with <1 ppm water content have been analyzed. IR spectroscopy showed the formation of $Li_2CO_3$ and a polymeric compound. ESCA analysis of the surface layer formed on electrochemically-deposited Li indicated the formation of two types of carbon compounds, related to the formation of $Li_2CO_3$ and polymer. ESCA analysis also showed that $LiClO_4$ decomposes to chlorine compounds with lower valency, with the higher-valent chlorine found in the outer film regions, lower-valent in the inner. In-situ X-ray diffraction confirmed the formation of $Li_2CO_3$ and polymeric compounds. An SEM study of the surface of electrodeposited Li showed a porous structure.

In-situ X-ray diffraction has been developed to study surface layers formed on lithium during deposition from nonaqueous electrolytes. Because of the high reactivity of lithium, use of in-situ techniques for the characterization of surface layers is essential. A collimated X-ray beam is directed toward the electrode surface at a glancing angle (6° from the surface) in order to enhance sensitivity for the surface region, and the diffracted X-rays are measured by a rotating detector. The cell containing the electrode was made of polypropylene and contained the working electrode of 1.9-cm diameter in the center, surrounded by a 3-mm wide counter electrode. A lithium reference electrode of 3-mm diameter was located between the working and counter electrodes.

Electrolyte could be injected and removed from the cell by the use of two syringes, which were connected to the cell with Teflon spaghetti tubing. Electrodes and electrolyte were separated from the atmosphere by a polyethylene or Mylar window of 0.3 mm thickness, through which the X-ray beam enters and exists. Permeation of water through the cell window from air over the time of the measurement was found to be negligible.

Three tests have been used to determine the stability of solutions of two nonaqueous solvents, propylene carbonate and 2-methly-tetrahydrofuran and their solutions of $LiAlCl_4$, $LiAsF_6$ and $LiClO_4$ in contact with lithium. The procedures identify the effect of surface layers, open-circuit stand, and anodic and cathodic polarization. They employ (1) contact with liquid Li amalgam and solid-sheet Li; (2) open-circuit potential measurements of cathodic deposits, and (3) anodic dissolution of deposits with ramped potential. The stability of solvents is found to depend on the dissolved electrolyte. Polymeric materials containing other products of the reaction between metal and electrolytes have been collected and identified by X-ray diffraction.

Publications


1. Gh. Nazri and R.H. Muller, "Surface layers on Lithium in Organic Battery Electrolytes", 35th Meeting of the International Society of Electrochemistry, Berkeley, CA, August 5-10, 1984. Extented Abstracts A4-16 (LBL-17710, May 1984).

2. Gh. Nazri and R.H. Muller, "In-Situ X-Ray Diffraction of Surface Layers on Lithium in Nonaqueous Electrolyte", submitted to J. Electrochem. Soc. (LBL-18194, July 1984).

3. Gh. Nazri and R.H. Muller, "Stability of Nonaqueous Electrolytes for Ambient-Temperature Rechargeable Lithium Cells", submitted to Chem. Engr. Comm. (LBL-18497, September 1984).

4. F. Schwager, Y. Geronov and R.H. Muller, "Ellipsometric Studies of Surface layers on Lithium", accepted by J. Electrochem. Soc. (LBL-13656 Rev., September 1984).

5. Gh. Nazri and R.H. Muller, "Composition of Surface Layers on Li Electrodes in PC, $LiClO_4$ of Very Low Water Content", submitted to J. Electrochem. Soc. (LBL-18197, September 1984).

6. Gh. Nazri and R.H. Muller, "Effect of Residual Water in Propylene Carbonate on the Nature of Films Formed on Lithium", submitted to J. Electrochem. Soc. (LBL-16094, August 1984).

Metal Couples in Non-Aqueous Electrolytes

(C.W. Tobias, Lawrence Berkeley Laboratory)

The objective of this project is to explore practical alternatives to aqueous, or high-temperature molten salt-systems, for the efficient electrochemical reduction and oxidation of reactive metals.

UV-visible spectroscopy experiments of iodine and bromine solutions have demonstrated that the stable form of the halogen in propylene carbonate (PC) is the trihalide. In the case of iodine, the equilibrium constant of the disproportionation reaction at 25°C was determined to be 0.85. Gas-chromatography analysis showed that chlorine attacks even dried, distilled PC (less than 7 ppm water), and that the extent of the reaction increases with increasing water content of the solvent. However, solutions of iodine in PC are stable for several months.

Conductivity experiments were performed to determine the extent of ion-pair formation of KI and KBr in PC. In addition, the conductivity of these solutions was measured as a function of the concentration of the corresponding halogen. Increased conductivity was noted for each solution, and a maximum was observed for equimolar iodide and iodine concentrations.

Cyclic voltammograms of KI in supported ($KAsF_6$) propylene carbonate show two anodic peaks. To characterize the voltammograms, the following sequence of reactions is proposed:

$$3I^- \rightarrow I_3^- + 2e^- \qquad \text{(i)}$$

$$2I_3^- \rightarrow 3I_2 + 2e^- \qquad \text{(ii)}$$

The validity of this mechanism was tested in an optically-transparent thin-layer cell by performing simultaneous cyclic voltammetry and UV-visible spectroscopy at a narrow-mesh gold working electrode. The sequence of formation and disappearance of triiodide and iodine according to (i) and (ii) was confirmed by the spectral scans repeated at 30-

second intervals.

A transport model for the simulation of the voltammograms was developed in collaboration with M. Matlosz and J. Newman, which takes into account the presence of two-electron transfer steps; the fact that these steps have a complex (i.e. not 1:1) stoichiometry; the effect of mass transfer of the three species; and the kinetics of the charge-transfer reactions. Results indicate that reaction (i) is kinetically inhibited while reaction (ii) is reversible.

Publications


1. K.J. Hanson and C.W. Tobias, "The Electrochemistry of the Iodide/Tri-Iodide/Iodine Redox System in Propylene Carbonate", Fall Meeting of the Electrochemical Society, New Orleans, LA, Oct. 7-12, 1984, Extended Abstracts 140, p. 211; LBL-18335.

2. K.J. Hanson, M. Matlosz, J. Newman, and C.W. Tobias, "Theory of Cyclic voltammetry for Reactions having Complex Stoichiometry", 35th Meeting of the International Society of Electrochemistry, Berkeley, CA, Aug. 5-10, 1984. Extended Abstracts, p. 950; LBL-18335.

3. K.J. Hanson (Ph.D. Thesis) with C.W. Tobias, "On the Electrochemistry of Halogen Electrodes in Propylene Carbonate"; LBL-18335.


Polymeric Electrolytes for Ambient-Temperature Lithium Batteries

(G.C. Farrington, University of Pennsylvania)

The objective of this program is to investigate the chemical and electrochemical characteristics of polymeric electrodes and electrolytes that have been proposed for use in high-specific-energy batteries. Included in this study are polyacetylene materials and solid electrolytes based on complexes of poly(ethylene oxide).

Reduction of Polyacetylene: Polyacetylene $[(CH)_x]$ can be easily reduced, either chemically or electrochemically, to form complexes of the type, $(Li_yCH)_x$. These complexes have been suggested as anode materials for use in high-energy-density lithium batteries.

The reduction of polyacetylene in an electrolyte of $LiClO_4$ in tetrahydrofuran occurs with high coulombic efficiency for doping levels of $y>0.10$. Reduced polyacetylene in this composition range appears to be quite stable in this electrolyte. The potential of $(Li_yCH)_x$ is 0.5

to 1.5 V more positive than that of Li in the same electrolyte. Compared with Li as a battery anode, $(Li_yCH)_x$ has considerably lower gravimetric and volumetric energy densities and higher electrochemical potential.

These findings indicate that reduced polyacetylene is not an attractive alternative to Li electrodes for high-specific-energy rechargeable, non-aqueous-electrolyte batteries. On the basis of these results and previous studies of the characteristics of oxidized polyacetylene, there is no indication that it will be used widely in this class of battery.

Polymeric Solid Electrolytes: Polymer complexes formed between poly(ethylene oxide) (PEO) and various alkali metal salts, such as $LiClO_4$ and LiSCN, have been proposed as solid electrolytes for solid state, rechargeable batteries using lithium anodes and ion-insertion compounds as cathodes. These electrolytes have significant cationic and anionic transport numbers. By suppressing the cation transport rate, it might be possible to develop a new class of solid electrolytes for anions. One approach is to form PEO complexes with salts of divalent cations and monovalent anions, so that the higher charge on the cation would tend to trap it in the polymer.

It is possible to form PEO complexes with $MgCl_2$ and $PbCl_2$. The $MgCl_2$ complexes were prepared over a range of compositions, from $MgCl_2(PEO)_4$ to $MgCl_2(PEO)_{24}$. Similar compositions were prepared with $PbCl_2$. Conductivity measurements of the films were made by using complex ac-impedance analysis. Samples of the divalent halide films were compared with a sample of a standard film of $LiCF_3SO_3(PEO)_9$ and with a film of pure PEO. The best conductor was $MgCl_2(PEO)_{16}$, which has a conductivity of about $10^{-10}$ $(ohm\text{-}cm)^{-1}$ at 30°C, which is about an order of magnitude less than the $LiCF_3SO_3$ complex. However, the $MgCl_2$ complex had a higher conductivity than that of the $LiCF_3SO_3$ complex above 60°C.

These remarkable new complexes may be a general group of high-conductivity solid electrolytes for anions. They may also provide new approaches toward optimizing the conductivity characteristics of the more conventional complexes that conduct $Li^+$.

Publications

1. G.C. Farrington, "The Electrochemical Oxidation of Polyacetylene and its Battery Applications", J. Electrochem. Soc. 131, 7 (1984).

2. R. Huq and G.C. Farrington, "Stability of Undoped and Oxidized Polyacetylene", J. Electrochem. Soc. 131, 819 (1984).

Novel Membranes for Lithium Batteries

(M. Litt, Case Western Reserve University)

The objective of this project was to synthesize block polymers with alternating crystalline blocks and amorphous, $Li^+$-solvating blocks for use in ambient-temperature rechargeable lithium batteries. Two approaches to synthesize the amorphous blocks were considered. The first approach was to use polyethylene oxide and the second approach was to use a polyethyleneimine block.

The crystalline blocks were made by polymerizing 2R-Δ2-oxazolines to produce poly (2-acyl or 2-aroyl ethyleneimines), which can crystallize into uniform lamellar domains. The amorphous blocks can also form lamellar domains. Thus, a film which consists of crystalline and amorphous blocks would exhibit high permeability through the amorphous domains and would have good mechanical strength because of the crystalline domains.

Initial experiments with poly (p-toluyl ethyleneimine) as the crystalline block were not successful. The blocks crystallized only with great difficulty, and the multiblock polymer was unstable due to the synthesis used to make it. In another series of experiments, poly(ethylene glycol) ditosylate was used as the initiator for polymerization of 2-isobutyl Δ2-oxazoline. This procedure should give a triblock polymer consisting of two crystalline blocks at the ends with an amorphous (or low melting) PEG (poly(ethylene glycol)) central block. However, initiation was very slow, which was contrary to previous experience and literature reports on tosylate esters. This slow initiation led to a mixture of di- and tri-block polymers with a broad molecular-weight distribution.

Monodisperse blocks of poly (N-isovaleryl ethyleneimine) were synthesized using a new reactive difunctional initiator. The living ends of the polymer were reacted with various diamine coupling agents. While coupling occurred, it stopped at about 50% reaction. Further heating tended to cleave the block polymers. Therefore, a new coupling method was used which finally gave reasonable block copolymers. Two-ended, monodisperse poly(N-isovaleryl ethyleneimine) with active ends was hydrolysed to transform the ends to hydroxyethyl amide groups. The Na salt of the hydroxyl end was formed and reacted with PEG ditosylate to make the block copolymer. While the reaction was still not complete, the final polymer had good mechanical strength, and it melted at the same temperature as the homopolymer. The unoriented films showed isotropic swelling, while the oriented films showed reversible anisotropic swelling in water (swelling was almost completely in the film plane). This is exactly what is expected if domains are oriented with the long axis perpendicular and the short axis parallel to the film surface. X-ray diffraction showed good crystallite orientation.

Due to the difficulties encountered in the synthesis procedures required to make the polymer films, effort on this project was ended.

Publications


1. A.X. Swamikannu and M.H. Litt, "Preparation and Characterization of p-Toluene Sulfonyl Ester and Amino Derivatives of Tri- and Poly(ethylene Glycol)", J. Polymer Sci, Chemistry Ed. 22, 1623 (1984).

2. M.H. Litt and A.X. Swamikannu, "Block Copolymers of Poly(ethylene Glycol) and Poly(N-isovaleryl Ethyleneimine)", Polymer Preprints 25, 242 (1984).

## G. CROSS-CUTTING RESEARCH

### Analysis and Simulation of Electrochemical Systems

(J.S. Newman, Lawrence Berkeley Laboratory)

The object of this program is to improve the performance of electrochemical cells used in the inter-conversion of electrical energy and chemical energy. Experiments and mathematical models are designed to identify the physical phenomena that govern these systems. The phenomena involved may include hydrodynamics, convective and diffusive mass transfer, ohmic potential drop, charge transfer, and heterogeneous and homogeneous kinetics. A thorough understanding of the interactions among the phenomena governing a given system leads to mathematical models that agree with experiment and predict system behavior. The models are useful in the identification of important parameters, and aid in the design and scale-up of electrochemical systems.

A mathematical model is being developed to calculate the concentration, potential, and current distribution in a thin-gap flow cell. While previous models have assumed that the inter-electrode gap is much larger than the diffusion boundary-layer thickness, the present model allows the gap to be thin enough for the diffusion-boundary layers to interact. In addition, the effects of multiple reactions at the electrodes are considered. This mathematical model requires the solution of the convective diffusion equation for concentration, and Laplace's equation for the potential. When the cell is operated below limiting current, the boundary conditions are complicated by the fact that, due to kinetic limitations, the concentrations vary along the electrode surfaces.

The Li-Al/$FeS_x$ battery is a candidate for electric vehicle propulsion and energy storage. Many aspects of its behavior, however, are poorly understood. A theoretical study reveals important system parameters, and suggests experiments that provide information needed to improve the design and operation of the battery. The mathematical model of the Li-Al/FeS battery has been used to predict important operating characteristics. A general energy balance for battery systems was developed and incorporated into the model.

A mathematical model of secondary battery systems with soluble active material has been developed. This model incorporates concentrated-solution theory to predict the effect of redistribution of active material on the cycle life of the battery. The development is general, and is useful in the design of battery systems encountering shape change problems, such as the Zn/NiOOH battery.

Publications


1. Tim Risch and John Newman, "A Theoretical Comparison of Flow-Through and Flow-By Porous electrodes at the Limiting Current," J. Electrochem. Soc. 131, 2569 (1984).

2. Alan Hauser, "The Corrosion of a Zinc Rotating Disk in One Molar Hydrochloric Acid," M.S. Thesis, April, 1984; LBL-17461.

3. John Van Zee, Greg Klein, Ralph E. White, and John Newman, "Extension of Newman's Numerical Technique to Pentadiagonal Systems of Equations", Electrochemical Cell Design, Ralph E. White, editor, Plenum Press, New York, NY (1984), p. 377.

4 Dawn Bernardi, Ellen Pawlikowski, and John Newman, "A General Energy Balance for Battery Systems", submitted to the Journal of the Electrochemical Society; LBL-17776 (1984).


Electrode Kinetics and Electrocatalysis

(P.N. Ross, Lawrence Berkeley Laboratory)

The objective of this project is to develop an atomic-level understanding of the processes taking place in complex electrochemical reactions at electrode surfaces. Physically-meaningful mechanistic models are essential for the interpretation of electrode behavior and are useful in directing the research of new classes of materials for electrochemical energy conversion and storage devices.

Two topics are currently being researched: 1) LEED studies of anodic reconstruction of metal surfaces, and 2) LEED studies of electrodeposition/dissolution.

LEED Studies of Anodic Reconstruction of Metal Surfaces: Anodic films formed on Pt(100) in 0.3M HF using a thin-layer electrochemical cell within a vacuum envelope were emersed and transferred to ultra-high vacuum for study by Auger electron spectroscopy (AES) and thermal

desorption spectroscopy (TDS). Comparison of the oxygen coverage determined in vacuum by AES with the oxygen coverage determined in solution by coulometry indicated that only films formed above 1.1 V (RHE) survived emersion and evacuation. As the emersion potential increased above 1.1 V (RHE), the integrated thermal-desorption signals for $H_2O$ and $O_2$ increased in parallel, with a constant $O:H_2O$ stoichiometry consistent with the formation of hydroxide-type layer, i.e. $Pt(OH)_x$. The oxygen coverage determined by both AES and TDS saturated at an emersion potential of 1.9 V (RHE), with formation of a surface phase containing 2.3 O/Pt and ca. 2 $H_2O$/Pt. Analysis of this surface phase by secondary-ionization mass spectroscopy (SIMS) indicated it is probably $PtO_2 \cdot H_2O$ rather than $PtO_2 \cdot 2H_2O$. Kinetic analysis of TDS lineshapes indicated a perimeter-controlled desorption model gave the best overall fit of lineshapes. This model is indicative of a growth mode for anodic films involving island formation and fusion, and the reverse occurring on reduction. The water-desorption peak temperature was 400°K, independent of film thickness, and a temperature much higher than that reported for surface-adsorbed hydroxyl groups produced by low-temperature (100°K) gas-phase coadsorption of $O_2$ and $H_2O$. The higher temperature for desorption is ascribed to the incorporation of hydroxyl ions into a surface phase with displacement of Pt atoms from their metallic lattice positions, i.e. place-exchange. Oxygen was evolved from the dehydrated anodic films at much lower temperatures than from gas-phase chemisorbed oxygen. The difference in the oxygen peak temperature is also ascribed to the subsurface state, but in this case (anhydrous oxide), the bulk phase has a heat of formation lower than the heat of adsorption. This unusual thermochemistry of the platinum-oxygen system is suggested to be the key to understanding the electrocatalytic properties of platinum.

<u>LEED Studies of Electrodeposition/Dissolution</u>: It is of considerable fundamental interest to determine whether electrode processes respond uniquely to long-range order on the surface. In chemisorption phenomena, it is well-known that short-range order, which establishes the adsorption-site symmetry, plays an important role in determining the strength of bonding of adsorbates. The role of long-range order is not as well understood, and it has not been the subject of systematic investigation. Only recently have surface-structure methods for long-range

order determination been developed for LEED. These developments in LEED analysis have renewed interest in studies of the effects of long-range order on adsorption phenomena. The underpotential deposition (UPD) of one metal on another is a type of adsorption phenomenon that occurs in electrodeposition. As a model system, UPD of Cu on Pt(100), (111), and (110) was studied with LEED to determine the range of order before and after UPD. LEED spot profile analysis of the vacuum-annealed low-index substrates indicated these surfaces initially had long-range order (ca. 100 A perfectly ordered domains). Post-UPD LEED analysis of the Pt surfaces emersed at ca. 0.6 V vs. Cu/Cu(II) indicated Cu UPD had a minimal residual effect on the surface structure, indicating that Pt-Cu place-exchange ("alloying") did not occur during Cu UPD. Oriented Pt surfaces with only short-range order were produced either by anodic cycling of the Pt, or by UHV treatment with argon-ion bombardment; both treatments produced similar types of surface structures. The comparison of the voltammetry revealed the effect of the short-range and long-range order in the surface on the UPD process. In short-range order, the orientation of the crystal (zone axis) determines the local symmetry of the majority of adsorption (ad-atom) sites on the surface. The primary UPD peaks occurred at the same potentials on both the short-range and long-range ordered surfaces, indicating, as expected, that the adsorption energy is determined by site symmetry due to the highly localized nature of adsorption bonding. Steps (or dislocations) had the effect of introducing sites with different adsorption energies. Long-range order appears to have a second-order effect which is manifested in the peak widths, i.e. a collective interaction which narrows the energy distribution.

Publications

1. P.N. Ross and P. Andricacos, "Diffusion Controlled Multisweep Cyclic Voltammetry: III. Deposition of Silver on Stationary and Rotating Disk Electrodes", J. Electrochem. Soc. 131, 1531 (1984); LBL-16734.

2. P. Andricacos and P.N. Ross, "The Underpotential Deposition of Cu on Pt Single Crystals Prepared in an Ultra-High Vacuum System", J. Electroanalytical Chem. 167, 301 (1984); LBL-17355.

3. P.N. Ross and F.T. Wagner, "The Application of Surface Physics Techniques to the Study of Electrochemical Systems, Chapter 2 in Advances in Electrochemistry and Electrochemical Engineering, Vol. 13, edited by H. Gerischer and C.W. Tobias, Wiley-Interscience, New York, NY (1984) p. 69.

4. P.N. Ross, "Hydrogen", Chapter 3, in Oxidation-Reduction Potentials of Aqueous Solutions: A Selective and Critical Source Book, Edited by A. Bard, J. Jordan and R. Parsons, Marcel Dekker, New York, NY (1984).

5. F.T. Wagner and P.N. Ross, "LEED Spot Profile Analysis of Electrochemically Cycled Pt(100) and (111) Surfaces", submitted to Surface Sci.; LBL-18498.

6. F.T. Wagner and P.N. Ross, "AES and TDS Studies of Electrochemically Oxidized Pt(100)", submitted to Appl.

## Analysis of Ambient-Temperature Sulfur Electrodes

(E.J. Cairns and F.R. McLarnon, Lawrence Berkeley Laboratory)

Efforts during 1984 have concentrated on producing efficient counterelectrodes, for possible use in photoelectrochemical and/or redox cells, based on the sulfide/polysulfide redox couple. The sulfide/polysulfide redox couple shows highest exchange current densities on transition-metal sulfides such as CuS, $MoS_2$ and CoS. Our approach has been to disperse these metal sulfides in a hydrophilic carbon matrix in order to maximize surface area. A small amount (~3 w/o) of PTFE was added to bind the electrode together, and the active material was hot pressed onto an expanded Ni mesh. the electrodes were less than 1-mm thick and had 15 $cm^2$ of projected area, with an active-material porosity of about 75%.

The electrodes have been tested in a parallel-plate electrochemical cell, in which the test electrode and counterelectrode were held about 3-mm apart. A Pt wire between the two electrodes served as a reference electrode. Steady-state current vs. electrode polarization curves were taken for each test electrode. In order to assist interpretation of electrochemical data, sections of the electrode have been examined with the scanning electron microscope and with a powder X-ray diffractometer. Transient experiments on smooth metal or metal-sulfide disks are planned in order to determine the kinetic parameters.

## Engineering Analysis of Electrolytic Gas Evolution

(C.W. Tobias, Lawrence Berkeley Laboratory)

The objective of this project is to establish the influence of electrode geometry and surface morphology, and of electrolyte composition, on bubble size and residence time, and to elucidate the role of free and forced convection as it affects overpotential behavior and ohmic resistance in electrode gas-evolution processes.

There has been continued interest in the effect of gas evolution on the performance of electrochemical cells. Existing theory for the effect of attached bubbles on an electrode reaction is limited to the primary current distribution. A model has been advanced which takes into account local concentration overpotentials due to charged and uncharged species, as well as charge-transfer overpotentials. The tertiary current distribution is substantially different from the primary case. In particular, the concentration overpotential of dissolved gas is substantially reduced near the bubble, causing an effective attraction of current to the region nearest to the point of attachment. The pseudosteady-state analysis accounts for migration and diffusion of each dissolved species in the vicinity of a single attached bubble within a Nernst diffusion layer. The resulting coupled boundary-value problem is solved by a finite-element routine. The standard condition involves the case of hydrogen evolution in 5.0 M KOH at 100 $mA/cm^2$, for a 10-micron tangent bubble within a 50-micron boundary layer. The current distribution is evaluated for various values of exchange current density. For cases of fast kinetics, the attached bubble causes a pronounced enhancement in local current density. For slower kinetics this enhancement is reduced until, in the irreversible limit (Tafel kinetics), product transport does not influence the rate, and hence there is no enhancement effect.

An electrolyte cell has been designed and constructed in which two identical (e.g. $H_2$-$H_2$) or different ($H_2$-$O_2$) gas bubbles generated on microelectrodes facing each other may be evolved at suitably low rates, to allow the observation of coalescence phenomena as the spherical bubbles come into contact. Preliminary results indicate that for bubbles

smaller than 1 mm in diameter, the coalescence event is completed within $10^{-5}$ seconds, and that earlier observations, here and elsewhere, according to which bubbles could touch without immediate coalescence, may have resulted from slight axial misalignment.

The effect of electrode morphology and attitude on bubble size and residence time is studied using high-speed cinematography. Electrodes of various geometries--flat horizontal, flat vertical, ridges and spheres--are masked with an insulating material so that a single row of bubbles can be viewed from the side. Overpotential measurements are obtained from the unmasked smooth and textured electrodes.

Three new sets of micromosaic electrodes have been produced for this program by Hewlett Packard Company and by Bell Laboratories. For these electrodes, more stable materials, such as tantalum silicide and titanium/palladium/gold, have been used to replace the aluminum and chromium in the original version, hopefully increasing the useful life of these valuable experimental tools.

Publications and Presentations


1. D.W. Dees and C.W. Tobias, "Experimental Observations of Free Convection Mass Transfer to a Horizontal Surface with a Micro-Mosaic Electrode", Spring Meeting of the Electrochemical Society, Cincinnati, OH, May 6-11, 1984, Extended Abstracts 84-1, p. 535; LBL-16176.

2. D.W. Dees and C.W. Tobias, "Mass Transfer at Gas Evolving Surfaces: A Microscopic Study", 35th Meeting International Society of Electrochemistry , Berkeley, CA, Aug. 5-10, 1984. Extended Abstracts, p. 717; LBL-16176.

3. C.W. Tobias and P.J. Sides, "Current Distribution Around, and Resistance by Gas Bubbles Adhering to an Electrode Surface", Presented at the International Meeting on Electrolytic Bubbles, Imperial College, London, England, Sept. 13-14, 1984. Extended Abstracts No. 11; LBL-11849.

4. C.W. Tobias and J.O. Dukovic, "Current Distribution at an Electrode with an Attached Bubble", Presented at the International Meeting on Electrolytic Bubbles, Imperial College, London, England, Sept. 13-14, 1984, Extended Abstracts No. 12; LBL-18818A. Electrochemically Oxidized Pt(100)", submitted to Appl. Surf. Sci.; LBL-17971.

## Bibliography of Convective Transport Correlations

(J.R. Selman, Illinois Institute of Technology)

The objectives of this project are to search the literature for references to experimentally established mass- and heat-transfer correlations useful for the design of electrochemical energy storage and conversion devices, and to compile this information as a bibliography in an easily accessible form.

During 1984 the draft bibliography has been completed and suggestions by reviewers have been incorporated in the final report. A review paper highlighting the scope and present status of mass-transfer measurements and correlations was prepared for Journal publication. The final report contains approximately 420 mass-transfer correlations from 260 sources and 450 heat-transfer correlations from 240 sources.

## IV. AIR SYSTEMS RESEARCH

The objectives of this project element are to identify, characterize and improve materials for air electrodes; and to identify, evaluate, and initiate development of metal/air battery systems and fuel-cell technology for transportation applications.

### A. SECONDARY METAL/AIR CELLS

#### Electrocatalysts for Oxygen Electrodes

(E. Yeager, Case Western Reserve University)

The objective of the research is to develop more effective electrocatalysts for $O_2$ reduction and generation which have good stability in acid and alkaline electrolytes. The emphasis of this research is on achieving a fundamental understanding of $O_2$ electrocatalysis. Research during the past year has involved:

1. Fundamental aspects of various macrocycles that were adsorptively-attached as monolayers and aggregates on carbon and other surfaces and in solution.

2. Thermally-treated macrocycles whose structures have been degraded to varying degrees, but nonetheless exhibit high catalytic activity for $O_2$ reduction and good stability.

3. Research on oxygen and carbon electrochemistry, including $O_2$ reduction on chemically-modified carbon surfaces.

The work has involved the use of a number of electrochemical, spectroscopic and theoretical approaches, and various macrocycles were examined. A considerable effort has been devoted to the purification and spectroscopic characterization of the transition-metal macrocycles and the corresponding metal-free species, particularly porphyrins and phthalocyanines. The iron tetra-sulfophthalocyanines (TsPc) are of special interest since they adsorb on electrode surfaces to catalyze the 4-electron direct pathway in alkaline electrolytes. Recent results with Raman spectroscopy, including depolarization measurements on monolayers adsorbed on silver single-crystal surfaces without activation, provide evidence that these complexes are oriented with the plane of the macrocycle ligand perpendicular to the surface. Mossbauer studies on bulk

crystalline Fe-TsPc and Fe-TsPc adsorbed at monolayer coverages on high surface-area carbon (Vulcan XC-72) suggest a μ-oxo or peroxo-Fe-TsPc complex for the adsorbed species.

The research has also focussed on understanding the processes occurring during heat treatment of macrocycles adsorbed on carbon and the role of the transition metal. The heat-treatment process has been studied using pyrolysis gas chromatography-mass spectroscopy, and the final material has been examined using transmission electron microscopy (TEM). The most striking difference between the behavior observed for the metal tetramethoxyphenyl porphyrins (TMPP) and that of the metal-free counterpart supported on high surface-area carbon is the lack of nitrogen-containing fragments in the chromatograms of the former, even at temperatures as high as 850°C. The TEM measurements on $(Fe\text{-}TMPP)_2O$/Vulcan XC-72 heat-treated at 800°C indicate the presence of small iron-oxide single crystals of ~60 nm diameter; this confirming the assignment made earlier based on Mossbauer spectroscopy. TEM also indicates that Co-TMPP/Vulcan XC-72 specimens, which were heat-treated at 800°C, contain single crystals of cobaltous oxides, in agreement with emission Mossbauer experiments reported earlier for samples of this type. Experiments are also in progress with Fe and Co oxides added to the mixtures of carbon and transition-metal macrocycle, both before and after heat treatment. Cobalt and iron salts have been heat-treated in combination with nitrogen-containing polymers, and some of the resulting catalysts were found to have high catalytic activity for $O_2$ reduction.

The research has indicated that various quinones, adsorptively-attached or chemically-bonded to graphite surfaces, catalyze $O_2$ reduction to $HO_2^-$ in alkaline solutions. A mechanism involving the quinone radical anion as a redox mediator has been proposed. In order to examine the effect of water as a proton donor, $O_2$ reduction on glassy carbon, pyrolytic graphite, the basal plane of highly-ordered pyrolytic graphite, and Au have been examined in an aprotic solvent with and without added water. Without water, $O_2$ reduction on these surfaces in acetonitrile proceeds only to the superoxide $O_2^-$ by an outer sphere, weakly adiabatic-electron transfer to $O_2$. In the presence of water, reduction proceeds to $HO_2^-$ on these surfaces, but the reduction of

superoxide to peroxide is much faster on Au than carbons, providing evidence for a catalytic role of the electrode surface for the conversion to peroxide.

Publications


1. R. Adzic, M. Hanson and E.B. Yeager, "Structure of Silver Single-Crystal (100) and (111) Surfaces Obtained by Chemical Polishing", J. Electrochem. Soc. 131, 1730 (1984).

2. E.B. Yeager, D. Scherson and B. Simic-Glavaski, "Mechanistic Aspects of Oxygen Electrochemistry", Proceedings of the Symposium on the Chemistry and Physics of Electrocatalysis, The Electrochemical Society, Inc., Pennington, NJ (1984) p. 247.

3. D. Tryk, W. Aldred and E.B. Yeager, "Carbon in Bifunctional Air Electrodes in Alkaline Solutions", Proceedings of the Workshop on the Electrochemistry of Carbon, The Electrochemical Society, Inc., Pennington, NJ (1984) p. 192.

4. Z. Zhang, D. Tryk, and E.B. Yeager, "Effect on Surface Treatment of Glassy Carbon on $O_2$ Reduction in Alkaline Solution", Proceedings of the Workshop on the Electrochemistry of Carbon, The Electrochemical Society, Inc., Pennington, NJ (1984) p. 158.

5. E.B. Yeager, J. Molla and S. Gupta, "The Electrochemical Properties of Graphite and Carbon," Proceedings of the Workshop on the Electrochemistry of Carbon, The Electrochemical Society, Inc., Pennington, NJ (1984) p. 123.

6. D. Scherson, C. Fierro, E. Yeager, M.E. Kordesch, J. Eldridge, R.W. Hoffmann and A. Barnes, "In-Situ Mossbauer Spectroscopy on an Operating Fuel Cell", J. Electroanal. Chem. 169, 287 (1984).

7. E. Yeager, "Electrocatalysts for $O_2$ Reduction", Electrochim. Acta 29, 1527 (1984).


## Corrosion of Non-Metallic Electrode Materials

(P.N. Ross, Lawrence Berkeley Laboratory)

In previous work, we showed that the presence of a dispersed cobalt-oxide phase ($Co_3O_4$) in acetylene black had a catalytic effect on the corrosion rate of the acetylene black at oxygen evolution potentials (> 450 mV vs. Hg/HgO). This catalytic effect was postulated to occur via a redox mechanism involving dissolved Co(II)/Co(III) species. To test this postulate, other transition metal oxides not having redox couples in this potential range were dispersed into acetylene black and their catalytic effect on corrosion was examined. The results were

surprising; $Co_3O_4$ actually had the lowest catalytic effect, the observed order being $Fe_2O_3$ > $Cr_2O_3$ > NiO > $Co_3O_4$. Fe and Cr do not have redox couples in this potential region, whereas Ni and Co do, but these latter two had the lowest catalytic effect. It appears therefore that the catalytic effect of these metal oxides on carbon corrosion is not via a redox mechanism. The noble metals Pt, Au and Ru are being examined for their effect on carbon corrosion. Extensive testing of graphitized furnace carbon blacks has identified only one type of material with a significantly lower corrosion rate than acetylene black, namely graphitized Sterling R (Cabot). All future studies of carbon corrosion will employ graphitized Sterling R.

Publications


1. P.N. Ross and H. Sokol, "The Corrosion of Carbon Black Anodes in Alkaline Electrolyte: I. Acetylene Black and the Effect of Cobalt Catalyzation", J. Electrochem. Soc. 131, 1742 (1984); LBL-16520.

2. P.N. Ross, "Corrosion of Carbon in Gas Evolving Electrodes"; LBL-17851 (1984).


## Iron/Air Battery Development

(E.S. Buzzelli, Westinghouse Electric Corporation)

Development work at Westinghouse on the iron/air battery system has concentrated on improving the performance and life characteristics of the bifunctional air electrode. Specific objectives have been to reduce polarization at the air electrode to achieve performance of -60 mV vs. Hg/HgO at 25 $mA/cm^2$ (discharge) and +480 mV at 12.5 $mA/cm^2$ (charge), and to extend cycle life to 1000 cycles for 8-hour cycles (4 hrs. discharge, 4 hrs. charge). Achievement of this goal will permit the fabrication of an iron/air battery system suitable for electric vehicle propulsion.

Three areas of research that were addressed are:

- carbon corrosion
- alternative binders
- electrocatalysts for bifunctional electrodes

A study on the corrosion of various types of carbon was conducted. Black Pearls 2000 (high surface-area furnace black), Shawinigan Black, (a medium surface-area acetylene black), and ENSAGRI Conductive Carbon (type "super S") were used in the corrosion tests. The measurements indicate that Shawinigan Black has the lowest corrosion rate and the highest activity for oxygen evolution of the three carbon blacks.

Fibrillated polyethylene and polypropylene were proposed as alternative binders to Teflon. These polyalkanes cost approximately 1/10 that of Teflon, thus reducing the price of the electrode. Performance of electrodes containing the alternative binder was comparable to Teflon-bonded electrodes.

The components previously identified as the active electrocatalysts in bifunctional air electrodes, i.e., Ni-Co-Fe, (with Ni-Co active in discharge and Fe-Ni for charge-reaction catalysis), were found to be more active when added to the electrode structure as hydroxides (-325 mesh particle size), instead of NiS, WC-12% Co and $FeWO_4$. An order-of-magnitude increase in the peroxide-elimination rate constant was observed in floating electrode-type studies, which corresponded to a ~15 mV improvement in performance of 40-$cm^2$ air electrodes in half-cell tests.

Development work on the iron/air battery at Westinghouse has been discontinued due to the limited life and performance of the bifunctional air electrodes using carbon blacks.

Publication

1. L. B. Berk, C. T. Liu, "New Binder System for Low Temperature Alkaline Electrodes", J. Electrochem. Soc. 131, 952 (1984)

Research and Development of Bifunctional Oxygen Electrodes

(M. Klein, Energy Research Corporation)

The major objective of this project is to develop bifunctional air electrodes utilizing perovskite metal oxides and low-loading gold catalysts. In addition, a preliminary design analysis of zinc/air batteries for electric vehicles will be conducted.

Initial efforts were directed toward the study of gold electrodes with a loading of less than 1 $mg/cm^2$. Both commercially-available gold powder and gold powder prepared by reduction of gold chloride were evaluated. Carbon, graphite, metal oxides, spinel oxides and nickel powder were used as electrocatalyst substrates. Both admixing and co-precipitation techniques were employed to form a catalyst substrate layer. Polarization tests were carried out in air and in pure oxygen, after which the electrodes were cycled (charge, 4 hours at 10 $mA/cm^2$: discharge 4 hours at 20 $mA/cm^2$) at ambient conditions. Electrodes without porous PTFE film deteriorated rapidly, started to show electrolyte weeping, and exhibited only a marginal improvement in polarization. Polarization data in pure oxygen exhibited a marked improvement compared to the values obtained in unscrubbed air. Data obtained to date indicate that among the substrates evaluated, the most promising catalyst support is graphite. Spinel oxides show a stable but high polarization.

Over 20 different compositions of perovskites were synthesized, and X-ray diffraction analysis of selected samples showed perfect matches to patterns of known phases. In addition, energy dispersive X-ray analysis confirmed that the bulk composition of material was identical to the desired formulation. Of the three samples analyzed, two were rhombic and one was cubic in crystal structure. The perovskites were prepared by evaporation and decomposition of the respective metal salts followed by sintering at 600 to 900°C for 4 to 72 hours in air. The perovskites were mixed with Teflon powder, and a hydrophobic catalytic layer was formed both by roll-bonding and by pressing the mix to form a pellet.

Experimental results obtained so far are as follows:

1. Catalyst layer in the form of pellets perform better than that prepared by kneading and rolling; but the pellets tend to develop cracks through which electrolyte permeates and causes deterioration.

2. Perovskites of the composition $LaNiO_3$ and $La_{0.5}Sr_{0.5}CoO_3$ are the best candidates among the ones tested.

3. The resistivities of perovskites are higher than desirable. Perovskites made with ruthenium exhibited very good conductivity.

4. In general, initial polarization values were good but the electrode performance degraded with cycling.

5. Addition of graphite to the perovskite resulted in more stable potentials during cycling. In addition, the instantaneous polarization showed a marked improvement after cycling. The reason for this is not clear at this time, and additional work remains to be carried out.

Work done during this calendar year indicates that perovskites show definite possibilities as an electrocatalyst for oxygen reduction, and the performance is comparable to electrodes made with noble-metal catalysts. Problem areas have been identified, and future experiments will emphasize improving electrode life. It is also planned that electrodes in an atmosphere of $CO_2$-free air will be tested.

Electrical and Electrochemical Behavior of Particulate Electrodes

(J.W. Evans, Lawrence Berkeley Laboratory)

The objective of this research is to provide the basic knowledge to enable particulate electrodes to be designed, evaluated and scaled up. The research is concerned with potential variations in particulate electrodes. Such potential variations are inherent in fluidized-bed electrodes and occur in both time and space, even when a constant voltage is applied to the electrodes. These variations affect the kinetics of the electrochemical reactions occurring in the cell and the morphology of the electrode; thereby the overall performance of the cell is affected.

Experimental work has been completed on potential transients within fluidized-bed electrodes and moving-bed electrodes. Of primary interest has been zinc deposition from (or dissolution into) alkaline zincate solutions (the electrochemistry of interest in the zinc-air battery), using Sorapec particles. These particles are zinc-coated polymer particles under development in France for use in particulate electrodes. Additional measurements have been carried out on copper particles and zinc-coated copper particles. Measurement of transient potentials have permitted the calculation of quantities such as time-averaged

potentials, standard deviation of the potential, etc., as a function of parameters such as position in the bed and bed expansion. Many of the results have been explained in terms of the hydrodynamic behaviour of fluidized beds; for example fluidized beds frequently exhibit "bubbling" behaviour. The "bubbles" referred to are not gas bubbles but regions of the bed that are almost free of particles; these regions rise through the bed and are roughly spherical in shape. Classical studies of fluidized beds have long since delineated the conditions under which bubbling occurs, and based on that work, it can be predicted that a bed of Sorapec particles will not have bubbles, but that a bed of zinc-coated copper particles (which are of much greater density) will. Measurements on the latter particles show a low-frequency potential variation that can be ascribed to bubbles, and this variation is absent in measurements on the former particles.

In a second series of experiments, a zinc rotating-disc electrode has been used for deposition of zinc from zincate solutions. The electrode potential is set by a potentiostat under the control of an Apple microcomputer; the potential can therefore be set at a constant value or varied in some controlled fashion. The latter option includes making the rotating-disc electrode experience potential fluctuations recorded by the potential-transient-measurement apparatus in the fluidized bed. The morphology of zinc deposited under various constant and fluctuating potential has been determined by scanning electron microscopy for various (time-averaged) current densities, solution compositions, rotational speeds, etc. It has been shown that fluctuation of the current density about some mean yields a very different morphology from that obtained at a constant current density equal to this mean.

An air electrode has been acquired and a cell designed and constructed wherein this air electrode is coupled with a fluidized electrode of Sorapec particles. Preliminary measurements of overall cell performance are in progress.

A short investigation of the production of zinc particles has been carried out. If zinc particulate electrodes reach commercial operation, there are three likely sources of zinc for electrodeposition to produce

the necessary particles: zinc sulfate, zinc chloride (obtained from zinc ores by hydrometallurgical techniques) and alkaline zincate solution ("spent" battery electrolyte). The last named would dominate if mechanical recharging is established, either or both of the first two are likely to be significant during the early stages of implementation of the technology (before the "pool" of spent electrolyte has grown to sufficient size). Fluidized-bed electrodeposition from zinc sulfate solution has been studied in the past and shown to be difficult but possible. A short (six month) investigation was carried out to determine the feasibility of deposition from zinc-chloride solution. This investigation showed that zinc particles can be grown from near-neutral zinc-chloride solutions in fluidized electrodes with high current efficiencies and space-time yields and energy consumptions (per unit of metal), which are comparable with conventional zinc electrodeposition.

Publications and Presentations


1. N.E. Tuffrey, V. Jiricny and J.W. Evans, "Fluidized Bed Electrowinning of Zinc from Chloride Electrolytes", LBL-18738.

2. V. Jiricny, T. Huh and J.W. Evans, "Fluidized Bed Electrodeposition of Zinc", Presented at the Spring Meeting of the Electrochemical Society", Cincinnati, OH, May 1984.

3. T. Huh and J.W. Evans, "Potential Distributions and Transients in Particulate Electrodes of Possible Use in Energy Storage," Presented at the 35th Meeting of the International Society of Electrochemistry, Berkeley, CA, August 5-10, 1984.


## B. ALUMINUM/AIR BATTERIES

### Aluminum/Air Battery Research and Development

(A. Maimoni, Lawrence Livermore National Laboratory)

The objectives of the Aluminum-Air Power Cell program are to develop an automotive energy source for general-purpose vehicles and to evaluate its ability to provide vehicles with the range, acceleration performance, and rapid refueling capability of current internal-combustion-engine vehicles. Recent calculations by LLNL suggest that the overall energy efficiency of an electric vehicle with an aluminum/air battery is 13-14% and 16-18%, if Al is produced by the Hall process and Alcoa smelting process, respectively.

The Lawrence Livermore National Laboratory (LLNL) conducts research and provides program direction for the development of the Al/air battery. Most of the work is done under a cost-shared contract with Eltech Systems Corporation which has formed a consortium with Alcan Aluminum Ltd., Case Western Reserve University (CWRU), and SRI International. The main thrusts of the research during 1984 were: a) air cathode development, b) hydrargillite crystallization and separation, c) integrated experiments involving a coupled cell/crystallizer, d) cell design, and e) development of improved aluminum anodes.

The development work has treated anode development, cell design, and crystallization development as independent problems. The close coupling between these aspects of the problem can no longer be ignored and will receive increased emphasis during 1985.

## Integrated Experiments

Two experiments were performed at LLNL during 1984 in which a single cell was coupled to a crystallizer to simulate the performance of an aluminum/air power-cell system. Both experiments ran for about 5 h at 120-A nominal current. While both experiments suffered from failures due to the tubing of the peristaltic pump feeding the hydrocyclone, which precluded obtaining good material balances and relating crystal growth parameters to operational conditions, a great deal of important system design information was obtained.

M3-3 Experiment: In the M3-3 experiment, Fig. 1, the cell was run at 14 A for 101 min, followed by 122 A for 269 min at 60°C with 4M NaOH electrolyte containing 0.06M sodium stannate as corrosion inhibitor; the overall current efficiency was 96%. Previous experiments used a commercial hydrocyclone sized for 30 to 50 cells; the M3-3 experiment used a hydrocyclone scaled for 1 to 5 cells. Peristaltic pumps were used instead of the centrifugal pumps from previous experiments; essentially no particle degradation occurred when peristaltic pumps were used to feed a hydrocyclone (1).

Analysis of the results obtained in the M3-3 experiment indicates reasonable agreement in the material balances, and in a comparison between the calculated M1-1 and experimental M-1 values of the mass of hydrargillite in the system.

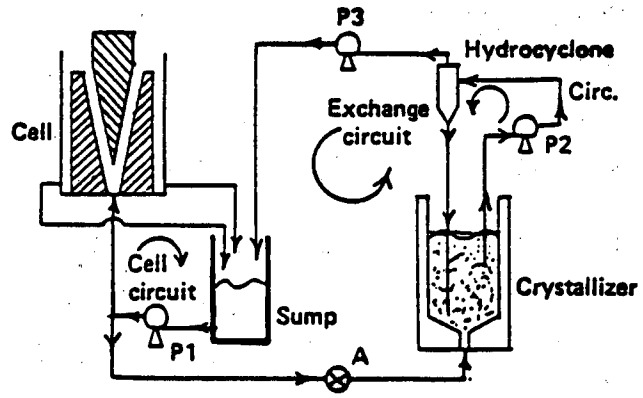


Fig. 1. Flow diagram for M3-3 experiment. There are two independent circulation loops: (1) cell recirculation loop, and (2) exchange flow between cell and the crystallizer. Exchange flow is regulated by pump P3 and valve A.

A more sensitive test of the material balances is the evolution in total crystal population as a function of time, given as the base 10 logarithm of the particle population for various times in Fig. 2. The main conclusion derived from Fig. 2 is that at 60°C, secondary nucleation produced an approximately 100-fold increase in the total number of fine particles. The time averaged value of particle growth rate for particles larger than about 17 μm was approximately size independent, at about 1.2 μm/h.

<u>M4-1 Experiment</u> The M4-1 experiment was the initial test of the M4 "reference cell", shown in Fig. 3. It was also the initial test of a new crystallizer and interconnecting piping; the first operation of coupled cell-crystallizer system at temperatures in the 70-80°C range; the initial test of a new data acquisition; system; the initial operational test of on-line Foxboro conductivity meters; and, the initial use at LLNL of a modified industry-standard method for the determination of sodium and aluminate concentrations.

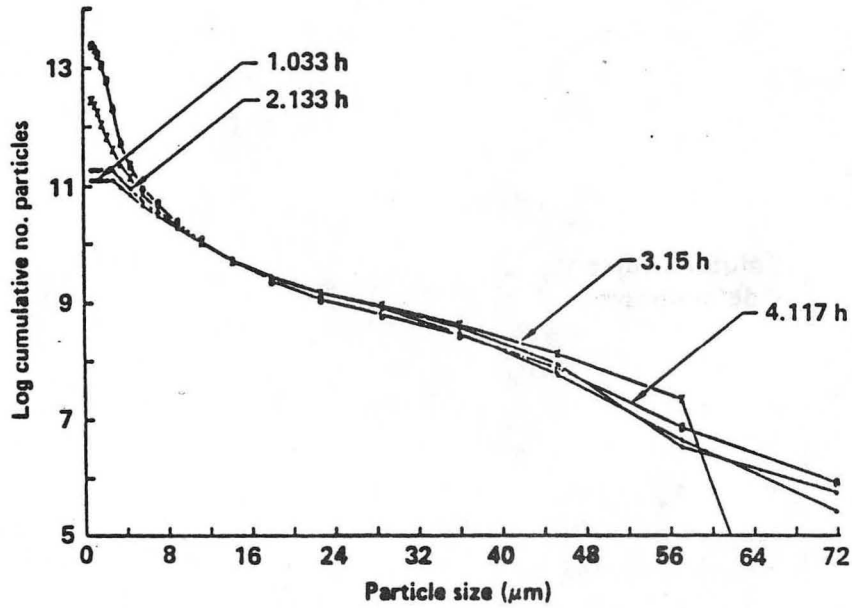


Fig. 2. Total particle population in the system at various times shown as the logarithm (base 10) of the total number of particles. The population of fine particles increased over 100 fold throughout the course of the experiment.

Most of the new components performed very well. The main operational problems were failures of the peristaltic pump tubing, accumulation of gas in one of the Foxboro meter housings, and plugging of an electrolyte return line from the cell by metallic tin and hydrargillite. The precipitation rate of tin in the 70-80°C range was approximately linear with time, about 17% of the initial tin content per hour. The M4-1 experiment was terminated when the electrolyte return from the cell began to overflow, due to plugging of the return flow to the crystallizer. The flow restriction that led to overflow in the cell return is likely to have occurred in the return line to the crystallizer.

The conditions required to obtain representative samples of the solids were determined prior to the M4-1 test; particle size-distribution data are still being analyzed. Detailed information about performance of the various system components is given in the following sections.

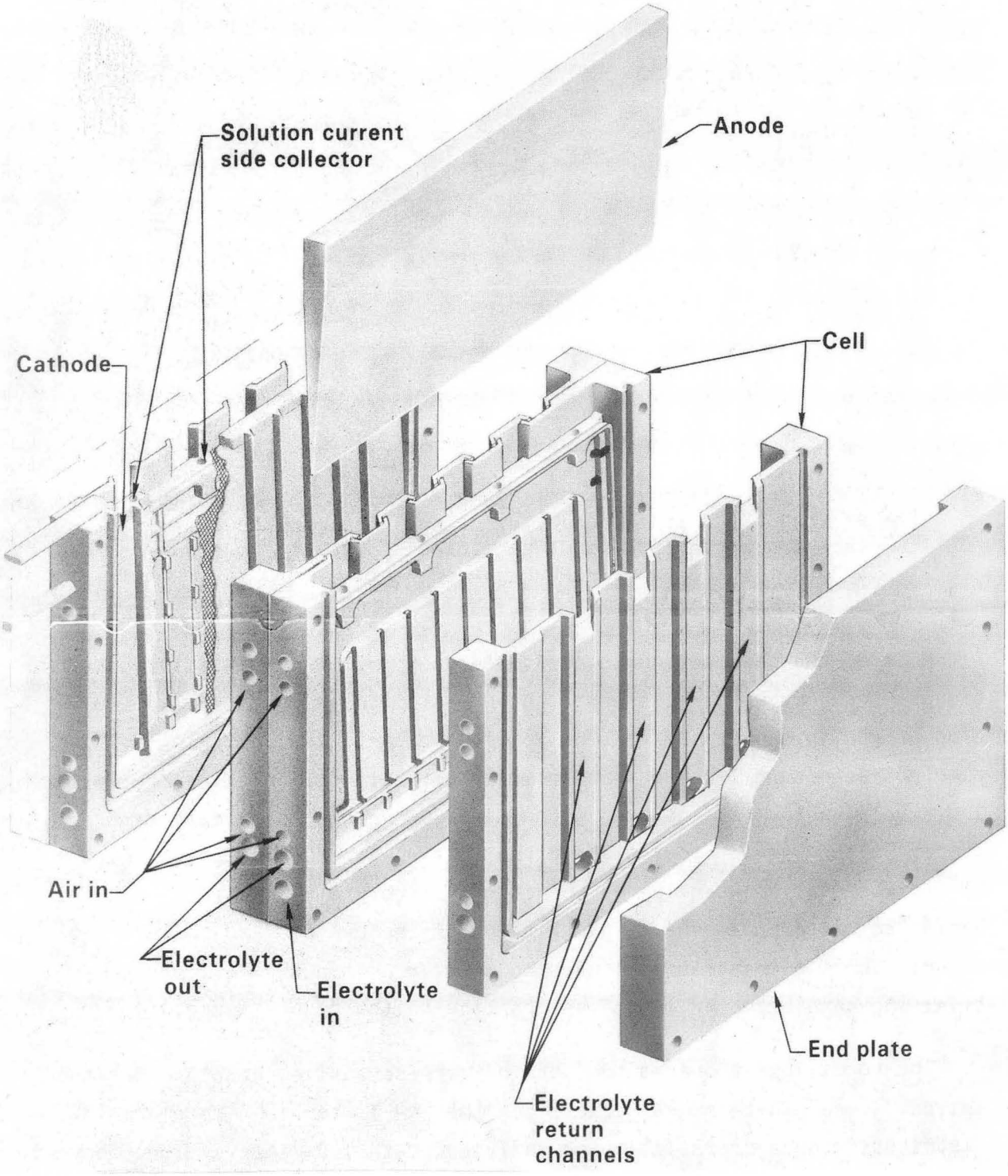


Fig. 3. The M4 Aluminum-Air Wedge Cell.

Individual Components

Air Cathode: Work in this important area has continued at Eltech, Electromedia, and Case Western Reserve University (CWRU). In previous work (2), the best electrode had a life in excess of 1400 simulated driving cycles, which may be equivalent to over two years of operating life in a vehicle. While attempts to duplicate this performance have not been successful, a great deal has been learned about the effect on operating life of various materials and fabrication variables. A number of steam-activated carbon blacks have performance as good as that of activated carbons; the most promising materials are classified RBDA and Norit Ultracarbon, containing a 5-10% loading of CoTMPP. Electromedia has obtained substantial improvement in the polarization characteristics of the air electrodes, as well as significant improvements in electrode life by using an alternative binder material instead of Teflon and by increasing the thickness of the wet-proof and active layers.

Work at CWRU has concentrated on three main areas:

1. Understanding the role of the transition metal: A transition metal is required, but it can be incorporated before or after heat treatment. Almost the same degree of activity was obtained when carbons with adsorbed $H_2$TMPP were treated with solutions of the transition metal. After heat treatment to 450°C and 800°C, some metal oxides are present. The catalytic activity decreases when the metal oxides are extracted with glacial acetic acid or 0.5M $H_2SO_4$, with a greater decrease in the activity of the 800°C heat-treated material.

2. Low-cost alternatives: A number of natural products have been examined for oxygen reduction activity. Hemin and hematin appear promising.

3. Optimization of the structure: Thinner layers improve the oxygen and electrolyte transport.

Aluminum Anodes: Statistical analysis of data obtained on various alloys and some Alcan proprietary alloys has continued at Eltech. The tests at Eltech have been performed at 60°C in 4M NaOH; they measure the Open Circuit Corrosion Rate (OCC), $mg/cm^2/min$, which is almost equivalent to a corrosion current in $mA/cm^2$; and, the Open Circuit Potential (OCP), -V vs Hg/HgO. In some tests they have incorporated 0.06M sodium stannate as corrosion inhibitor; in others, 1M of dissolved

alloy. Polarization testing has been performed on the most promising alloys. Statistical analysis of data on alloys containing In, Tl, and Ga indicates that Ga does not significantly influence the OCC. Ga does have a strong effect in the OCP, and cross terms are significant. The models predict improved voltage only at the expense of increased corrosion rate. One of the best alloys, ESC-3, in the presence of 1M dissolved alloy in the electrolyte, has an OCC of 0.029 (Zn yields .011) at an OCP of 1.78 V. The voltage decreases to 1.31 V at 600 $mA/cm^2$.

Two Alcan proprietary alloys show promise with OCC of 0.12 and OCP of 1.84 V; one of these alloys gave 1.5 V at 500 $mA/cm^2$ in 4M NaOH at 60°C.

The work at SRI is aimed at developing a fundamental understanding of the processes taking place at the anode surface. They have calculated thermodynamic activities of the important species, and will interpret the results of complex-impedance measurements in terms of the thermodynamics and kinetics of the various possible reactions. Experimentally, they have recently completed a cell with a well-defined hydrodynamic flow pattern to simultaneously measure the partial anodic and cathodic reactions occurring at the surface.

Carbon Dioxide Scrubber: The detailed design has been ignored thus far because the amounts of carbon dioxide involved are small, less than 6 kg/yr. However, since the atmospheric $CO_2$ concentration is about 330 ppm and the current specification calls for 2-5 ppm, about 99% removal of atmospheric $CO_2$ is required at air flow rates as high as $10^4 cm^3/s$. A preliminary calculation was made of the size of a packed tower absorber. The results of the calculations indicate that a packed tower absorber for vehicle application is at least 9-in diameter by 68-in high. While it is realized that packed columns are not appropriate, the above analysis does indicate that careful design is required.

Electrolyte Flow: In the M4 cell, electrolyte feeds from both sides into a flow distribution plenum; however, only one feed port was used in the M4-1 experiment. During the experiment, metallic tin and hydrargillite deposited in the flow distribution plenum, starting about 7.5 cm from the inlet. A substantial amount of solids had also accumulated at

the bottom of the wedge and in the anode/cathode gap. The deposit was heaviest at locations opposite to the electrolyte inlet.

The M4-cell overflow feeds the internal return manifold through a series of openings in the back of each cell pod. Caked deposits of hydrargillite were formed during the experiment on the internal-cell-electrolyte-return manifold of one of the cell pods. The loosely adhering deposits, about 0.5-mm thick, were not likely to have been the source of plugging in the return line.

Subsequent experiments at Eltech with M4 cell pods have shown that the electrolyte flow past the anode/cathode space is not uniform. It is low at both ends of the electrode chamber; however, this was easily remedied by inserting a flow distributor into the inlet distribution plenum. The lack of uniformity in electrolyte flow reflected on the consumption of the aluminum anode; at the end of the run, it was about 7 mm longer near the edges than in the center.

In contrast to previous cells, the M4 cell is very easy to assemble and disassemble, thus it was possible to readily examine the result of system malfunctions without damaging the cell.

Air Flow: The M4 cell has air flow across the cell. There is concern that the unequal oxygen concentration on the two sides of a cell pod might lead to uneven consumption of the anode. At least for relatively short (4 h at 120 A) periods, anode consumption is relatively insensitive to oxygen concentration.

Air Cathode Assembly: Platinum-catalyzed cathodes were used in the assembly of the M4-1 cell. The edges of the cathodes were glued to the pods using epoxy. A good bond was obtained with no pinhole air leaks, and with seams intact after the M4-1 experiment.

Good electrical connection to the metallic screen of the cathodes was more difficult to obtain. Two methods were used: soldering and conductive epoxies. Soldering was accomplished using a low-melting (93°C) indium solder; it gave a very good joint. Two pods were assembled using conductive epoxy; the bond failed in the first pod during assembly. A

tougher epoxy was used for the second assembly. It appeared to be satisfactory after oven cure, but the current and voltage records of the M4-1 experiment indicate that the conductive epoxy bond failed during the run.

Cell Design at Eltech: Six M4-cell pods were given to Eltech for their cell development work. They found the electrolyte flow to be uneven, but also found an easy solution to the problem. The main emphasis of Eltech's work is in developing techniques for inexpensive assembly of air cathodes into cells. They are studying a number of configurations in which the air cathode is assembled on a conductive frame and then the assembly is mounted onto the cell pod. Several methods of attaching the air cathode to its conductive frame are being evaluated.

## Crystallization

Experimental: Experimental studies on crystallization and separation of hydrargillite from the electrolyte were carried out at LLNL and at Alcan. The LLNL M3-3 and M4-1 experimental results have already been described; this section will highlight the crystallization experiments at Alcan.

Crystallization Experiments: Alcan has carried out a large number of crystallization experiments at 60-80°C in 4M NaOH, as well as a few experiments using KOH and KOH-NaOH mixtures. A schematic diagram of their equipment is shown in Fig. 4. The supersaturated aluminate solution (about 2.9M) was added at a constant rate to the crystallization tank.

Alcan obtained a very good correlation for their experimental crystal growth rates (correlation coefficient 0.9985). In the NaOH system, the fastest growth rate (3.1 μm/h) occurs at 2.6M aluminate at 80°C. It is about 15% lower at both 70° and 90°C. Precipitation from KOH yields approximately the same rate, provided the seed was grown from KOH solution, but it is lower with seed from NaOH solution.

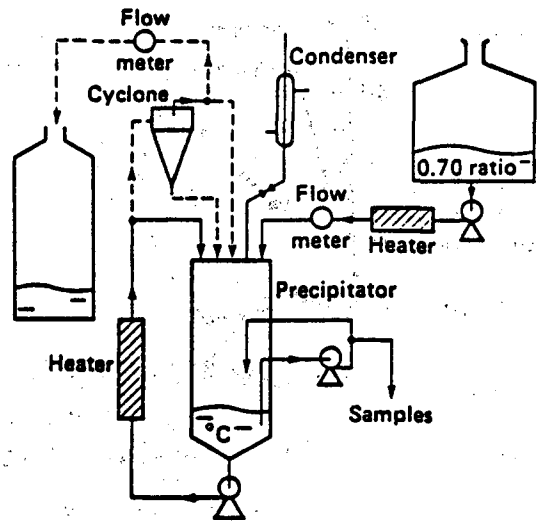


Fig. 4. Schematic of Alcan's crystallization equipment.

Agglomeration Experiments: Very significant results have been obtained at Alcan regarding agglomeration of hydrargillite. Under "high turbulence" conditions, agglomeration does not proceed beyond the 10-20 μm size; under "low turbulence" conditions, the particles continue to agglomerate. The optimum agglomeration temperature for both NaOH and KOH appears to be about 80°C. Figure 5 shows the evolution of the particle size distribution during a 2-h run at 84°C under low turbulence conditions; almost no secondary nucleation occurs at this temperature. The < 10 μm fraction of the population is negligible after 50 min; the 10-20 μm fraction has population peaks at about 50 min and is negligible after 105 min; the 30-40 μm population begins to increase rapidly at 90 min and is peaking at 145 min; the greater than 40 μm population begins to grow at about 110 min and constitutes about 25% of the total product weight after 2 h. Thus, agglomeration can provide the desired product particle size in reasonably short times.

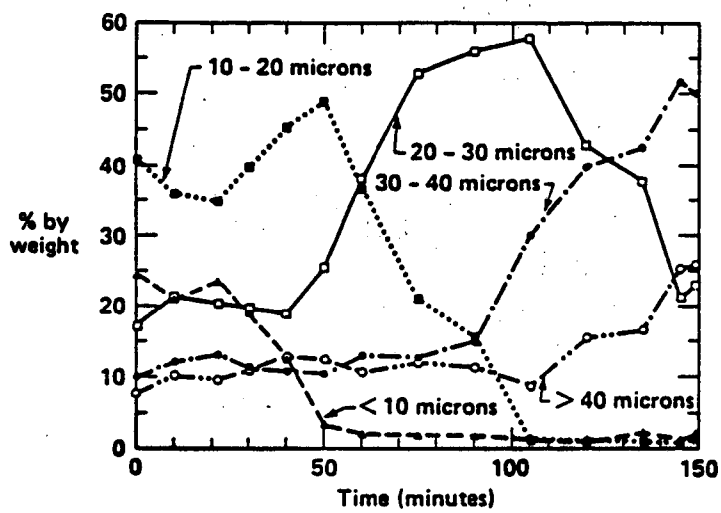


Fig. 5. Agglomeration and particle growth during crystallization experiment at Alcan.

Crystallization Modeling: A computer code CRYSP, written at LLNL, predicts how the particle size distribution evolves as a function of vehicle operating conditions. CRYSP was written as a main driver code, which handles the input-output and describes the system configuration by the interconnections between the various components, and a collection of subroutines which describe in detail the behavior of the various components. In its present configuration it has subroutines which describe: 1) cell performance parameters (power, heat balances, material balances, water evaporation and make-up, etc.), 2) a mixed suspension and mixed product removal (MSMPR) crystallizer, 3) hydrocyclone, 4) mixing blocks, 5) particle growth using Alcoa's correlation, and 6) an arbitrary secondary nucleation source.

A good fit to the M3-3 results (particle size distributions vs time) was obtained when the nucleation source was set to match the experimental value of the M3-3 run. As additional experimental data and correlations are obtained, the particle description in CRYSP will be modified with subroutines to describe secondary nucleation, particle attrition and agglomeration. No effort is being devoted at present to further code development.

References

1. M. Newman, Development of Hydrocyclones for Aluminum-Air Battery Applications, Lawrence Livermore National Laboratory, Livermore, CA, UCID-20061, (1984).

2. L.A. Knerr and D.J. Wheeler, "Aluminum/Air Battery Development, Final Report Under Contract No. 5033001," Eltech Systems Corp, Fairport Harbor, OH. Limited distribution report of February 15, 1985.

## C. FUEL CELL RESEARCH

### Fuel Cells for Vehicles

(J.R. Huff, Los Alamos National Laboratory)

The objectives of this program are to conduct basic research in electrochemistry, to investigate the kinetics and mechanisms of methanol fuel processing, to explore the potential of fuel-cell systems for use in transportation applications. Efforts in CY 84 were directed at research on electrode kinetics and electrocatalysis of fuel-cell reactions; characterization of electrodes and electrocatalysts, both experimentally and by *ab initio* quantum-mechanical calculations; physicochemical characterization of electrolytes; evaluation of electrode and fuel-cell performance under simulated-vehicle operating conditions; evaluation of methanol fuel-processing kinetics and mechanisms; and fuel-cell system simulations.

### Electrode Kinetics and Electrocatalysis

Research was conducted by United Technologies Corporation (UTC) to increase overload capability and efficiency, and to reduce catalyst cost and start requirements for vehicular phosphoric-acid fuel cells. The goal of the program is to improve cathode performance by using macrocyclic catalysts and to increase anode CO-tolerance by using metal alloy catalysts. At temperatures from 100°C to 150°C, pyrolyzed macrocyclic compounds are reported to match platinum activity for oxygen reduction in phosphoric acid, but with limited high power density in the electrodes tested. Cobalt and iron phthalocyanines (PC), tetraazaannulenes (TAA), and tetramethoxyphenylporphyrins (TMPP) were selected for evaluation. The objectives were to select the catalyst with the highest intrinsic activity, to identify factors limiting the performance of the

catalyst in fuel-cell electrodes, and to develop approaches for their improvement. On the basis of the best apparent activity and stability in preliminary tests, iron TMPP (FeTMPP) was chosen for further study.

Catalysts were prepared with FeTMPP supported on a variety of carbon powders with a range of surface characteristics and particle morphologies. They were characterized by physical and electrochemical methods. Measurement of electrode performance as a function of loading and electrode thickness indicated that the cathode performance of FeTMPP supported on RB and Black Pearls carbons, which were heat-treated at 880°C, is limited by diffusion losses and as yet undefined internal resistance.

The performance of Black Pearls, catalyzed by sequential adsorption and heat-treatment with 1 to 4 monolayers of FeTMPP-catalyst, had a maximum performance at 2 monolayers, perhaps due to increasing resistance to electron transfer by the multiple catalyst layers. The performance of the two-monolayer catalyst was the best observed (to date) at 140°C, i.e., 100mA/cm$^2$ at 700 mV on oxygen.

The performance of heat-treated FeTMPP appears to be stable in half-cell tests. However, stability has to be demonstrated in full-cell endurance tests. The first full-cell test of FeTMPP-catalyzed RB carbon was on load for 550 hours at 100°C. Decay in performance occurred, which could be due either to instability of the catalyst or to flooding of the electrode structure.

Possible temperature stability limitations of macrocyclic catalysts may require anode catalysts with increased tolerance to CO to allow cell operation at temperatures below 150°C. In the UTC program, the CO-tolerance of CSV-11 (a proprietary platinum-based catalyst) was measured over a range of CO partial pressures and temperatures. Results for test temperatures of 80°C to 180°C at CO partial pressures from 0.3% to 5.0% confirmed that this anode catalyst can operate satisfactorily at cell temperatures below 140°C on fuel gases containing CO.

A program was initiated at the University of Virginia to alter the microstructure of electrocatalytic alloys by metallurgical techniques and to determine the effect the nonequilibrium phases on the rate and path of oxygen reduction. Based on the results of other investigators, the platinum-chromium alloy system was chosen. The metallurgical characterization of platinum-chromium samples containing 0, 10, 25, 80, and 100 atomic percent (at%) chromiun was completed. The microscopic evaluation and successful quenching in of the disorder in the 25 at% Cr alloy was completed. The successful quenching was verified by the diffraction patterns of the sample in which the quenched condition contained none of the order peaks observed in the "as cast" sample. This was a pleasing result because previous investigators reported that it is not possible to retain disorder in samples of this composition.

The microscopy observations documented the type of grain structures and precipitates (impurities) and revealed segregation in the 80 at% Cr sample. This was due to a dendrite-type solidification process when the material was cast and should be fairly easy to anneal out. An X-ray diffraction trace verified that the intermetallic was obtained.

Initial electrochemical tests were completed in reagent grade, 85 wt% phosphoric acid at room temperature. Linear sweep and cyclic voltammetry at various sweep rates were conducted on all specimens. Although quantitative examination of the voltammograms was not completed, several observations can be made. The solid-solution specimens of 10 to 25 at% Cr were very similar to pure platinum. The hydrogen adsorption and desorption peaks were not well-resolved. Peak potentials related to oxide formation and reduction shifted slightly with increasing chromium content. These high Pt-content samples were qualitatively equivalent, yielding the classic voltammogram for Pt and indicating no major changes in reactions. Microscopy of these specimens did not reveal any surface changes due to the voltammetry.

The 80 at% Cr intermetallic behaved very differently. Hydrogen bubble formation occurred at lower potentials and oxygen formation occurred at slightly higher potentials than on previous samples. An extra peak was observed, indicating a reaction not present on pure platinum. This

peak disappeared after the initial sweep but returned after a pretreatment of hydrogen evolution for several minutes or after the sample was allowed to sit for longer than one to two hours. The behavior of this sample was also very different from that of pure Cr, because in the case of pure Cr, vigorous oxygen evolution was not observed.

Because of the low operating temperature of the proton-exchange membrane (PEM) system (105°C or lower), the anode catalyst must be CO-tolerant. Six different catalysts (based on the platinum/ruthenium/tungsten oxide system) were selected for evaluation at LANL. Base-line performance was established for both hydrogen/oxygen and hydrogen/air. Membrane and electrode assemblies (M&E's) fabricated from five of the catalysts showed varying degrees of tolerance to carbon monoxide using a fuel of 0.17% CO, 24.8% $CO_2$, and the balance $H_2$. Two other anode catalysts (based on the platinum/rhodium/tungsten oxide system) were evaluated. Their performance was superior to any catalysts previously tested on the 0.17% CO gas mixture, i.e., 740 mV at 500 ASF.

A cell configured with a base-line M&E and a CO-tolerant anode catalyst (platinum/rhodium) accumulated 3079 hours of test at 180°F, 30 psig $H_2$, 30 psig $O_2$ and 500 ASF. At this point, a routine performance test revealed gas cross-over in the cell. At 2906 hours, no leakage across the membrane was detected. The voltage decay during the test was from 740 mV to 675 mV. This decay appeared to be caused by increasing diffusion losses, but determination of the exact cause of the losses was prevented by cross-over of gases.

Several fuel cells were operated at high current densities (up to 1800 $A/ft^2$ at 280 mV) to determine the performance level and the effect of high current density on performance and endurance. Operating at 220°F, 135 psig $O_2$ and 30 psig $H_2$, no adverse effects were observed. However, base-line M&Es have exhibited cathode diffusion losses when operated at 400 $A/ft^2$ on oxygen. To determine if the diffusion loss could be reduced by increasing the cathode Teflon content, a series of M&Es was fabricated with Teflon contents of 16 to 36%. The Teflon content of the anode remained at the base-line level of 15%. The M&Es were evaluated on various gases at 180°F and 222°F. No significant

differences between base-line performance and the performance of M&Es with up to 22% Teflon was observed. With 22% Teflon, the performance curves at 30 psig and 135 psig $O_2$ were parallel, indicative of improved diffusion characteristics. The parallel behavior was evident using Teflon contents up to 36%, but at that level activity losses were experienced. Poor endurance on high-pressure (135 psig) air, which is related to nitrogen diffusion across the membrane interferring with the anode diffusion rate, was significantly improved by increasing the Teflon content of the anode layer to 33%.

A M&E with lower catalyst loading (2 $mg/cm^2$ vs 4 $mg/cm^2$) was tested. Initial performance was 680 mV at 200 $A/ft^2$ on $H_2$ and $O_2$ at 15 psig and 180°F. After solving operational problems with fuels containing CO, the results showed that the reduced loading did not affect cell performance.

## Characterization of Electrodes and Electrocatalysts

Extensive calculations were performed at LANL on the ground and first excited states of the PtO molecule to determine the potential energy surfaces and to establish the bonding and electronic structure as a function of internuclear separation. The ground-state electronic structure was completely determined. Computer-generated plots of the variation of the $\sigma$-bond, $\pi_x$ pair of electrons, and the oxygen 2s pair, respectively, for internuclear distances ranging from 5 Å to the experimentally-observed equilibrium distance, R = 1.72726 Å, were obtained. These plots revealed the molecule has only one bonding pair of electrons that form $\sigma$-bonds. There is no evidence of $\pi$-bonding in the molecule. The Pt 6s electron does not participate in either bonding or non-bonding orbitals, but it is transferred to the oxygen $\pi$ system resulting in a high ionic character with a basic electron configuration of the form $Pt^+O^-$. Ground-state dissociation produces $Pt^+$ and $O^-$, a configuration approximately 7.5 eV above the respective neutral atoms ground-state energy. The ground state of the PtO molecule, at the experimental equilibrium distance, exhibits a charge transfer of 0.34 electrons from the Pt atom toward the O atom, and this transfer comes exclusively from Pt d-type electrons into p-type orbitals in the O atom.

A study of the $Pt_2$ molecule was initiated. Correlated wavefunction calculations for the $Pt_2$ molecule were carried out using a set of programs. Results were obtained for this system as a function of internuclear separation for a Hartree-Fock calculation, a Generalized Valence-Bond calculation, Configuration Interaction including single and double excitations from the Hartree-Fock configuration, a Coupled Cluster calculation, and fourth-order Moller-Plesset perturbation theory. These calculations gave a consistent value for the $Pt_2$ bond length of 2.33 Å. Excellent agreement was obtained for calculated and experimental vibrational frequencies for the molecule. The nearest Pt-Pt distance in bulk Pt metal is 2.746 Å, indicating that larger clusters may have Pt-Pt internuclear separations in the range of 2.30-2.75 Å.

## Physicochemical Characterization of Proton Exchange Menbranes

The program at the General Electric Company (GE) includes efforts to find membranes that are less expensive than Nafion, but that perform similarly in fuel-cell operation. Membranes were obtained from several vendors and characterized alone and in M&Es. Three tests with one membrane exceeded 100 hours of operation before being shut down, and they exhibited good initial performance levels of 0.729 V at 500 $A/ft^2$, 180°F, 15 psig $H_2$, and 30 psig $O_2$. A sample of this membrane was successfully treated with peroxide inhibitor and fabricated into an M&E. It was operated at 180°F, 30 psig $O_2$, and 30 psig $H_2$ for 198 hours when cross-cell leakage was detected. The membrane was degraded at the oxygen inlet between the catalyst layer and the seal area. A second M&E was fabricated with an improved configuration to assist in the prevention of membrane degradation at the cell oxygen inlet. Over 1200 hours of operation were accumulated at 180°F, 30 psig $O_2$, and 30 psig $H_2$ on a cell using this membrane.

Impedance data were obtained at LANL for the hydrogen electrode reaction on a smooth platinum electrode pressed against a Nafion 1170 membrane. A palladium hydride reference electrode was used. All gases were pre-humidified before introduction into the cell. Impedance measurements spanned a frequency range from about 50 kHz to 0.5 Hz and were made in the presence and absence of hydrogen gas.

A number of impedance and cyclic-voltammogram experiments were carried out using either one or two woven platinum grids in contact with the Nafion membrane. At sweep rates at which it is usually possible to obtain reasonable cyclic voltammograms (for example, 50 mV/s), no details were observed. At much lower sweep rates, however, details became observable in the hydrogen adsorption region. Because the adsorption-desorption reactions are rapid, it appears that some other process was hiding the details of the response at shorter times. It appears as if much more of the platinum is available for adsorption of hydrogen than is electrochemically active, in the sense of area available for charge transfer. It is also likely that the low-frequency diffusion process observed in the impedance studies may be due to or associated with surface diffusion of hydrogen on platinum. The process is sufficiently slow that it "smears" out the details of the voltammograms taken at faster scan rates. This also explains why the steady-state currents measured on the grid electrodes were higher than those on smooth platinum, even through the interface resistance was apparently larger for the grid electrodes. A further complication involved in the analysis of data obtained on grids was the current distribution at small contact areas on thin films of electrolytes. Such considerations appeared to explain why higher electrolyte resistance and smaller double-layer capacitances were measured on grids than were expected on the basis of surface areas of contact.

## Fuel-Cell Testing

A six-station, phosphoric acid, single-cell test and measurement system was used to investigate the effects of rapid current pulsing, slow load-current ramping, and temperature cycling on electrodes. The cathode reactant for all of the cells is filtered, compressed air. The anode fuel is hydrogen for all stations except station 1, where $CO_2$ is added to the fuel stream. All cells are maintained at 200°C when under load. Cells 1 and 2 operated at a constant and continuous 200 $mA/cm^2$. Cell 3 was pulsed at a constant and continuous 1 kHz between no load and 400 $mA/cm^2$ to simulate chopper control. Cells 4 through 6 underwent a varying load current that took 7.5 s to go from no-load to 400 $mA/cm^2$ and returned to no-load in 2.5 s. Cell 4 operated in this mode

continuously. Cells 5 and 6 operated in this mode for 3 hours and then were unloaded for 21 hours. Cell 5 was kept at temperature while unloaded, but cell 6 was allowed to cool to ambient temperature.

Rutherford Backscattering Spectroscopy (RBS) has been used to examine possible catalyst movement within the cells. RBS analysis was performed on electrode assemblies from cells 1 and 2 and on two control electrode assemblies. The control electrode assemblies consisted of (1) a cathode and anode assembled and left at open circuit in phosphoric acid at 200°C for 3 days and (2) a cathode and anode assembled, loaded with phosphoric acid and later disassembled. Neither of the control electrode assemblies displayed any platinum redistribution. The cathode and anode assemblies from cells 1 and 2 had run for 2000 hours. The electrochemical behavior of both assemblies showed a gradual loss of activity with time under constant load. The RBS analysis demonstrated that some platinum redistribution had occurred.

X-ray photoelectron spectroscopy (XPS) was performed on a second set of anode assemblies from cells 1 and 2 that also had run for 2000 hours. Again, cell 1 showed very little loss in electrochemical activity; however, cell 2 demonstrated a significant loss of activity. XPS confirmed the loss of Pt from the cathode, which appears as a significant electroplated-Pt deposit on the anode. In addition, the signal position identifies this deposit at the anode as being largely pure platinum. Both the unused and the anode assemblies from cell 1 demonstrated rather broad and low signal-to-noise ratio expected from a highly dispersed catalyst. Although not definitive, the signals for these two electrodes suggest that significant amounts of Pt oxide are present in contrast to the anode from cell 2, which was largely pure Pt.

As a part of the contract with GE to investigate new membrane-catalyst assemblies for solid polymer electrolyte (SPE) systems, two test fixtures were delivered to LANL. Testing with these fixtures was done at LANL to verify contractor results and to update and revise previous performance projections for SPE fuel cells. Tests were run to establish performance baselines, to assess endurance, and to determine anode tolerance to CO. Test reactant gases used were hydrogen/oxygen,

hydrogen/air, and premixed simulated-methanol reformate with oxygen and air. The reformate mixtures used had carbon monoxide volume percentages of 0 to 1%.

The cell conditions used to determine basic individual cell performance were 82°C with 30 psig $H_2$ and 30 psig $O_2$. The desired operating point at these conditions is at least 700 mV at 500 A/ft$^2$. The average of all tests made under these benchmark conditions was 726 mV at 500 A/ft$^2$. Numerous tests at various conditions were made to ensure that there were good correlations between data obtained by LANL and GE for the same M&E formulations.

Several series of tests were made at LANL using reformate/air, including the use of reformate without CO to establish separately the $CO_2$ dilution effect. These tests were of particular interest because of the need to revise projected SPE performance data. In one specific series, a cell running on hydrogen and air at 102°C was switched to CO-free reformate and air to determine the dilution effect, and then to 0.17% CO reformate and air. The cell was run for six hours to determine long-term effects of CO poisoning of the anode. Finally, a return to hydrogen and air was made to find if any permanent degradation in performance could be seen. There was no permanent degradation, and after the initial performance decreased due to the introduction of CO, no discernible further degradation was seen. Furthermore, a large portion of the decrease of cell voltage with reformate was due to $CO_2$ dilution. This series verified the fairly good anode CO-tolerance of the test electrode. Some voltage decrease at high currents was observed after returning to hydrogen operation. This is thought to be due to diffusion losses from build-up of water at the cathode, which is a frequent problem.

## Methanol Fuel Processing - Kinetics and Mechanisms

LANL has identified the ability of the methanol-steam reformer to follow transient load requirements as a problem area. One key to solving this problem is an understanding of the mechanism of the reforming process. Experiments to study the process of catalyst activation and

the mechanism of methanol steam reforming on these active catalysts are underway.

Thermogravimetric studies of catalysts were made using either oxygen, hydrogen, or inert (argon) atmospheres. The data showed a rather complete picture of catalyst activation. Fresh catalysts showed reduction of the CuO (in hydrogen atmospheres) to Cu metal. Zinc oxide is not reduced in these temperature regions (up to 400°C), even with pure hydrogen. Examination of spent catalyst under oxygen atmospheres showed a two-step oxidation, apparently the step-wise conversion of copper metal, through Cu(I), back to CuO. Moreover, the spent catalysts showed an additional peak at ~700°C, that represents a weight loss, most likely the result of oxidation of deposited carbon.

Infrared spectroscopic studies showed similar trends to those suggested by the thermogravimetric experiments. Fresh catalyst showed numerous bands for CuO and $CuCO_3$ species. Following reduction to activate the materials, these were generally absent.

Considerable effort was directed at studies on methanol steam reforming. Fourier-Transform Infrared Spectroscopy (FTIR) was used to analyze the output from a microcatalyst system. A small volume of methanol-steam mixture was pumped through the catalyst at 200°C and then into a heated cell. Water-rich streams gave low CO levels, measured by the ratio of CO to $CO_2$. As the water is decreased in concentration, more CO is formed. With low water levels (90% methanol), appreciable amounts of a compound that appears to be methyl formate is produced. Introduction of $D_2O$ along with methanol gave deuterated products including $CD_3OH$. This C-D bonding did not appear immediately, suggesting that the bed of catalyst slowly exchanged deuterium (as part of the reforming reaction). When the entire bed was deuterated, then the $CD_3OH$ species exited. These data strongly supported a mechanism that involves the generation of hydrogen radicals on the catalyst surface.

Work was also completed on other alcohols, especially isopropanol and ethanol. These compounds are typical of what can be expected as contaminants in methanol. They also serve as model molecules that permit additional testing of proposed hypotheses because the carbon-carbon

bonds are not readily severed, and thus products are useful to suggest a methanol reforming mechanism.

Isopropanol produces acetone when it reacted at an active catalyst. Ethanol, on the other hand, was converted to acetaldahyde. In both cases, the carbon-carbon bond was maintained, and the carbon bonded to oxygen was oxidized to a carbonyl-like group. These data explained the odor that is apparent when methanol reformers are fed fuel that contains $C_2$ and $C_3$ alcohols. These products also point to a mechanism that involves a molecular attachment to the catalyst through the oxygen atom. The rapid reaction of methanol results from the fact that, following that step, only carbon-hydrogen bonds are severed, leaving an oxidized carbon species, $CO_2$.

Other efforts were directed at identifying the source of oxygen in the product carbon dioxide. Mass-spectroscopy techniques were used with specially-prepared methanol and water, both with $^{18}O$. Data showed that the catalytic reaction with water is the process that releases carbon dioxide. It is suspected that reaction with alcohol results in an effective "reduction" of a surface site. However, experiments where first methanol and then water was injected produced no product carbon dioxide until the water was introduced. This behavior showed that the water "oxidation" is the step that generates product carbon dioxide. Oxygen-18 labeling showed clearly that the carbon—oxygen bond is not maintained during the reaction. Rather, when normal methanol was reacted with water containing $^{18}O$, carbon dioxide of mass 44 was the principal product. This result is the normal trend; the oxygen content of product $CO_2$ reflects the oxygen isotopic content of reactant water, not of reactant methanol. These data are best explained by assuming rapid oxygen exchange on the catalyst surface, at rates that are fast compared to the lifetime of the methanol species or its product on the surface. Thus, these reforming catalysts work by scrambling both hydrogen and oxygen atoms. These data indicate that the catalyst works by rapid oxygen migration, prompting exchange of surface oxygen atoms with molecular compounds that reside there.

## Fuel Cell Vehicle Systems Simulations

The 20-kW fuel cell system was completed in April 1984 at Energy Research Corporation (ERC). ERC ran preliminary tests, and LANL personnel participated in limited testing at ERC in May 1984. Site preparation was completed at LANL, including instrumentation and sensor installation, check-out, and field calibration; ventilation-hood installation; load-bank installation; and data-acquisition system installation and software development. The scope of the test was reduced somewhat due to delays in completion of the test article.

The fuel-cell system was delivered to LANL in June 1984, and two days of operation were achieved while ERC personnel were present. Sixteen days of testing were accomplished with the system under load for thirty-four hours. The projected nominal operating point was 124 V and 170 A, or 21.1 kW. Initially, a nominal operating point of 115 V and 182 A or 20.9 kW was achieved at LANL. This was somewhat better than the performance observed at ERC. Using reformate fuel, the maximum power attained at LANL was 26.2 kW (103 V, 254 A), and the minimum power was 15.5 kW (124 V, 125 A).

A sudden decrease in performance was seen after about nineteen hours of operation on load. The nominal operating point changed to 21.6 kW at 108 V and 200 A. Original system efficiencies were approximately 30% at the design point. The efficiency after the performance change dropped to 26%. Efficiencies do not take into account cooling fan power which has been measured at 1.5 kW. The performance decrease has not been explained yet. Some acid loss was observed coincident with the problem, and there is also evidence that the reformer is not performing at its original level.

A subset of the overall test procedure was to map the reformer performance. Tests were made at various reformer flows, temperatures, and fuel utilization to measure reformer conversion efficiency, CO content of the product gas, and system efficiency. Little decrease in fuel-cell performance was observed at design operating temperatures (400°F) with CO contents of up to 5% by volume. Dynamic response of the system to load changes was observed. The reformer catalyst-bed temperature has a

time constant of about fifteen minutes in response to changes in the heat rate of the reformer burner. Reformer start-up time is about twenty minutes. System instability was seen during attempts to operate at lower power levels (less than 15 kW) on tail gas, where hydrogen-depleted reformate is returned from the fuel cell to be burned as a heat source for the reformer.

Overall, the system has performed reasonably well, even though power density and efficiency fell somewhat below the original projections. Valuable experience and insight into operational, design, and control problems and possible solutions was gained.

Publications


1. P.J. Hyde, C.J. Maggiore, and S. Srinivasan, "Use of a Nuclear Microprobe in the Study of Fuel Cell Electrodes," Proceedings of the Sixth Australian Electrochemistry Conference, Geelong, Australia, February 19-24, 1984.

2. J.R. Huff, J.B. McCormick, D.K. Lynn, R.E. Bobbett, G.R. Dooley, C.R. Derouin, H.S. Murray, and S. Srinivasan, "Applications of Fuel Cells to Transportation," Proceedings of the Eleventh Energy Technology Conference, Washington, DC, March 19-21, 1984.

3. 5. A. Carubelli, S. Srinivasan, M. Babai, and S. Gottesfeld, "Pseudo-Capacitance Technique to Determine Anion Adsorption on Gold and Effects of Anion Adsorption on the Oxygen Reduction Kinetics," presented at the spring Meeting of the Electrochemical Society, Cincinnati, OH, May 6-11, 1984.


## Advanced Chemistry and Materials for Fuel Cells

(J. McBreen, Brookhaven National Laboratory)

The objectives of this project are to develop electrocatalysts that minimize or eliminate the need for noble metal catalysts in fuel cells and to enhance the kinetics of oxygen reduction and the oxidation of carbon monoxide/hydrogen mixtures. In 1984, research was focused on studies of the interaction of fuel-cell reactants with platinum, the synthesis and evaluation of tetrasulfonated-metal-phthalocyanine electrocatalysts, and an investigation of the solid polymer electrolyte/electrocatalyst interface.

Fuel Cell Reactants on Platinum Surfaces: The interaction of several reactants (water, oxygen, carbon monoxide and methanol) with platinum (111) single crystal were investigated using high-resolution electron energy-loss spectroscopy (HREELS). A method was devised for detection of reaction intermediates. The temperature was increased in steps to permit various reactions to occur, and after each temperature increase, the sample was cooled rapidly (10°K/s) to quench the reaction, and the intermediates were then observed in the spectrometer. Several reactions of importance to fuel cells were studied. At 100°K, co-adsorbed $O_2$ and $H_2O$ react to form surface OH species. Two pathways for methanol decomposition were observed, one involving the formation of surface species such as formaldehyde, formate and carbon monoxide; and the other, formation of formate and carbon monoxide. On clean platinum, the adsorption of CO could be clearly seen and vibrational spectra for Pt-C and C-O were observed. On platinum covered with O and OH groups, the situation was more complex and has not been resolved.

Synthesis and Evaluation of Phthalocyanine Catalysts: So far tetrasulfonated metal phthalocyanine (M-TsPc) compounds with the following centers have been prepared: $H_2$, VO, Cr, Mn, Fe, Co, Ni, Cu, Zn, Ga, Ru, Os, Rh, In and Re. All except Re-TsPc have been purified.

A spectrophotometric study of the homogenous reaction between most of the M-TsPc compounds and $H_2O_2$ was carried out in an aqueous solution consisting of $1x10^{-5}$M M-TsPc and $1x10^{-3}$M $H_2O_2$. The M-TsPc compounds of Mn, Fe, Co and Ru were unstable to $H_2O_2$. However, more recent results with Co-TsPc adsorbed on pyrolytic graphite indicate that adsorption on graphite imparts stability to M-TsPc in the presence of $H_2O_2$.

Electrochemical characterization of the M-TsPc compounds was started. This included cyclic voltammetry studies in 1M $H_3PO_4$ and 1M KOH and investigations of the interactions of M-TsPc with $O_2$, $H_2O_2$, CO, $CO_2$, $CH_4$ and $H_2$. All of the M-TsPc compounds show some activity for $O_2$ reduction, and the compounds of Co, VO and Ga were active for $H_2O_2$ oxidation. The Cu-TsPc catalyst oxidizes CO in $H_3PO_4$. In alkaline solution, the compounds of Zn, Mn and Ga catalyze the reduction of $O_2$. None of the materials interacted with $CH_4$ or $H_2$.

The electrocatalytic activity of Co-TsPc in conductive polypyrrole films was investigated. A number of effects were observed, including an enhancement of the activity for oxygen reduction, an improvement in the stability of the polypyrrole film, and a change in the mechanism of oxygen reduction that coincided with the change in oxidation state of the Co-TsPc.

The Solid Polymer Electrolyte/Electrocatalyst Interface: Further investigations were made on the solid polymer electrolyte/ electrocatalyst interface and on the current generation mechanism of electrodes in contact with Nafion membranes. Experiments with platinum black and with single and multiple layers of platinum screens confirmed the fact that platinum sites remote from the Nafion/electrocatalyst interface could be utilized for electrochemical adsorption and desorption of hydrogen and oxygen species. A mechanism based on the fast mobility of adsorbed hydrogen and hydroxyl groups was proposed. A series of critical experiments, in which gold screens or carbon felt were interposed between the platinum and Nafion membrane, confirmed the proposed mechanism. These findings have important implications regarding solid-polymer-electrolyte fuel cells and the type of catalyst support that should be used to disperse catalysts and reduce catalyst loading in fuel cells with ionomeric membranes.

Publications and Presentations


1. M. I. Florit, W. E. O'Grady, T. Skotheim and M. Rosenthal, "Conducting Polymers for $O_2$ Reduction", Extended Abstract #415, Spring Meeting of the Electrochemical Society, Cincinnati, OH, May 6-11, 1984.

2. M. I. Florit, W. E. O'Grady, A. Schuler and C. A. Linkous, "Adsorption of Cobalt Tetrasulfonated Phthalocyanine on Gold: The $O_2$ Reduction Reaction", Abstract #628, Fall Meeting of the Electrochemical Society, New Orleans, LA, October 7-12, 1984.

3. C. A. Linkous, "Decomposition Kinetics of Phthalocyanine Electrocatalysts by Hydrogen Peroxide, Abstract #651, Fall Meeting of the Electrochemical Society, New Orleans, LA, October 7-12, 1984.

4. A. Melo, W. E. O'Grady, G. Chottiner and R. Hoffman, "Study of Hydroxyl Formation on Pt(111) Surface by EELS and Low Temperature Reaction Quenching", Presented at the 6th Symposium on Applied Surface Analysis, Dayton, OH, June 1984.

## Alternative Electrolytes for Fuel Cells

(E.J. Cairns and F.R. McLarnon, Lawrence Berkeley Laboratory)

Alkaline electrolytes have long been known to support higher oxygen-reduction kinetic currents than those observed in acid electrolytes. However, recent fuel cell work has avoided hydroxide electrolytes because carbonation can occur in the presence of the $CO_2$ in the hydrogen-rich gas that results from the steam-reforming of carbonaceous fuel. $CO_2$-rejecting electrolytes such as $Cs_2CO_3$ were investigated in 1964 by Cairns and Bartosik(1). This early work demonstrated electrolyte invariance in a methanol/oxygen single cell, where $CO_2$ is produced at the anode. Overall cell performance was shown to be promising but no measurements of the oxygen-electrode kinetics were made.

Preliminary kinetic results obtained with the rotating ring-disk electrode technique in dilute $Cs_2CO_3$ showed higher currents and lower ring-currents than KOH at the same concentration, indicating a possible change in reaction mechanism. To study the carbonate-anion effect in a manner independent of pH differences, increments of potassium carbonate were added to the well-characterized electrolyte 0.1M KOH. An increase in kinetic current was observed with a series of carbonate additions (0.1M $Cs_2CO_3$ and 0.1M $K_2CO_3$). The causes for this behavior have not yet been identified. Ring currents due to peroxide formed at the disk were also found to depend on carbonate concentration. Negligible ring currents (<0.1 μA) were observed in the pure 0.1M $Cs_2CO_3$ solution (pH = 11.4), whereas significant peroxide was detected in the higher-pH solutions.

Changes in oxygen solubility due to the increase in ionic strength of the solution would result in the opposite trend in kinetic currents; however, other effects of the ionic strength are possible. Future work will focus on determination of the reasons for the positive anion effect, as well as an investigation of the extent. Experiments with more concentrated electrolytes are planned.

Reference

1. E.J. Cairns and D.C. Bartosik, "A Methanol Fuel Cell with an Invariant Alkaline Electrolyte," J. Electrochem. Soc. 111, 1205 (1964).

Publication

1. K.A. Striebel, P.C. Andricacos, E.J. Cairns, P.N. Ross, and F.R. McLarnon, "Oxygen Reduction in Tetrafluoroethane-1,2-Disulfonic Acid", Presented at the 166th Meeting of the Electrochemical Society, New Orleans, LA (1984), Paper No. 410; LBL-19088 (1984).

This report was done with support from the Department of Energy. Any conclusions or opinions expressed in this report represent solely those of the author(s) and not necessarily those of The Regents of the University of California, the Lawrence Berkeley Laboratory or the Department of Energy.

Reference to a company or product name does not imply approval or recommendation of the product by the University of California or the U.S. Department of Energy to the exclusion of others that may be suitable.

*LAWRENCE BERKELEY LABORATORY*
*TECHNICAL INFORMATION DEPARTMENT*
*UNIVERSITY OF CALIFORNIA*
*BERKELEY, CALIFORNIA 94720*